GULF GENERAL ATOMIC

Gulf-GA-B12340

FORT ST. VRAIN PROOF TEST ELEMENT NUMBER TWO DESIGN, FABRICATION, AND ASSEMBLY REPORT

by

W. J. Scheffel, B. F. Disselhorst, and S. Langer

Prepared under
Contract AT(04-3)-633
for the
San Francisco Operations Office
U.S. Atomic Energy Commission

This document, which was prepared primarily for internal use, may contain preliminary or incomplete data. It is informal and is subject to revision or correction; it does not, therefore, represent a final report.

Date Published - May 21, 1973

MASTER

GULF GENERAL ATOMIC COMPANY
P.O. BOX 81608, SAN DIEGO, CALIFORNIA 92138

DISCLAIMER

NOTICE

GULF GENERAL ATOMIC

Gulf-GA-B12340

FORT ST. VRAIN PROOF TEST ELEMENT NUMBER TWO DESIGN, FABRICATION, AND ASSEMBLY REPORT

Work done by:

C. C. Adams
N. L. Baldwin
J. N. Graves
V. H. Pierce
E. E. Borders
P. R. Macy
P. T. Mattson, Jr.
B. A. Czech
R. J. Colburn
R. H. Arnold
C. S. Luby
W. Wayles

Report written by:

W. J. Scheffel
B. F. Disselhorst
S. Langer

Prepared under
Contract AT(04-3)-633
for the
San Francisco Operations Office
U.S. Atomic Energy Commission

Gulf General Atomic Project 900

Date Published - May 21, 1973

GULF GENERAL ATOMIC COMPANY
P.O. BOX 81608, SAN DIEGO, CALIFORNIA 92138

CONTENTS

FIGURES

FIGURES (continued)

FIGURES (continued)

TABLES

TABLES (continued)

1. INTRODUCTION

As part of the overall fuel element research and development program for the Public Service Company of Colorado Fort St. Vrain Nuclear Generating Station, Unit One Reactor, one or more prototype proof test fuel elements are to be irradiation tested in a high-temperature gas-cooled reactor (HTGR) environment. This report discusses the design details, fuel characteristics, and assembly of the second proof test element (PTE-2) in a series of five prototype proof test elements built for the Fort St. Vrain Nuclear Generating Station.

The purpose of the fuel element irradiation program is to demonstrate that the Fort St. Vrain (FSV) fuel element will meet its design objectives. This will be demonstrated by irradiating a test element(s) in the Peach Bottom HTGR at temperature gradients typical of that expected in FSV to at least one-third of the design lifetime fuel burnup. PTE-2 will achieve the desired total burnup in approximately 300 full-power days of irradiation in Peach Bottom.

It should be noted that PTE-2 was built in 1968, prior to the introduction of pitch-bonded, natural-flake graphite matrix which was eventually chosen for use in the FSV initial core.

2. GENERAL COMPARISON OF PTE-2 TO THE FSV FUEL ELEMENT

PTE-2 was designed to model the FSV fuel element wherever possible within the limitations of the Peach Bottom reactor. In Table 2-1 a comparison is made of various criteria for PTE-2 and the FSV fuel element. Because of the objectives of the test and the Peach Bottom neutronics, it was not possible to use the reference Th/U ratio of 4.25 to 1. Rather a ratio of 0.58 to 1 was used to achieve both the desired fuel temperatures and the objective of one-third FSV peak fuel particle burnup in 300 equivalent full power days of irradiation. The hole pattern in PTE-2 is consistent with a duplicate of the pattern in the FSV fuel element as shown in Fig. 2-1.

TABLE 2-1
PTE-2 AND FSV FUEL ELEMENT CRITERIA COMPARISON

	PTE-2	FSV Reactor
Element type	Hex block with internal coolant passages, no purge flow	Hex block with internal coolant passages, no purge flow
Body graphite	GLCC H-327 and Speer 9567	GLCC H-327
Fuel - coolant hole pitch, in.	0.740	0.740
Fuel hole diameter, in.	0.474, 0.521	0.500
Fueled length, in.	28.63 (Zones 2 and 3 only)	29.10
Coolant hole diameter, in.	0.454, 0.626	0.625
Width across flats, in.	3.540	14.172
Fuel bed type	Rods	Rods
Fuel rod diameter, in.	0.467, 0.514	0.490
Fuel rod length, in.	1.00, 5.93, 11.53, 14.31	1.94
Fuel particle type: Fissile	$(Th,U)C_2$ TRISO	$(Th,U)C_2$ TRISO
Fertile	ThC_2 TRISO	ThC_2 TRISO
Fissile particle Th/U ratio	0.58	4.25
Fuel rod matrix type	Resin mix binder and graphite flour, cold injected	Pitch binder and natural flake graphite filler, hot injected
Average fuel rod linear heat rating, watt/in. of fuel rod	220	99
Maximum fuel rod linear heat rating, watt/in. of fuel rod	288	257
Maximum fuel rod centerline temperature, °F	2270	2300
Fuel rod ΔT, °F	235	210

TABLE 2-1 (Continued)

	PTE-2	FSV Reactor
Maximum graphite ΔT between fuel surface and adjacent coolant hole surface, °F	200	130
Maximum axial tensile stress, psi	900	450
Maximum axial compressive stress, psi	1100	450
Maximum radial tensile stress, psi	370	200
Maximum radial compressive stress, psi	410	300
Average fuel rod burnup, Mwd/Tonne initial U + Th[(a)]	26,000	100,000
Maximum fuel rod burnup, Mwd/Tonne initial U + Th[(a)]	34,000	120,000
Average fast fluence (E > 0.18 Mev) nvt x 10^{21}[(a)]	1.15	5.5
Maximum fast fluence (E > 0.18 Mev) nvt x 10^{21}[(a)]	1.5	8.0

[(a)] Assumes 300 equivalent full-power days in Peach Bottom.

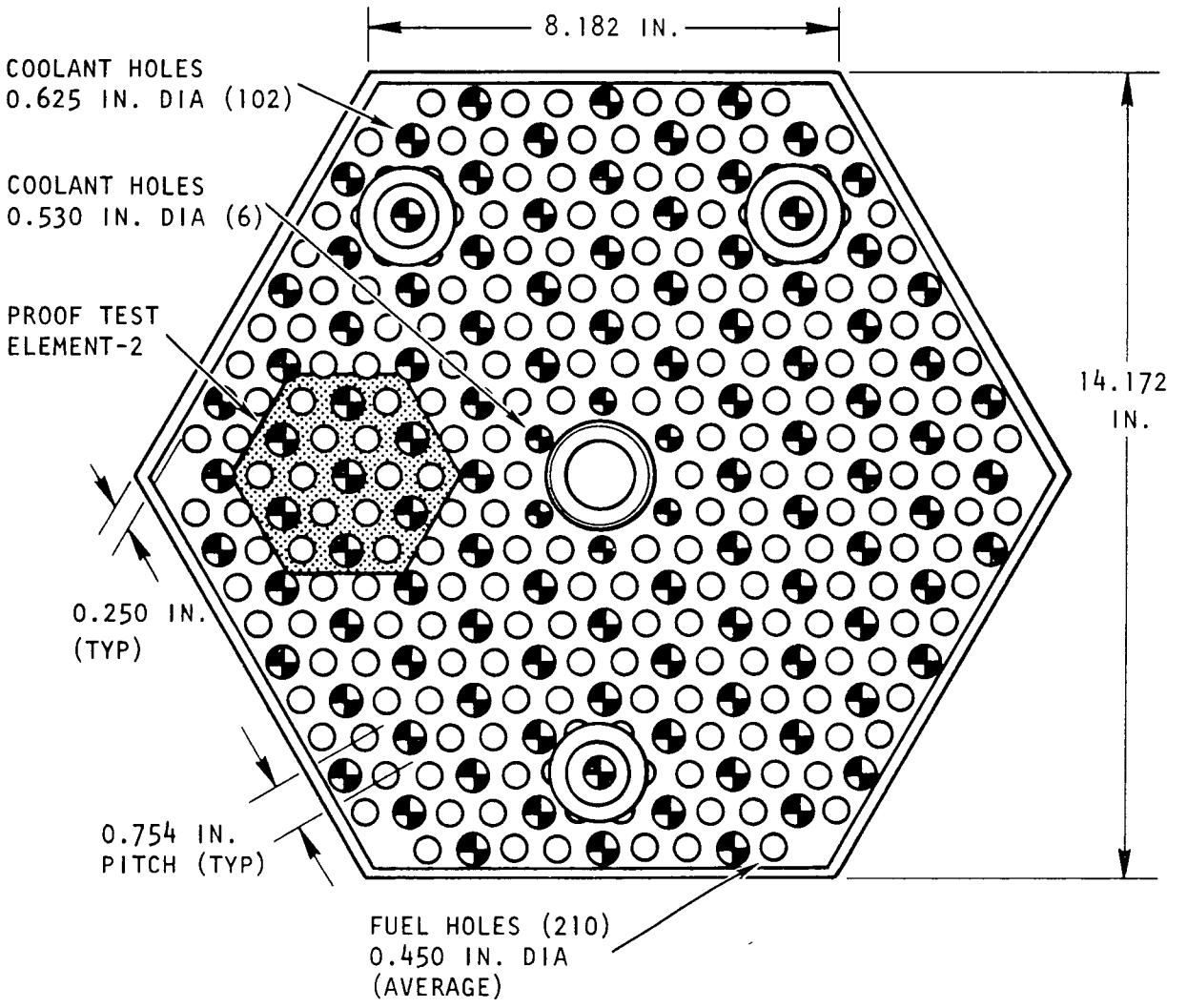

Fig. 2-1. Typical Fort St. Vrain fuel element

3. PTE-2 DESCRIPTION

3.1. GENERAL DESIGN DESCRIPTION

The proof test element was designed to replace a standard instrumented element in the Peach Bottom core. The test element contains an array of fuel beds and coolant channels within a hexagonal graphite structure having an external width across the hexagonal flats equal to the outer diameter of a Peach Bottom element. Figure 3-1 shows the hexagonal test element surrounded by an array of cylindrical Peach Bottom elements. A comparative view of the test element and a standard element is shown in Fig. 3-2.

3.2. ARRANGEMENT OF COMPONENTS

The test element assembly consists of seven graphite sections joined together. The sections are, from bottom to top, a bottom connector, a bottom reflector, four fuel zones, and a top reflector. An assembly view of the element is shown in Fig. 3-3. The bottom portion of the element is cylindrical, with a transition to a hexagonal shape in the bottom reflector section. The active fuel zones are hexagonal, and the width across the flats is equal to the diameter of the intermediate spacers of the regular elements. The width across the flats of the hexagonal top reflector is equal to the diameter of the top spacer of a regular element. The length of the test element is the same as a regular fuel element excluding the handling knob.

The element, in cross section, contains 12 fuel beds and 7 coolant channels, as shown in the plan view in Fig. 3-4. The fuel and coolant hole centerlines are located on a 0.740-in. triangular pitch, the same as the FSV fuel element. The hole pattern, from the center out, consists of a coolant channel, a ring of fuel beds, a ring of coolant channels, and another ring

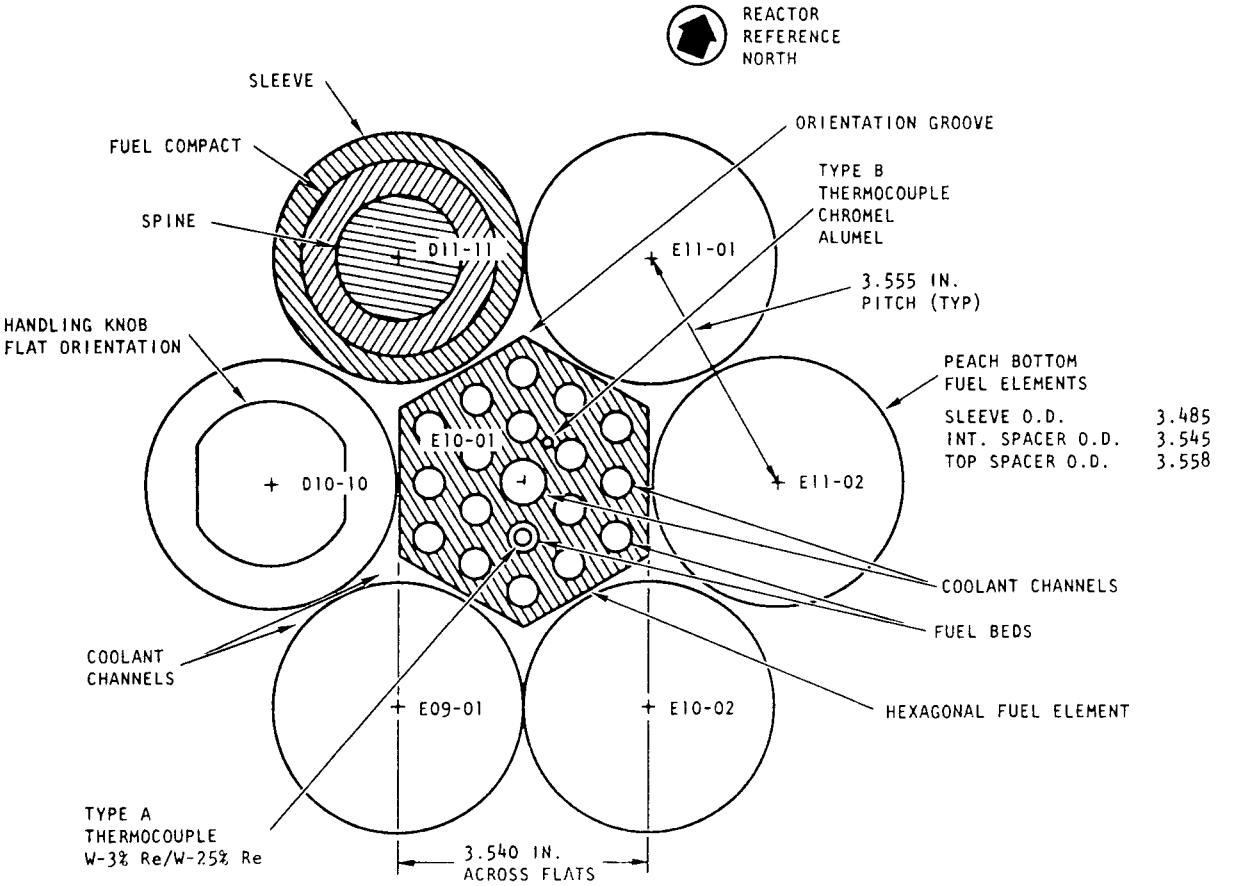

Fig. 3-1. Second proof test fuel element orientation in the Peach Bottom core

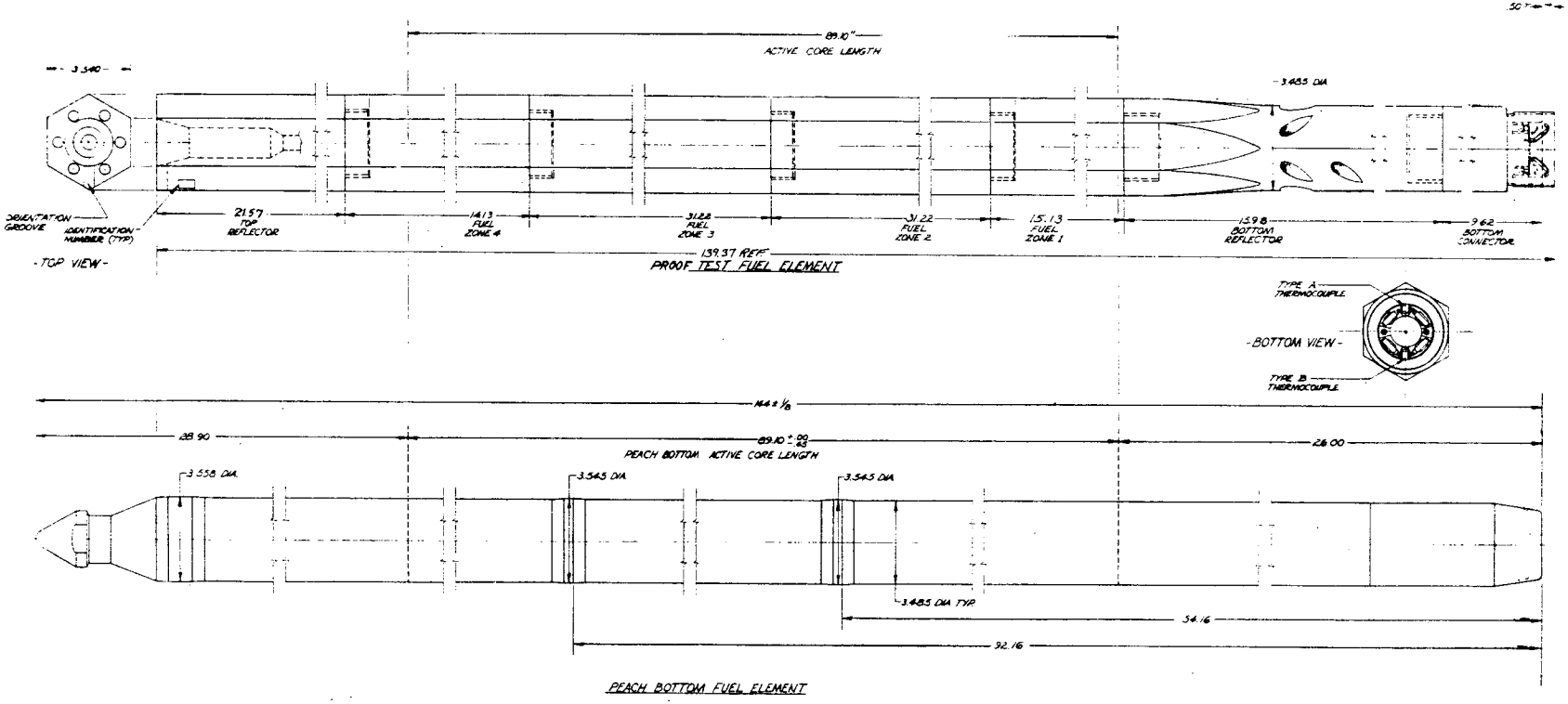

Fig. 3-2. Comparative view of the proof test fuel element and Peach Bottom fuel element

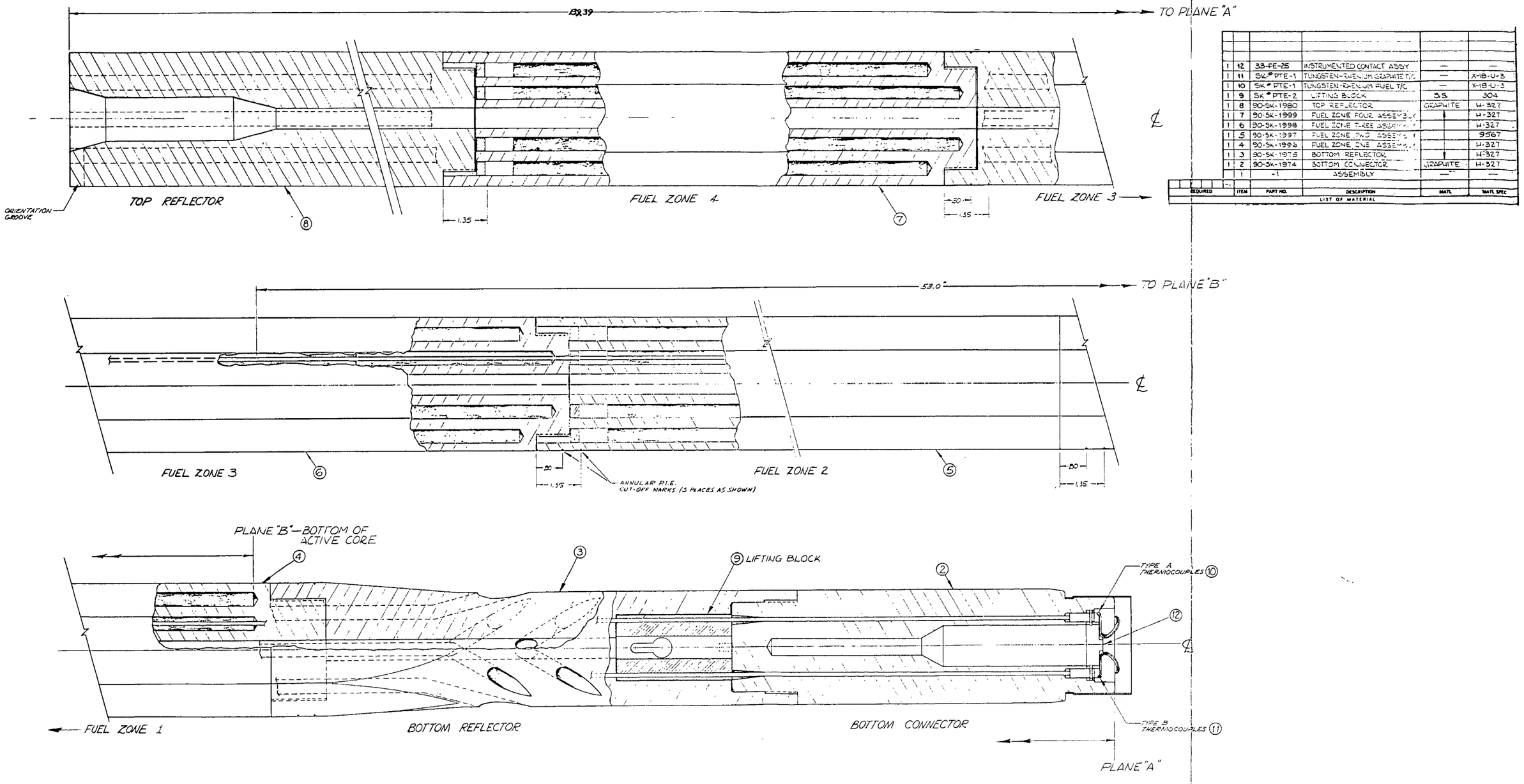

REQUIRED	ITEM	PART NO.	DESCRIPTION	MATL	MATL SPEC
1	12	33-FE-25	INSTRUMENTED CONTACT ASSY	—	—
1	11	SK-PTE-1	TUNGSTEN-RHENIUM GRAPHITE T/C	—	X-18-U-3
1	10	SK-PTE-1	TUNGSTEN-RHENIUM FUEL T/C	—	X-18-U-3
1	9	SK-PTE-2	LIFTING BLOCK	S.S.	304
1	8	90-SK-1980	TOP REFLECTOR	GRAPHITE	H-327
1	7	90-SK-1999	FUEL ZONE FOUR ASSEMBLY	"	H-327
1	6	90-SK-1998	FUEL ZONE THREE ASSEMBLY	"	H-327
1	5	90-SK-1997	FUEL ZONE TWO ASSEMBLY	"	9567
1	4	90-SK-1996	FUEL ZONE ONE ASSEMBLY	"	H-327
1	3	90-SK-1975	BOTTOM REFLECTOR	"	H-327
1	2	90-SK-1974	BOTTOM CONNECTOR	GRAPHITE	H-327
1	1	-1	ASSEMBLY	—	—

LIST OF MATERIAL

Fig. 3-3. Test element assembly

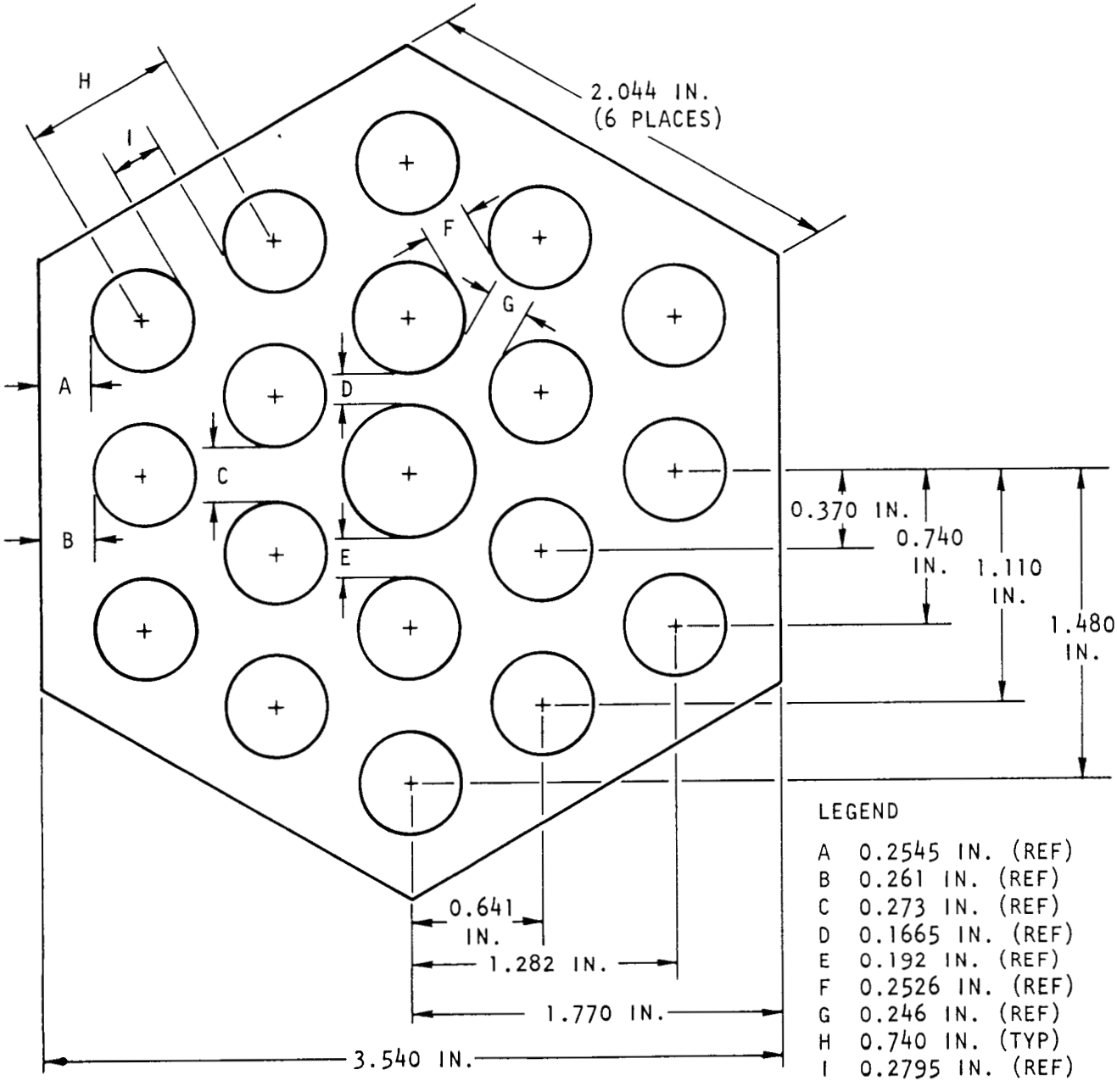

Fig. 3-4. Test element plan view

of fuel beds located near the corners of the hexagon. The fuel and coolant holes are arranged in the same manner as those in the FSV element, as seen in Fig. 2-1.

The test element is cooled both by the seven internal coolant channels and the six modified tricuspidal channels adjacent to the element. The coolant enters the internal coolant channels just below the region where the element undergoes the transition from a cylindrical to a hexagonal shape. The coolant flows up through the active fuel section and discharges out of the top reflector.

The active portion of the fuel element is composed of the four fuel zones joined together axially by cemented threaded joints. Each fuel zone contains twelve blind fuel holes drilled from the top of the zone to within 0.4 in. of the bottom. The details of the fuel zones are shown in Fig. 3-5. The diameter of each of the regular fuel holes is 0.474 in. The fuel hole that will contain the annular fuel rods is 0.514 in. in diameter. A thermocouple will be placed through the center of these rods. The seven coolant channels are continuous from the top to the bottom of the zone and are aligned with the channels in adjacent zones to form continuous internal coolant channels over the full length of the fuel element. The alignment of the coolant channels is maintained by controlling the hole location during machining, and by precise alignment of the flats of the hexagons during assembly. The diameter of the center coolant channel is 0.626 in. The diameter of each of the six outer coolant channels is 0.454 in.

The test element is not purged and therefore does not provide a flow of helium to the purge line in the reactor standoff pin.

The test element graphite (excluding the bottom connector) is composed of high-density, high-strength, extruded, nuclear-grade needle-coke graphite. Two similar types of needle-coke graphite were used in the test element and represent the two leading candidates of material for the FSV reactor. Fuel zones one, three, and four, plus the top and bottom reflectors, are made from H-327 graphite supplied by the Great Lakes Carbon Corporation (GLCC).

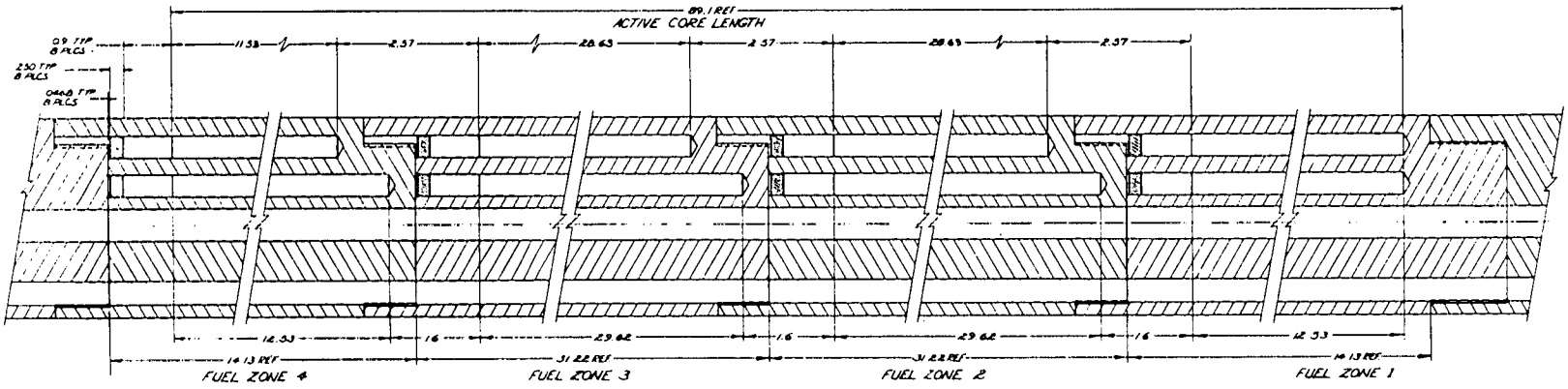

Fig. 3-5. Fuel zone details

Fuel zone two is made from Grade 9567 graphite supplied by the Speer Carbon Company. Physical and mechanical properties of the two types of graphite are listed in Table 3-1. The bottom connector graphite is made of highly impregnated stock to minimize helium inleakage to the standoff pin and is the same type of material as that used for the standard fuel element bottom connectors.

The test element is instrumented with two thermocouples, as shown in Figs. 3-3 and 3-6. One thermocouple is in the center of an inner fuel rod and the other is in the graphite structure between two inner fuel holes. The thermocouple junctions are about 53 in. above the bottom of the active core at the plane of expected maximum fuel temperatures. The thermocouple contained within the annular fuel rod is the W-25% Re/W-3% Re type with a molybdenum sheath and niobium cladding. The thermocouple contained within the graphite is a Chromel-Alumel type with an Inconel sheath and niobium cladding. The tungsten-rhenium thermocouples are designated type A and the Chromel-Alumel are designated type B. The type B thermocouple is on the side of the element containing the loading mark. This loading mark faces reactor north after installation.

An identification number is imprinted on the top reflector of each element. Also, a horizontal orientation groove from the center coolant hole to the corner of the hex is machined on the top face of the top reflector. The groove is aligned with the type B thermocouple and faces reactor north after installation, as shown in Fig. 3-1.

The fuel for the test elements is composed of close-packed coated fuel particles bonded into cylindrical fuel rods. The details of the fuel particles and fuel rods are discussed in Sections 5 and 6 of this report.

3.3. PTE COMPOSITION

The as-built composition of the test fuel element over the active core section is as follows:

TABLE 3-1
NEEDLE-COKE GRAPHITE PROPERTIES

Parameter	GLCC H-327	Speer 9567
Tensile strength, psi		
parallel	1600	1310
perpendicular	900	1125
Compressive strength, psi		
parallel	4700	∿4500
perpendicular	4200	
Coefficient of thermal expansion, /°F		
parallel	1.17×10^{-6}	1.16×10^{-6}
perpendicular	2.22×10^{-6}	2.43×10^{-6}
Density, gm/cm^3	1.73	1.76
Modulus of elasticity, psi		
parallel	1.86×10^{6}	1.75×10^{6}
perpendicular	0.66×10^{6}	1.0×10^{6}

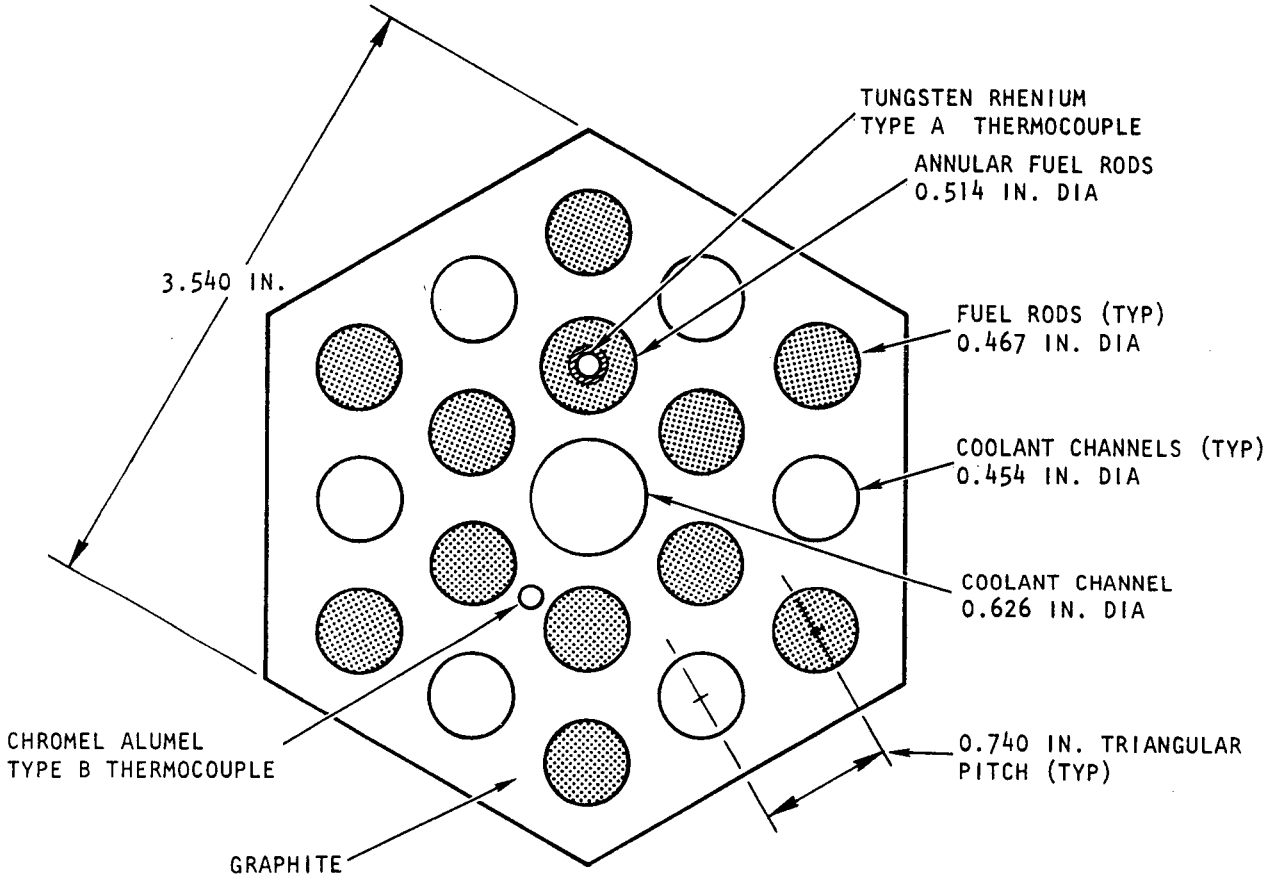

Fig. 3-6. Radial thermocouple locations

Uranium (93.15% U-235)	450.18 g
Thorium	2,153.41 g
Particle coatings (carbon plus silicon) and matrix carbon	3,261.12 g
Fuel zone structural graphite	20,692. g
Two thermocouples	260.0 g
Thermocouple contactor	93.0 g
Top reflector	5,687.0 g
Bottom reflector	3,395.0 g
Bottom connector	2,753.0 g
Latch block	1,218.0 g
Total	39,962.71 g (88.10 lb)
Handling tool	4,917 g (10.84 lb)
Total element weight with handling tool	44,879.71 g (98.94 lb)

3.4. FUEL ELEMENT HANDLING

The test elements are inserted and removed from the core with a special handling tool and the fuel transfer machine. It is necessary to use a special handling tool because the test element does not have a handling knob on the top of the element as does the standard Peach Bottom element. After insertion of the handling tool, the fuel transfer machine handles the test element in essentially the same manner as the standard fuel and hexagonal reflector elements.

The handling tool assembly is shown in Fig. 3-7. The main components of the tool are the handling knob, compression spring, extension rod, and lifting tee. The handling knob, compression spring, and a part of the extension rod are shown in Fig. 3-8. The tool engages a metal lifting block, which is built into the lower reflector of the test element as seen in Fig. 3-3.

The handling tool is latched to the test element in the following manner. The fuel transfer machine lowers the tool into the element through

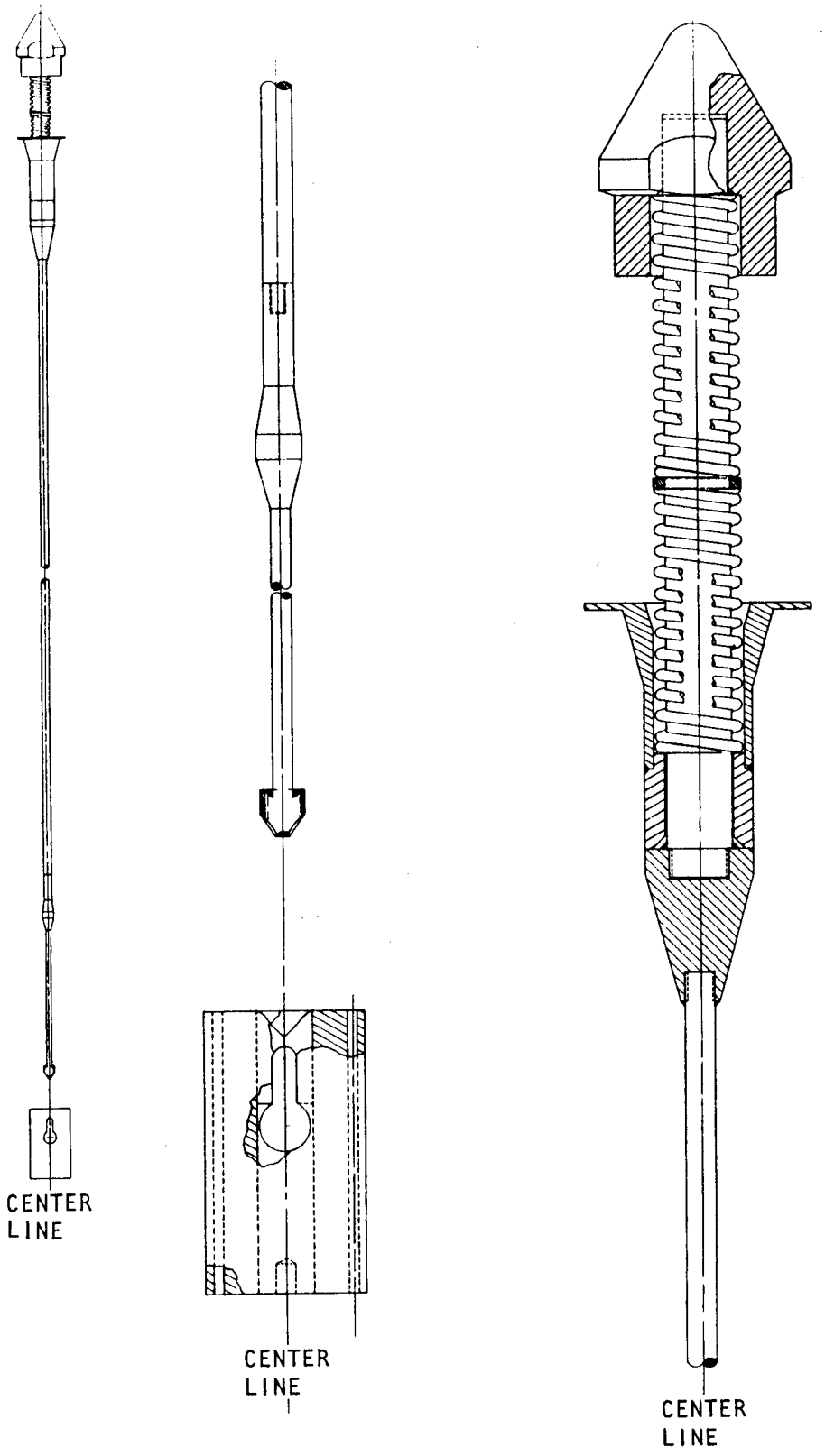

Fig. 3-7. Handling tool assembly

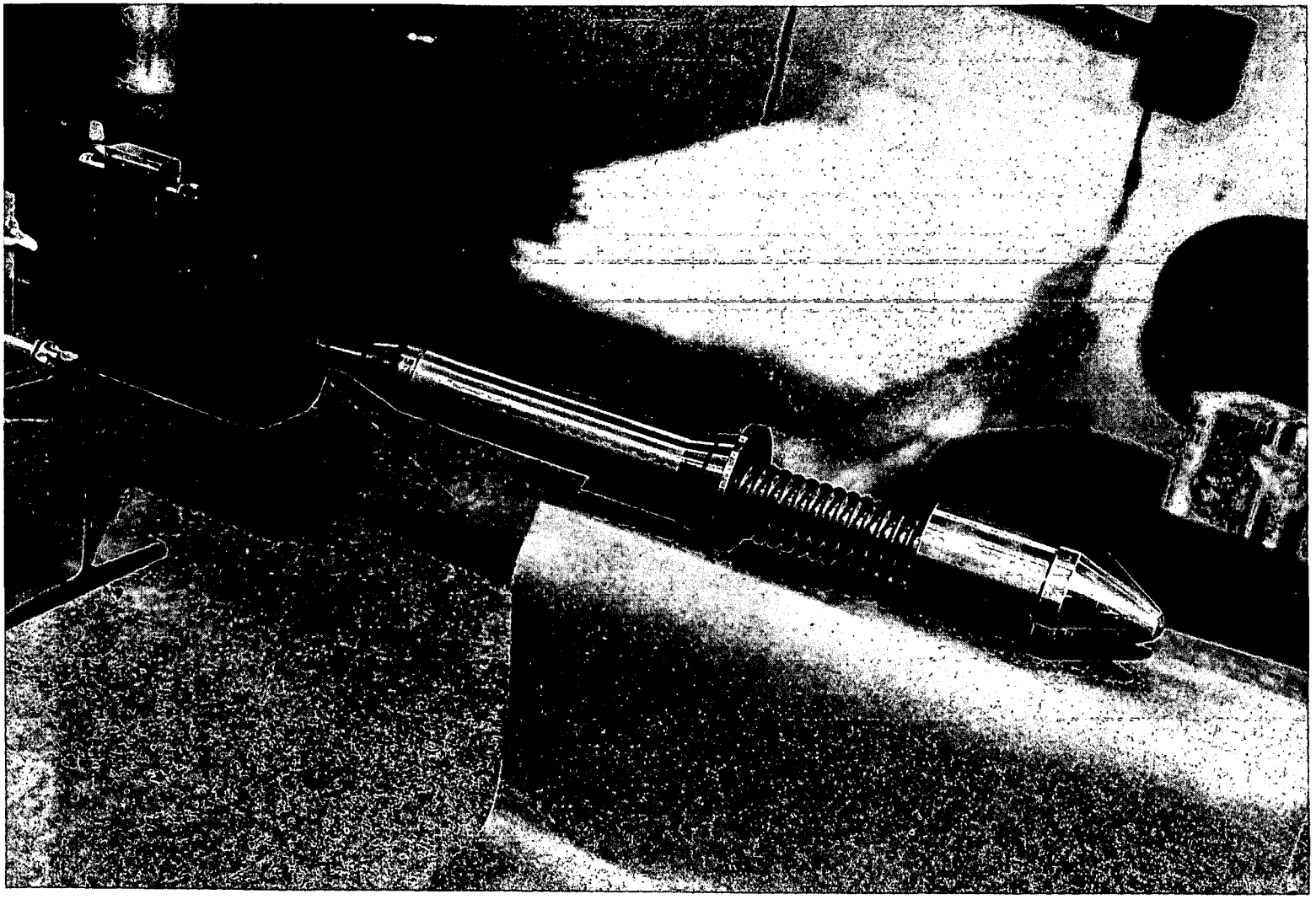

HT66521

Fig. 3-8. Upper portion of handling tool within PTE-2

the center coolant hole. As the tool becomes fully inserted within the element, the spring assembly starts to compress against the top of the fuel element. When the tool is fully inserted, it is rotated 90 deg and then raised to allow the lifting tee on the bottom of the tool to engage the recessed slot in the lifting block. At this point the tool is in the latched position and the element is ready to be handled. The latching sequence between the tee and lifting block is shown in Fig. 3-9. With the tool in the latched position, the spring assembly is compressed and exerts a compression force of about 70 lb on the element.

The function of the spring assembly is to keep the tool firmly latched to the test element during handling operations. When the tool is in the latched position, the lifting tee is pushed against the top of the recessed slot of the lifting block with a force of about 70 lb. To unlatch the tool from the element, the spring must be compressed with a minimum force of approximately 110 lb, and the tool rotated 90 deg. In addition to the downward force exerted by the spring, the weight of the element (approximately 88 lb) will be bearing on the lifting tee. Thus, an upward force of at least 200 lb is required to raise the element seat from the lifting tee to a point where it can be rotated and delatched from the test element.

The element fits into a standard canister, and after irradiation can be transferred to the spent fuel storage pit in the same manner as a standard element.

In the unlikely event of a failed proof test element, a design arrangement and study layout of a failed PTE removal tool was prepared and evaluated and the feasibility of the tool established.

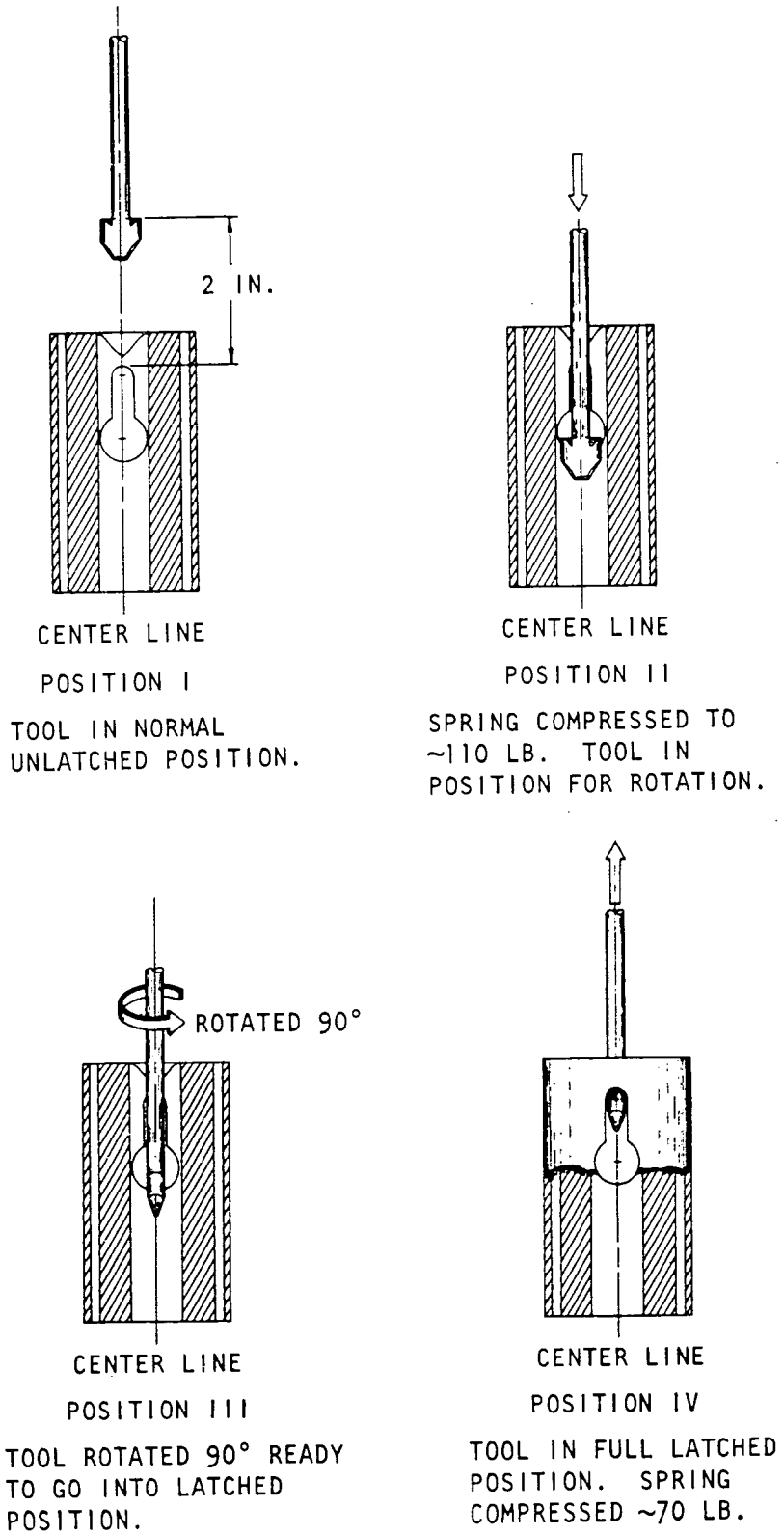

Fig. 3-9. Handling tool latching sequence

4. PTE PERFORMANCE ANALYSIS

4.1. ELEMENT POWER AND FUEL LOADING

The test element will produce 225 kW of thermal energy at core location E10-01 which has an initial local to core average power ratio of 1.61. The power produced in the replaced Peach Bottom element is 145 kW. Thus, the power produced in the test element is 1.55 times greater than in the replaced element and 1.61 times greater than in an average element. The average linear heat rating for the test element is 220.0 W/in. With an axial peaking factor of 1.31, the element maximum linear heat rating is 288.0 W/in.

The as-built fuel loading in the test element is 450.18 g of fully enriched uranium (93.15% U-235) and 2153.41 g of thorium. This compares to 312 g of enriched uranium and 1563 g of thorium in the typical core-1 Peach Bottom element and 250 g of enriched uranium and 1374 g of thorium in the typical core-2 Peach Bottom element. The Th:U ratio in the test element is 4.78:1 as compared to 5:1 in the regular core-1 elements and 5.5:1 in the regular core-2 elements. The test elements do not contain any rhodium or boron poisons as do some of the regular fuel elements. The higher fuel loadings in the test element are required to meet the test element objectives as stated in Section 1.

The tolerance on the uranium loading in the test element was as follows. Ideally, all the fuel rods have a constant value of 0.45 g uranium per in. However, certain variations are expected during fabrication of the fuel rods and therefore uranium loading tolerances were set for each fuel zone of the test element. The nominal uranium loading for fuel zones one through four is 67.1, 157.4, 157.4, and 65.1 g, respectively. The uranium loading tolerance of each fuel zone was set at ±5% of the nominal design value. The uranium loading for the assembled test element was 447 g ±3%. The thorium loading

was allowed to vary in order to accommodate variations in fuel particle and fuel rod parameters during fabrication. The nominal thorium loading for the element was set at 1660 g. It was expected that this value would not vary more than ±15% in the element. In PTE-2 the design value was, however, exceeded by 29.7%.

The effect of the greater thorium loading on the performance of PTE-2 was quantitatively evaluated. During irradiation for the planned 300 equivalent full-power days (EFPD), the extra thorium will have very little effect on the power density. The maximum increase in the predicted end-of-irradiation test element power density due to the extra thorium is about 2% after 300 days of irradiation. As previously stated the total element power decreases during the irradiation period. The extra Pa-233 produced in the test element due to the higher thorium loading, if fully decayed to U-233, could only increase the subsequent startup power density by a maximum of 0.3%. The equilibrium steady-state concentration of Pa-233 in the core is obtained after about 300 full-power days. The concentration after about 150 full-power days is about 97% of the equilibrium value. Therefore, if the plant is shut down for an extended period of time after approximately 150 days of operation, the increase in U-233 concentration from decayed Pa-233 could only increase the power density of the test element a maximum of 0.3% when the plant is brought back to power. This is an insignificant change.

The additional conversion of thorium to U-233 from the extra thorium will not cause the test element power to increase with time. The fissile uranium burnup in the element will cause the power to decrease a minimum of 3% over 300 days. Expected control rod motions should produce an additional 3% to 6% decrease in the test element power over 300 days of full-power operation. Therefore, the expected limit on the power decrease of the test element over a period of 300 days is from 1% to 7%.

4.2. NUCLEAR ANALYSIS

The effect on overall core reactivity of inserting the test element into the Peach Bottom core is negligible. The calculated core reactivity

increase due to the higher fuel loadings is 0.00012 $\Delta\rho$ per element. Two-dimensional, x-y geometry diffusion calculations show that no measurable tilting of core flux or power is produced with the test elements in the core.

The axial fission power profile for the test element is very similar to the Peach Bottom element except for the very localized power peaks at the unfueled joints between the fuel zones. The axial power shape for the test elements is shown in Fig. 4-1. The test element has a negligible effect on the fission power generation in the adjacent Peach Bottom elements. The fission power generated by the test element increases almost linearly with the additional fuel loading. The power produced by the test element, compared to adjacent elements, is 1.55 times greater for the heavier U-235 fuel loading of 1.61 times the average-power standard element loading.

Burnup calculations show that the conversion ratio in the test element is not significantly different than a Peach Bottom element, even for the lower Th:U ratio, and the element power production over a 300-day irradiation period will be essentially constant. The conversion of thorium to fissionable U-233 during the irradiation period is very low. Thus, the fission power produced in the test element is relatively insensitive to any variation in the thorium loading in the test element during the 300-day irradiation period. If one of the test elements is left in the reactor for an extended period of time, its fission power will decrease with continued irradiation because the lower thorium loading will not produce sufficient U-233 to replace the consumed U-235.

During the 300-day full-power irradiation period, the test element will receive an average fast-neutron dose (>0.18 MeV) of 1.15×10^{21} nvt and a peak dose of 1.50×10^{21} nvt. For an 800-day, full-power irradiation period, the test element will receive a fast-neutron dose of 3.07×10^{21} nvt and a peak dose of 4.00×10^{21} nvt. This compares to a maximum dose of about 4.5×10^{21} nvt for the regular elements at the end of 3 yr of full-power operation.

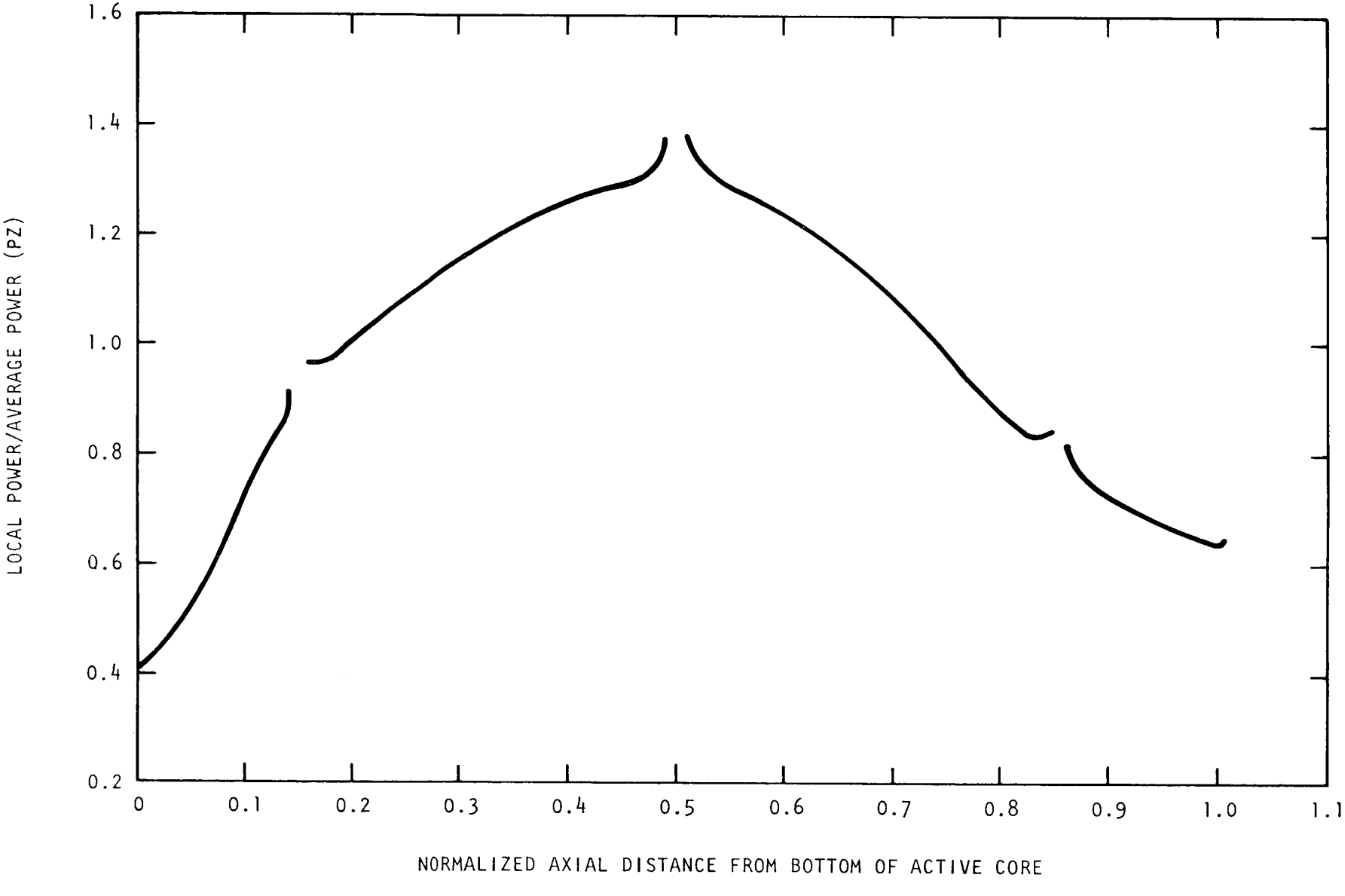

Fig. 4-1. Test element normalized axial power distribution

The test elements contain no boron or rhodium as do some of the regular elements. Detailed nuclear analyses have shown that the absence of boron and rhodium in the test elements will have no measurable change on the total core reactivity or the core negative temperature coefficient.

4.3. THERMAL AND COOLANT FLOW ANALYSIS

A detailed thermal and flow analysis of the test element shows that the temperatures of the fuel, graphite, and coolant are less than the calculated maximum temperatures for the hottest element in the Peach Bottom reactor. The maximum coolant exit temperature from the modified tricuspidal channels around the element is about 135°F greater than in the Peach Bottom reactor. However, this increase in local coolant exit temperature does not produce excessive fuel or graphite temperatures. Also, the small streams leaving these channels will be well mixed with other coolant a short distance above the core and before flowing over any internal reactor component structures or into ducts.

The following reactor operating conditions were used for the thermal analysis of the second test element:

Reactor vessel inlet temperature	598°F
Average core inlet temperature	616°F
Average core outlet temperature	1327°F
Vessel outlet temperature	1300°F
Core pressure drop	2.76 psi
System pressure	350 psia

The actual plant operating conditions during irradiation of the test elements may vary some nominal amount from the assumed design conditions. Because the calculated maximum temperatures are conservative and represent an upper limit, variations in plant operating conditions will have no significant effect on the performance of the test element.

The maximum calculated fuel rod centerline temperature is 2270°F and occurs in the lower end of fuel zone three in the inner row of fuel holes. This compares to a maximum fuel compact temperature of 2428°F in the hottest regular fuel element (Ref. 1). The 2270°F fuel temperature is based on a conservative thermal conductivity value for the fuel rod of 1.2 Btu/hr-ft-°F. This is the measured value for an unirradiated bed of loose, coated fuel particles. The unirradiated thermal conductivity for a bonded rod is around 4.0 Btu/hr-ft-°F. The loose-bed value was used for the calculations to account conservatively for any possible fast-neutron irradiation effects on the bonded-bed conductivity during operation. If the unirradiated bonded-rod value is retained during irradiation, the peak fuel temperatures will be significantly lower than the calculated value given above. A conductivity value of 16 Btu/hr-ft-°F was used for the structural graphite. This is the expected conductivity value of needle-coke graphite after significant fast-neutron irradiation. A conductivity value of 15 Btu/hr-ft-°F was used for the graphite of the adjacent fuel elements.

The axial distribution of temperatures in the test element is shown in Figs. 4-2 and 4-3. The outer ring of fuel rods runs slightly cooler than the inner ring, as seen in Fig. 4-2. The maximum fuel rod ΔT is approximately 640°F based on the conservative loose-bed thermal conductivity value. This would reduce to approximately 235°F for the unirradiated bonded-rod conductivity value. The graphite ΔT values between the fuel and adjacent coolant holes are modest, with a value of about 200°F. Figure 4-4 shows the radial temperature profiles in the element at the plane of maximum fuel temperature. The calculated overall maximum graphite ΔT across the graphite cross section is 280°F. A maximum graphite temperature of 1740°F occurs at the top of the fuel element. This compares to a maximum sleeve temperature of about 1950°F predicted for the hottest regular fuel element.

The above listed fuel and graphite temperatures are based on conservative conductivity values that may occur after a significant ($>1 \times 10^{21}$ nvt) fast-neutron dose. The test element will not accumulate this great a fast-neutron dose until near the end of 300 days of irradiation. Beyond 300 days, thermal conductivity changes are small with further accumulation of fast-neutron exposure.

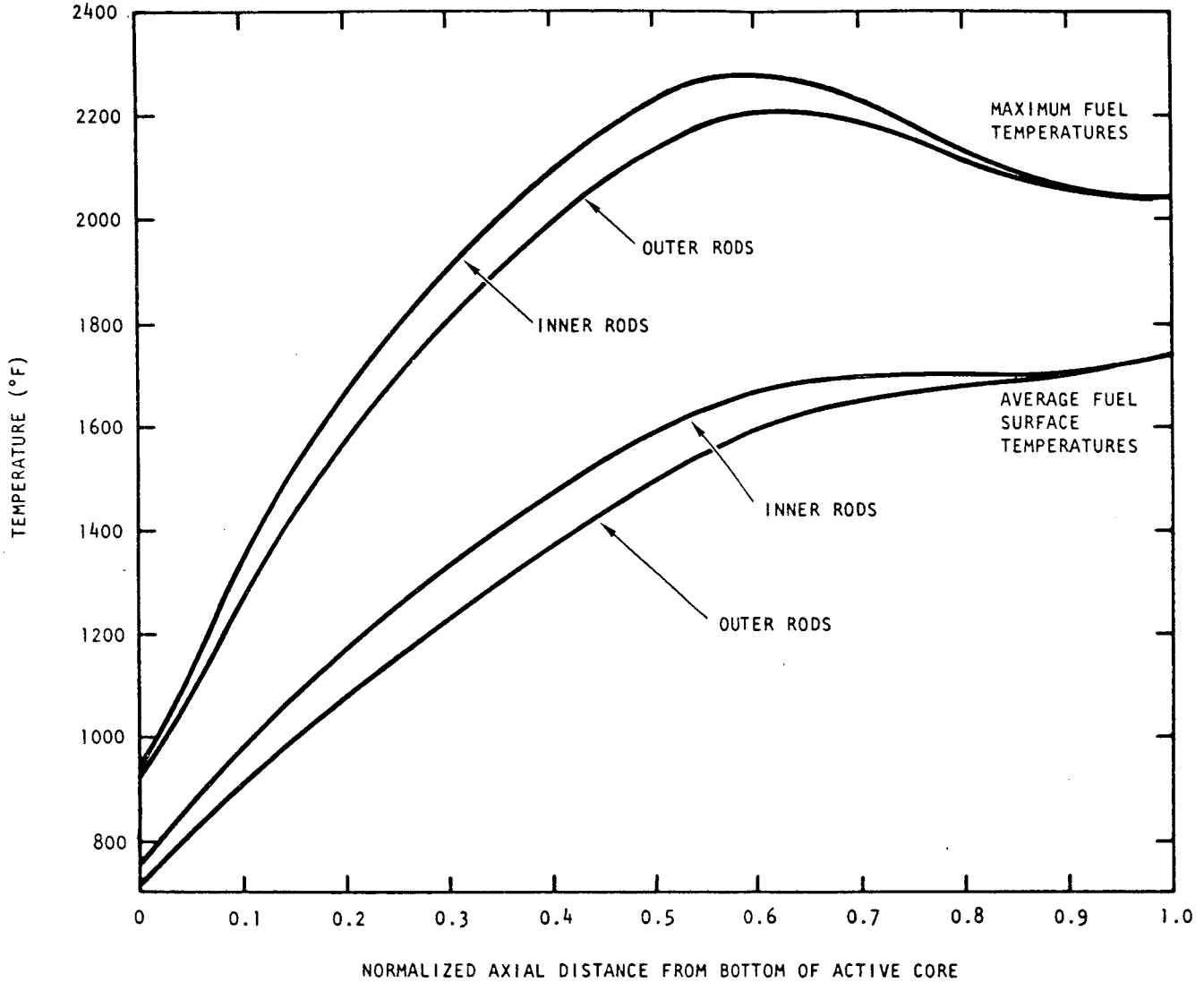

Fig. 4-2. Fuel rod axial temperature profiles

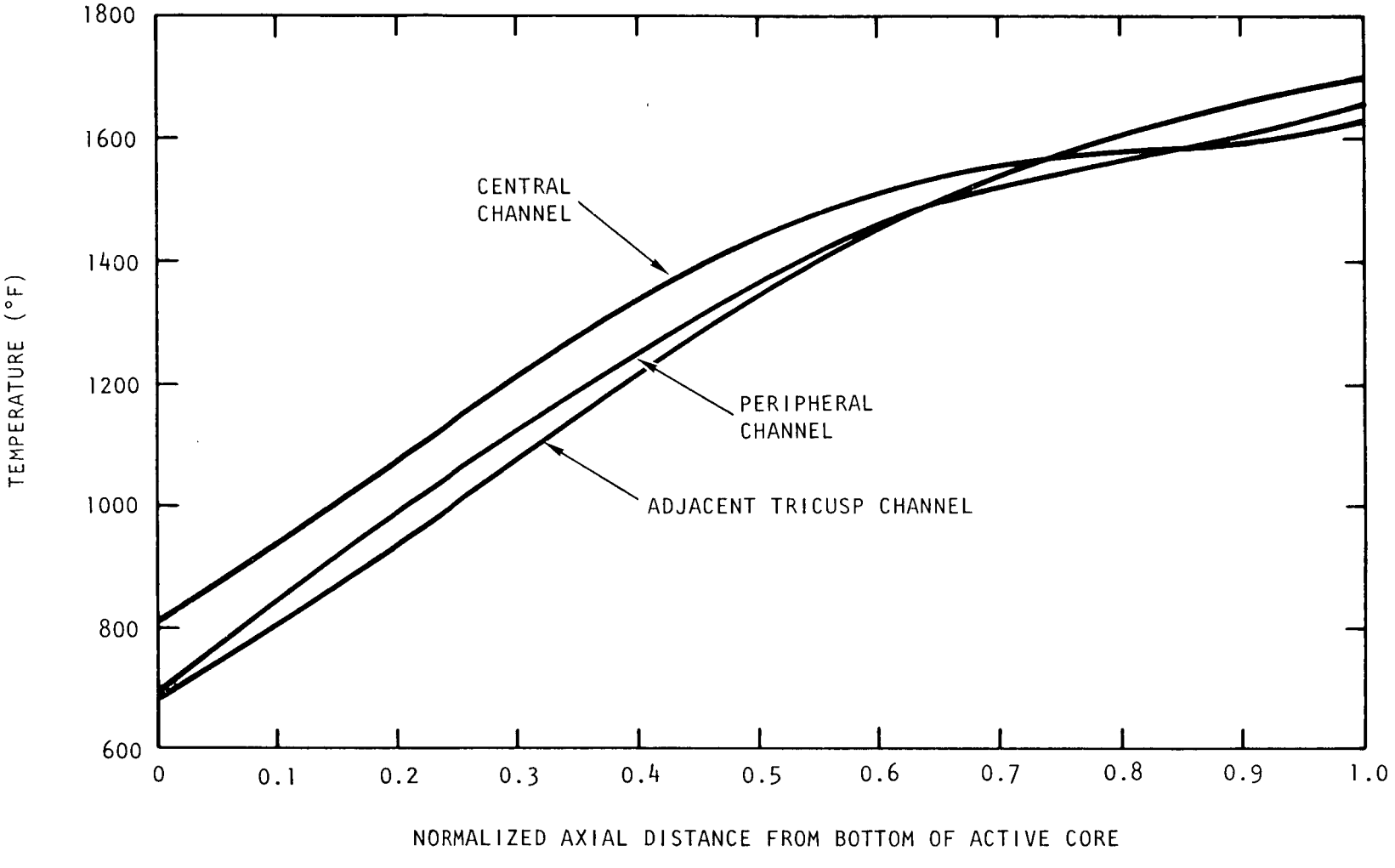

Fig. 4-3. Graphite coolant surface axial temperature profile

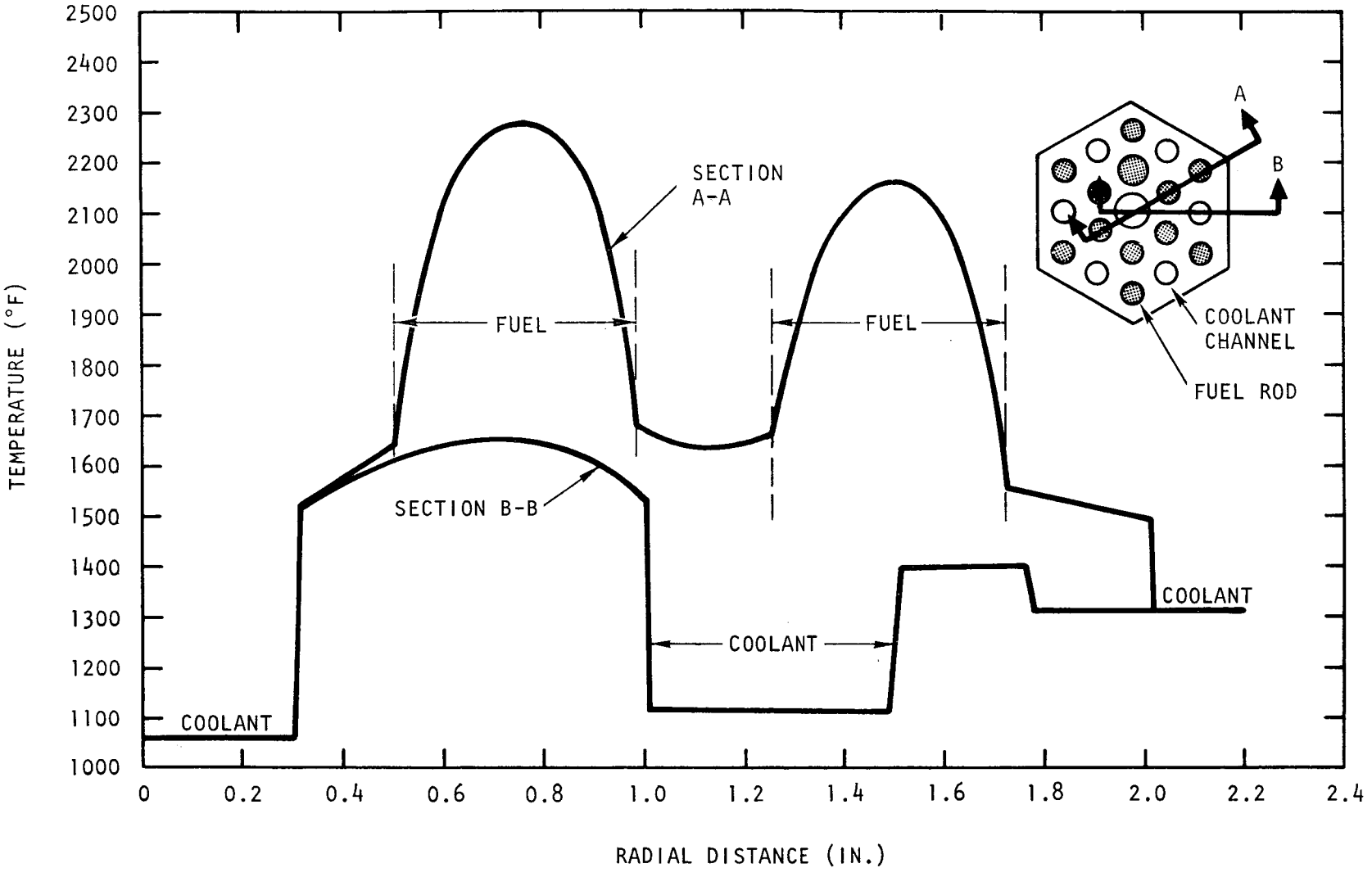

Fig. 4-4. Radial temperature profile at plane of maximum fuel temperature

The calculated coolant flow rates for the center and outer cylindrical and modified tricuspidal coolant changes are 49.5, 139, and 149 lb/hr, respectively. The axial profiles of coolant temperatures in the three types of coolant channels are shown in Fig. 4-5. The hottest coolant temperatures occur in the modified tricuspidal channels with an exit temperature of 1650°F. The 0.454-in.-diameter coolant channel has an exit temperature of 1440°F and the center channel an exit temperature of 1330°F. The maximum exit gas temperature of 1650°F is about 50°F less than the maximum calculated hot-channel exit coolant temperature in the Peach Bottom core (Ref. 1).

For the Peach Bottom elements next to the test element, the tricuspidal coolant channels on the sides away from the test element run cooler than the modified tricuspidal channels. Because of the difference in the coolant temperatures, the temperature of the graphite sleeve in the adjacent Peach Bottom element varies around its circumference. The sleeve side next to the test element is the hottest side, and can be a maximum of 250°F above the cooler side. This maximum occurs at the top of the active core. The temperature difference produces a thermal bending stress in the sleeve of approximately 330 psi and causes the axial midspan of the adjacent elements to bow toward the test element. This bending stress is quite moderate and presents no problems.

The maximum fuel compact temperature in the adjacent elements is increased about 120°F because of the higher coolant temperature in the channels surrounding the test element. The maximum fuel temperature is 2150°F, less than the core maximum of 2428°F.

The maximum steady-state operating temperature of the metal engagement block in the lower reflector is calculated to be 690°F.

4.4. STRESS ANALYSIS

Analysis of the stresses in the graphite structure was made for the test element assuming total irradiation times of both 300 and 800 EFPD.

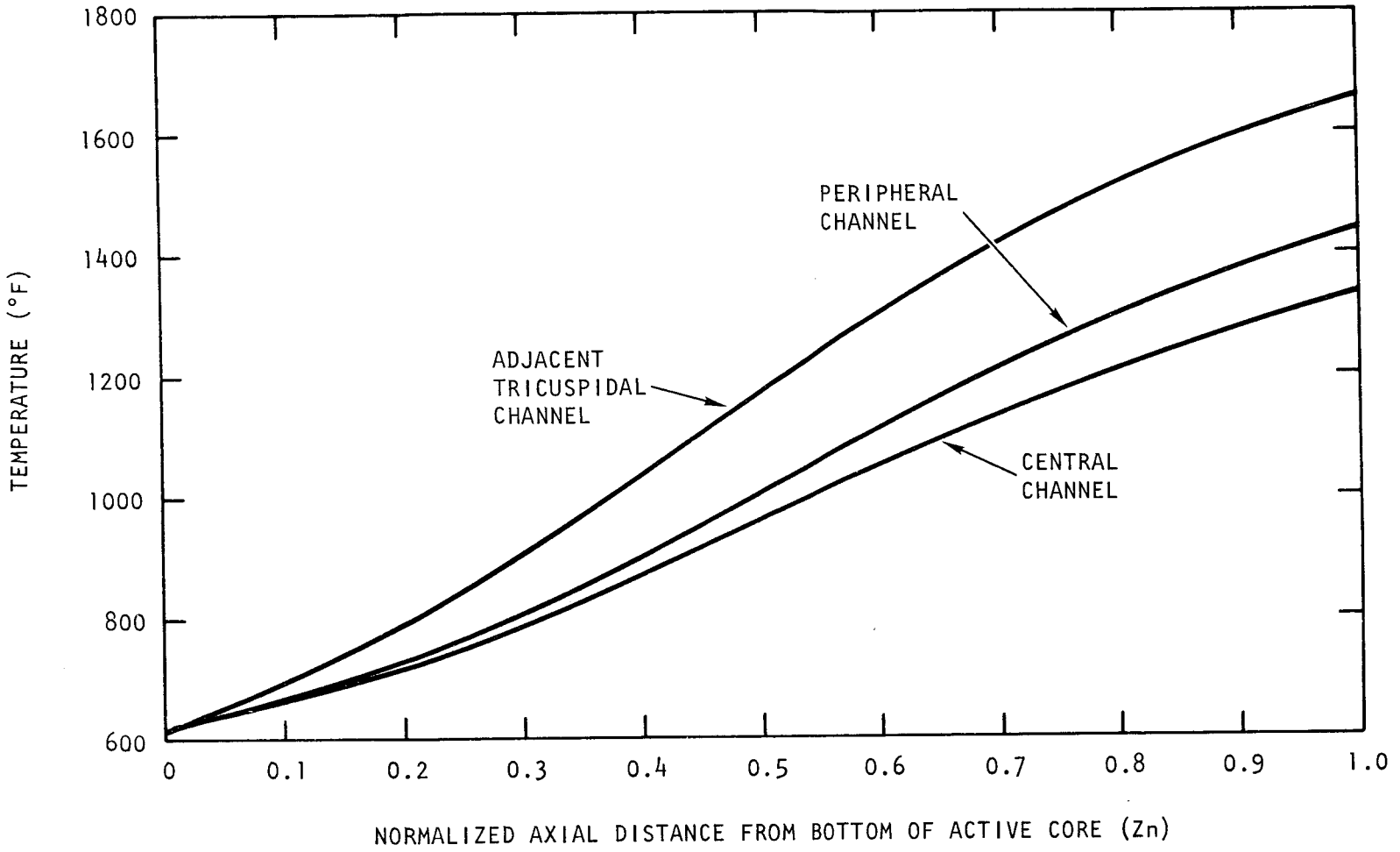

Fig. 4-5. Coolant channel axial temperature profiles

Stresses in the graphite structure are caused by thermal gradients and differential graphite contraction due to fast-neutron irradiation. The maximum stresses occur near the bottom of fuel zone three, which has the largest temperature differences across the graphite structure and the maximum fast-neutron dose. The graphite properties listed in Table 3-1 were used for this analysis.

The major axial stresses are produced by temperature-dependent fast-neutron irradiation contraction of the structural graphite. The amount of contraction will vary according to the local temperature and will result in tensile stresses in some areas and compressive stresses in other areas.

The axial stresses increase with irradiation and reach a maximum at the end of the 800-day irradiation period. The maximum axial tensile stress under operating conditions is 780 psi and occurs adjacent to the inner ring of fuel holes. For 300 days this stress, under the same conditions, is 540 psi. The maximum axial compressive stresses under operating conditions are 350 psi and occur next to the outer tricuspidal coolant surface. When the reactor is shut down, the local elastic thermal strains add to the local residual elastic contraction strains and act to increase the residual stress. At shutdown the maximum tensile stresses are 1080 psi for 800 EFPD and 900 psi for 300 EFPD, and the compressive stresses are 620 psi for 800 EFPD and 1100 psi for 300 EFPD. These stresses occur in the GLCC H-327 graphite, which has a nominal tensile strength of 1600 psi. The maximum axial stresses in the Type II graphite used in fuel zone two are less than the calculated maximum stresses in the Type I graphite because of the lower thermal power and accumulated fast-neutron dose for zone two. The stresses were calculated with conservative unidirectional models and represent an upper limit for the expected stresses.

The most significant stresses in the radial direction are thermal stresses since fast-neutron contraction rates are lower in this direction. The maximum thermal stresses are 460 psi compression for 800 EFPD and 410 psi compression

for 300 EFPD next to the inner fuel hole, and 180 psi tension for 800 EFPD and 370 psi tension for 300 EFPD next to the outer corner of the hexagon.

The test elements will be located in regions of uniform thermal and fast-flux distributions. No significant bowing deflections or stresses are predicted for the test elements.

4.5. FISSION-PRODUCT CONTROL

The retention of fission products within the test element is controlled primarily by the highly retentive coating on each individual fuel particle. The adsorption and retention properties of the carbon bonding matrix and the graphite are an effective secondary control system, especially for the metallic fission-product species. The highly retentive coatings on the fuel particles are of two types. One type, which includes the majority of the particles, is a high-density isotropic pyrolytic carbon coating. The other type is similar, but also includes a coating of high-density silicon carbide.

Because of the highly retentive characteristics of the fuel particles, the element is not purged and does not require low-permeability graphite.

Irradiation performance of retentive-type coated fuel particles (Refs. 2,3) and the investigation of fission-product transport and retention (Ref. 4) in fuel element graphite have demonstrated the retention characteristics of this type of fuel element for both gaseous and nongaseous fission-product species. Under the General Atomic In-Pile Loop (GAIL) irradiation program, two elements of the Peach Bottom type, GAIL III-A and GAIL III-B (Ref. 5), and an advanced element, GAIL IV (Refs. 6,7), were irradiated for long periods. The GAIL III-B element was representative of the standard purged fuel element design for the Peach Bottom reactor. Fuel, graphite, and helium temperatures were similar to the Peach Bottom design values for the GAIL III-B and GAIL IV elements. Heat flux and power density, comparable for GAIL III-B and GAIL-IV elements, were about twice the corresponding

Peach Bottom design values. The GAIL IV element contained retentive-type fuel particles and was irradiated part of the time without purge flow. The GAIL IV operation was for a total of 9700 hr at full power, producing a total of 670 MWh thermal energy.

As part of the Gulf General Atomic fuel development irradiation program, coated particles of the same general types as those to be used in the test element have been irradiated at high temperature to high burnup. Both types of particles have demonstrated excellent integrity to high burnup at temperatures comparable to the maximum fuel temperatures in the test element (Refs. 8-11).

The calculated gaseous fission-product releases from the test elements are listed in Table 4-1. Included were all isotopes with fission yields greater than 0.1% and with half-lives greater than one minute and less than 10^4 yr. The important short-lived noble gases, 33s Kr-90, 10s Kr-91, 41s Xe-139, and 16s Xe-140, have also been included. The fission-product release is calculated using the measured steady-state release fractions from the GAIL IV irradiation experiment. The calculated contribution of gaseous fission products to the primary reactor circuit from each test element being irradiated is less than 0.25% of the calculated beginning-of-life (BOL) (Ref. 12) gaseous activity in the primary reactor circuit. The gaseous fission-product releases from the test elements are therefore well within the established limits for safe operation of the plant. Nongaseous metallic fission products will be retained within the test element graphite to the same high degree as the standard Peach Bottom fuel elements.

In addition, gaseous fission-product release from the second test element was calculated using measured in-pile fuel rod release data. Release measurements were made of one specimen fuel rod taken from each production batch. The rods were irradiated in the TRIGA reactor at a temperature of 1000°C for the gaseous fission-product release measurement.

The contribution of gaseous fission-product activity from PTE-2 to the Peach Bottom reactor circuit, as calculated using as-built measurements of fuel rod batches used in the element, is summarized in Table 4-2 for the significant gaseous fission-product isotopes. The estimated total activity contribution from the second test element at full power is calculated to be <0.1 Ci as indicated by the Cary electrometer.

TABLE 4-1
COMPARISON OF CALCULATED GASEOUS FISSION-PRODUCT RELEASE

	Calculated Coolant Gaseous Fission-Product Activity from One PTE (Ci)	BOL Calculated Coolant Gaseous Activity from One Peach Bottom Fuel Element (12) (Ci)	Reactor Total Coolant Gaseous Activity (12) Calculated	
			BOL (Ci)	Design (Ci)
Total	0.21	0.14	108.6	4224.6
Kr and Xe	0.17	0.046	36.7	615.6
I-131	0.00004	0.00009	0.07	3.4

TABLE 4-2
FULL-POWER PRIMARY COOLANT GASEOUS ACTIVITY
CONTRIBUTION FROM PTE-2

Isotope	Activity (Ci)
Kr 85m	0.002
Kr 87	0.006
Kr 88	0.005
Kr 89	0.024
Xe 133	0.0003
Xe 135	0.004
Xe 138	0.021
I 131	2×10^{-6}
Total:	0.062

5. COATED FUEL PARTICLES

5.1. REQUIREMENTS AND TYPES OF PARTICLES

The fuel particles used in the test element are of TRISO design, and are of two general types: a fissile particle, containing a mixture of thorium and uranium carbide in the kernel in a Th:U ratio of 0.58:1, and a fertile particle, containing only thorium carbide in the kernel. The nominal sizes are detailed in Table 5-1. All particles were fabricated by the Fuel Operations Department (FOD).

The particles were fabricated to the particle specification listed in Section 11. Forty-two individual batches of material were evaluated for use in the element; twenty-three of these were included in the final assembly.

5.2. BATCH IDENTIFICATION NUMBERS

The 23 individual batches of fuel particles were identified during their fabrication with an FOD Batch Identity, which is listed in Table 5-2. Batches were then assigned a Data Retrieval Number (also listed in Table 5-2) for subsequent evaluation and rod fabrication. Table 5-3 lists the blending program that was used, and the batches that were used for fuel rod fabrication.

5.3. CHARACTERIZATION OF FUEL CORES

The coated particles of fissile material were made using three batches of substrate material. All kernels were screened to be in the size range of 150 to 250 micrometers in diameter. The coated particles of fertile material were made using six batches of substrate material, which were screened to be 300 to 500 micrometers in diameter. Table 5-4 contains relevant data on the fuel kernel substrate material.

TABLE 5-1
NOMINAL DIMENSIONS OF COATED FUEL PARTICLES

	Fissile	Fertile
Kernel diameter, μm	150-250	300-500
Buffer thickness, μm	50	50
Inner Iso thickness, μm	20	20
Silicon carbide thickness, μm	20	20
Outer Iso thickness, μm	30	40
Total coating thickness, μm	120	130

TABLE 5-2
BATCHES USED IN FUEL TEST ELEMENT

FOD Batch Identity	Number for Data Retrieval
1. T-103 AL - High Density	4000-711
2. T-103 CL - High Density	4000-713
3. T-105 BH	4000-715
4. ET-109 CL - Low Density	4000-745
5. T-161 BL - High Density	4000-720
6. T-169 AH	4000-725
7. ET-170 A(2)H	4000-729
8. ET-170 BH	4000-730
9. ET-170 CL - High Density	4000-731
10. ET-171 BL - High Density	4000-732
11. ET-171 CL - Low Density	4000-744
12. T-176 AL - Low Density	4000-741
13. T-176 BL - High Density	4000-733
14. T-176 CH	4000-734
15. T-212 BL - Low Density	4000-739
16. T-213 AL - Low Density	4000-737
17. T-213 BL - Low Density	4000-738
18. T-229 BL - Low Density	4000-740
19. T-236 BL - High Density	4000-752
20. T-237 BL - High Density	4000-742
21. T-253 BL - Low Density	4000-750
22. T-253 CL - Low Density	4000-751
23. ET-255 AL - Low Density	4000-747

NOTE: An "ET" prefix designates fissile material and a "T" prefix indicates fertile. An "H" suffix designates HTI material and an "L" suffix designates LTI material.

TABLE 5-3
COATED PARTICLE BATCHES USED IN FUEL ROD FABRICATION

	Batches Used for Fuel Rod Fabrication	Individual Batches From Which a Blended Batch Was Made
Fissile HTI	4000-701	
		4000-729
		4000-730
Fertile HTI	4000-702	
		4000-715
		4000-725
	4000-734	
Fissile LTI - higher density	4000-703	
		4000-731
		4000-732
Fertile LTI - higher density	4000-704	
		4000-711
		4000-713
		4000-720
	4000-733	
	4000-752	
	4000-742	
Fissile LTI - lower density	4000-745	
	4000-744	
	4000-747	
Fertile LTI - lower density	4000-706	
		4000-738
		4000-740
		4000-741
	4000-707	
		4000-739
		4000-750
		4000-751

TABLE 5-4
FISSILE AND FERTILE SUBSTRATE MATERIAL

Type	Batch Number	Th/U	Carbon (%)	Density (g/cm^3)	Average Diameter (μm)
Fertile	XTS-3548	-	10.39	8.72	393
	XTS-3564	-	10.53	8.67	390
	XTS-3596	-	10.60	8.51	387
	XTS-3602	-	10.50	8.64	378
	XTS 3543 3545	-	10.37	8.63	392
	XTS-3543	-	10.37	8.58	400
Fissile	PT-3003 ETS	0.585	9.75	9.82	194
	PT-3004 ETS	0.587	9.49	10.10	202
	PT-3005 ETS	0.590	9.74	10.06	198

5.4. CHARACTERIZATION OF FUEL COATINGS

The coatings are of the TRISO design: buffer, PyC, SiC, and PyC. The measurements made on the various coatings are listed in Table 5-5. In the table, the term high density refers to the fourteen batches with an outer isotropic PyC density of between 1.90 and 1.98 g/cm^3. The term low density refers to the nine batches with an outer isotropic PyC density of between 1.80 and 1.90 g/cm^3.

5.5. CHEMICAL COMPOSITION

A chemical analysis of the 23 coated-particle batches used is included in Table 5-6. It can be seen that for fissile particles, the heavy metal content is 34 wt %, the SiC is 22 wt %, and the free carbon is 44 wt %. For fertile particles, the corresponding values are 50 wt %, 13 wt %, and 37 wt %.

5.6. DEFECTIVE FUEL PARTICLE EVALUATION

Each of the 23 batches used in the element was evaluated by a radiographic technique for defective particles. For each fissile batch, 7000 particles were examined; for each fertile batch, 3500 particles were examined. Various classifications were used for the evaluation in an attempt to develop a standard format for reporting the data. Table 5-7 contains a recent interpretation of the data. The category of serious defects includes particles with any one coating layer missing. Also included is a defect of a cracked SiC layer, which would allow the escape of fission-product gases. Other defects seen were of a minor nature and are not tabulated; these included kernel diffusion and coated debris.

5.7. FISSION-PRODUCT-RELEASE EVALUATIONS OF FUEL PARTICLES

Fission-product-release measurements on material for Fort St. Vrain Proof Test Element No. 2 were a part of the fuel evaluation and quality

TABLE 5-5
COATING MEASUREMENTS ON BATCHES USED IN TEST ELEMENT

Data Retrieval Number (4000-)	Batch Number	Preseal Thickness (μm)	Buffer Thickness (μm)	Buffer Density (g/cm^3)	Seal No. Thickness (μm)	Inner Isotropic Thickness (μm)	SiC Thickness (μm)	SiC Density (g/cm^3)	Outer Isotropic Thickness (μm)	Outer Isotropic Density (g/cm^3)	Isotropic Coating Type	BAF	Total Coating Thickness (μm)
-711	T-103-A	2	41	1.05	1	18	20	3.19	45	1.90	LTI	1.01	124
-713	T-103C	2	41	1.05	1	18	20	3.16	44	1.91	LTI	1.10	121
-715	T-105B	5	39	1.16	4	20	21	3.17	41	1.94	HTI	1.04	127
-720	T-161-B	5	38	1.13	1	16	25	3.20	39	1.92	LTI	1.07	123
-725	T-169-A	3	39	1.14	1	23	19	3.19	46	1.92	HTI	1.08	128
-729	ET-170-A-2	2	42	1.16	1	16	21	3.19	33	1.93	HTI	1.00	112
-730	ET-170-B	2	42	1.16	1	16	20	3.23	33	1.92	HTI	1.02	112
-731	ET-170-C	2	42	1.18	1	16	20	3.21	32	1.97	LTI	1.10	108
-732	ET-171-B	1	43	1.31	1	15	20	3.20	32	1.97	LTI	1.11	107
-733	T-176-B	2	38	1.12	5	20	19	3.17	36	1.98	LTI	1.03	122
-734	T-176-C	2	38	1.12	5	20	19	3.18	44	1.91	HTI	1.07	128
-737	T-213-A	2	44	1.12	1	17	20	3.18	44	1.91	LTI	--	119
-742	T-237-B	3	46	1.05	6	22	19	3.21	37	1.97	LTI	1.12	128
-739	T-212-B	3	40	1.03	1	20	19	3.22	41	1.87	LTI	1.08	115
-738	T-213-B	2	44	1.12	1	17	20	3.18	45	1.87	LTI	1.10	124
-740	T-229-B	2	47	1.12	3	19	21	3.20	43	1.81	LTI	1.09	126
-741	T-176-A	2	38	1.12	5	20	18	3.20	45	1.90	LTI	1.03	132
-744	ET-171-C	1	43	1.31	1	15	21	3.17	34	1.88	LTI	1.13	116
-745	ET-109-C	5	38	1.20	4	25	20	3.21	27	1.83	LTI	1.08	112
-747	ET-255-A	1	45	1.03	1	17	21	3.23	29	1.87	LTI	1.10	113
-750	T-253-B	1	44	1.00	3	21	23	3.21	34	1.87	LTI	1.05	120
-751	T-253-C	1	44	1.00	3	21	21	3.21	36	1.84	LTI	1.03	118
-752	T-236-B	2	41	1.13	1	24	17	3.20	37	1.93	LTI	1.10	119
	Total	53	957	25.81	52	436	464	73.51		43.82		23.49	
(all)	Number	23	23	23	23	23	23	23		23		22	
	Average	2.30	41.61	1.12	2.26	18.96	20.17	3.20		1.91		1.07	
(fissile)	Total								220				780
	Number								7				7
	Average								31.43				111.43
(fertile)	Total								657				1974
	Number								16				16
	Average								41.06				123.38
(nigh density)	Total									27.08			
	Number									14			
	Average									1.93			
(low density)	Total									16.74			
	Number									9			
	Average									1.86			

TABLE 5-6
CHEMICAL COMPOSITION OF BATCHES USED IN TEST ELEMENT

Data Retrieval Number (4000-)	Batch No.	Chemical Composition				
		% U	% Th	% SiC	% C	Closure (%)
-711	T-103-A	--	52.27	11.70	36.13	100.10
-713	T-103-C	--	52.81	11.25	35.57	99.63
-715	T-105-B	--	49.77	12.20	38.33	100.30
-720	T-161-B	--	49.86	13.97	35.92	99.75
-725	T-169-A	--	49.26	12.09	39.37	100.72
-729	ET-170-A-2	21.74	12.80	21.30	44.80	100.64
-730	ET-170-B	22.48	12.90	21.17	43.77	100.32
-731	ET-170-C	21.71	12.58	20.47	45.79	100.52
-732	ET-171-B	22.79	13.27	21.64	43.50	101.20
-733	T-176-B	--	51.45	12.09	35.43	98.97
-734	T-176-C	--	51.13	11.35	38.06	100.54
-737	T-213-A	--	51.30	11.20	37.54	100.04
-742	T-237-B	--	48.97	12.97	38.07	100.01
-739	T-212-B	--	50.55	12.74	36.11	99.40
-738	T-213-B	--	48.82	15.29	36.07	100.18
-740	T-229-B	--	48.51	13.32	37.95	99.78
-741	T-176-A	--	49.75	12.45	37.07	99.27
-744	ET-171-C	21.17	12.63	20.86	45.80	100.46
-745	ET-109-C	21.19	11.99	22.96	43.92	100.06
-747	ET-255-A	20.54	11.84	23.68	44.29	100.35
-750	T-253-B	--	49.75	14.70	35.75	100.20
-751	T-253-C	--	51.16	13.73	35.47	100.36
-752	T-236-B	--	49.60	13.61	36.40	99.61
Fissile	Total	151.62	88.01	152.08	311.87	
	Number	7	7	7	7	
	Average	21.66	12.57	21.73	44.55	100.51
Fertile	Total		804.96	204.66	589.24	
	Number		16	16	16	
	Average		50.31	12.79	36.83	99.93

TABLE 5-7
PERCENTAGE OF PTE-2 FUEL PARTICLE
BATCHES WITH SERIOUS DEFECTS

Type of Particle	Number of Batches	Number of Batches With Listed Percentage of Serious Defects		
		0.2	0.1	<0.05
Fissile	7	--	--	7
Fertile	16	1	3	12

Note: The category of serious defects includes particles with any one of the four coating layers missing.

control program. Metallic fission-product-release annealing experiments were carried out on samples of candidate batches of fuel material, and fission gas release experiments were carried out on specimens of fuel rods prepared along with each production lot of rods. The metallic fission-product-release measurements on fuel particles are reported in this section, and the gas release experiments on fuel rods are reported in Section 6.3.4.

The purpose of the metallic fission-product-release experiments (also called postactivation release annealing experiments) is to determine the relative quality of the fuel particle lot by measurement of its metallic fission-product release from all sources, without determining the release from each individual source.

The release of fission products from TRISO-coated fuel particles under reactor conditions arises from three sources:

1. The release of fission products born in the fission of uranium contamination in the outer pyrolytic carbon coating. For the metallic fission products strontium and barium, the steady-state fractional release from this source is assumed to be unity since the pyrolytic carbon does not constitute a barrier to the metals.

2. The release of fission products born in defective particles. For the metallic fission products this includes not only those particles with broken or incomplete coatings, but also those with broken, thin, or totally absent silicon carbide layers. However, since the kernel of such particles still retains the metallic elements to some extent, it is assumed that the steady-state fractional release from this source is about 0.5. (This is probably a minimum value under steady-state conditions.)

3. The intrinsic release of fission products from intact high-quality particles. The steady-state fractional release from this source is thought to be very low (perhaps $<10^{-7}$).

Postactivation fission-product-release measurements detect metallic nuclides released from all of these sources, but cannot discriminate between them without specialized techniques. The measurement is, therefore, a relative screening procedure designed to determine whether lots of manufactured particles meet certain standards of quality without being able to specify why a given lot fails to meet the standards.

The technique of postactivation, fission-product-release annealing measurement has been described previously (Refs. 13, 14), and a detailed presentation of the method and its rationale is in preparation (Ref. 15). In the studies reported herein, the releases of Sr-91 and Xe-135 were measured. The coated-particle specifications for material in this test element (Ref. 16) prescribe a limit for the Sr-91 release only. The release of Xe-135 is reported only as an indication of the level of surface contamination, but is not used as a criterion for rejection or acceptance.

Postactivation annealing experiments for particle evaluation were carried out for 5 hr at 1400°C after activation in the TRIGA reactor at room temperature. The specification (Ref. 16) limits the release of acceptable fissile particles to 5×10^{-4} and acceptable fertile particles to 5×10^{-3} under these conditions. Since the measurement was intended to represent the quality of the particles used in rod fabrication, these limits applied to unleached samples. (Since some samples were inadvertently leached prior to their irradiation, these data are also reported.)

5.7.1. Fissile Particles

Seven lots of fissile particles were used in PTE-2. Two blended batches were prepared from four of these lots. The remaining lots were used individually. No release experiments were carried out on the blended lots. The detailed release data for the fissile particles are given in Table 5-8. The detailed data are then summarized in Table 5-9, where the total fractional release values at 5 hr are given.

TABLE 5-8
FRACTIONAL RELEASE FROM FISSILE TRISO-COATED
FUEL PARTICLES FOR PTE-2 AT 1400°C

Data Retrieval No.	FOD No.	Leached or Unleached	Anneal Time (hr)	Fractional Release	
				Xe^{135}	Sr^{91}
4000-729	ET170(A)	L	Recoil	2.3×10^{-8}	
			1		9.5×10^{-5}
			3		3.5×10^{-4}
			5	6.7×10^{-7}	4.1×10^{-4}
4000-729	ET170(A2)	U	Recoil	1.2×10^{-8}	
			1		1.9×10^{-6}
			3		6.6×10^{-6}
			5	4.8×10^{-8}	1.3×10^{-5}
4000-730	ET170(B)	L	Recoil	5.4×10^{-5}	
			1		4.8×10^{-5}
			3		1.2×10^{-4}
			5	5.0×10^{-6}	1.8×10^{-4}
4000-730	ET170(B)	U	Recoil	4.4×10^{-7}	
			1		7.0×10^{-6}
			3		1.1×10^{-5}
			5	5.6×10^{-7}	1.4×10^{-5}
4000-731	ET170(C)	L	Recoil	1.9×10^{-8}	
			1		1.7×10^{-7}
			3		7.5×10^{-7}
			5	1.8×10^{-7}	1.4×10^{-6}
4000-731	ET170(C)	U	Recoil	2.1×10^{-8}	
			1		9.9×10^{-7}
			3		2.3×10^{-6}
			5	2.4×10^{-8}	6.4×10^{-6}

TABLE 5-8 (Continued)

Data Retrieval No.	FOD No.	Leached or Unleached	Anneal Time (hr)	Fractional Release	
				Xe^{135}	Sr^{91}
4000-732	ET171(B)	L	Recoil	6.3×10^{-9}	
			1		3.9×10^{-7}
			3		1.8×10^{-6}
			5	1.6×10^{-8}	5.7×10^{-6}
4000-732	ET171(B)	U	Recoil	8.3×10^{-8}	
			1		3.4×10^{-6}
			3		1.2×10^{-5}
			5	1.8×10^{-8}	1.9×10^{-5}
4000-744	ET171(C)SL	U	Recoil	2.6×10^{-8}	
			1		1.7×10^{-7}
			3		5.6×10^{-7}
			5	1.2×10^{-8}	1.6×10^{-6}
4000-745	ET109(C)SL	U	Recoil	6.6×10^{-9}	
			1		2.3×10^{-6}
			3		2.8×10^{-6}
			5	2.3×10^{-8}	4.7×10^{-6}
4000-747	ET255PBIL(A)SL	U	Recoil	2.3×10^{-8}	
			1		1.1×10^{-6}
			3		2.2×10^{-6}
			5	1.5×10^{-9}	4.9×10^{-6}

TABLE 5-9
SUMMARY OF FISSION-PRODUCT RELEASE DATA
ON FISSILE PARTICLES USED IN PTE-2

Data Retrieval No.	FOD Batch No.	Coating Type[a]	Fractional Release[b]			
			Xe-135		Sr-91	
			Leached	Unleached	Leached	Unleached
4000-729	ET170A2H	FH	6.7×10^{-7}	4.8×10^{-8}	4.1×10^{-4}	1.3×10^{-5}
4000-730	ET170A2H	FH	5.0×10^{-6}	5.6×10^{-7}	1.8×10^{-4}	1.4×10^{-5}
4000-731	ET170CL	FLHD	1.8×10^{-7}	2.4×10^{-8}	1.4×10^{-6}	6.4×10^{-6}
4000-732	ET171BL	FLHD	1.6×10^{-8}	1.8×10^{-8}	5.7×10^{-6}	1.9×10^{-5}
4000-744	ET171CL	FLLD		1.2×10^{-8}		1.6×10^{-6}
4000-745	ET109CL	FLLD		2.3×10^{-8}		4.7×10^{-6}
4000-747	ET255AL	FLLD		1.5×10^{-9}		4.9×10^{-6}

(a) FH = Fissile particle, HTI coating
FLHD = Fissile particle, LTI high-density coating
FLLD = Fissile particle, LTI low-density coating

(b) Total fractional release in 5 hr at 1400°C

Examination of the data in Tables 5-8 and 5-9 shows that all sample lots of fissile particles easily met the metallic fission-product-release specification. Several lots were 2 to 2-1/2 orders of magnitude below the specification, indicating material of very high quality. If these data are interpreted in terms of the presence of BISO-coated particles or their equivalent in terms of Sr-91 release (5×10^{-2} fraction in 5 hr), then several of the fissile sample lots in PTE-2 have roughly the equivalent of two BISO-coated particles per 10^5 particles.

Four of the fissile sample lots were studies of both leached and unleached particles. Analysis of the data in Table 5-9 shows that in two cases the leached samples had a lower Sr-91 release than the unleached samples by factors of 3 to 5. In the other two cases, the unleached samples exhibited a lower release by factors of approximately 10 and 30. While no firm conclusions concerning the relative amounts of surface contamination on the particles or the effect of leaching can be drawn from these isolated four pieces of datum, the indications are that the statistical variations from sample to sample exert a stronger effect on the measured release than does the surface contamination. Leaching appeared to have little effect on the Xe-135 release.

One rather firm conclusion that can be drawn from the data in Table 5-9 is that fissile particles with high-temperature isotropic (HTI) outer pyrolytic carbon coatings have a higher Sr-91 release than those with low-temperature isotropic (LTI) coatings.

5.7.2. Fertile Particles

Sixteen lots of fertile particles were used in PTE-2. Four blended batches were prepared from 11 of these lots, each of the blended lots representing one of the types of coating parameters used (see Section 5.2). The remaining sample lots were used individually. No release experiments were carried out on the blended lots. The detailed release data for the fertile particles are given in Table 5-10, and the release data at 5 hr are summarized in Table 5-11.

TABLE 5-10
FRACTIONAL RELEASE FROM FERTILE TRISO-COATED
FUEL PARTICLES FOR PTE-2 AT 1400°C

Data Retrieval No.	FOD No.	Leached or Unleached	Anneal Time (hr)	Fractional Release	
				Xe^{135}	Sr^{91}
4000-711	T103PBIL(A)	L	1		2.8×10^{-6}
			3		1.4×10^{-5}
			5	1.5×10^{-6}	2.6×10^{-5}
4000-711	T103PBIL(A)SH	U	1		1.6×10^{-4}
			3		5.1×10^{-4}
			5	2.5×10^{-4}	9.3×10^{-4}
4000-713	T103PBIL(C)SH	L	1		1.5×10^{-5}
			3		3.0×10^{-5}
			5	1.6×10^{-6}	4.8×10^{-5}
			8		4.9×10^{-5}
4000-713	T103PBIL(C)SH	U	1		1.0×10^{-4}
			3		4.1×10^{-4}
			5	N.D.	6.5×10^{-4}
4000-715	T105PBIL(B)SH	L	1		5.1×10^{-4}
			3		1.0×10^{-3}
			5	2.4×10^{-6}	1.5×10^{-3}
4000-715	T105PBIL(B)SH	U	1		1.8×10^{-4}
			3		1.2×10^{-3}
			5	2.8×10^{-4}	1.3×10^{-3}
4000-721	T161(B)SH	L	1		5.3×10^{-4}
			3		2.1×10^{-3}
			5	3.3×10^{-6}	3.6×10^{-3}
4000-721	T161(B)SH	U	1		1.3×10^{-4}
			3		3.2×10^{-4}
			5	4.5×10^{-5}	5.5×10^{-4}

TABLE 5-10 (Continued)

Data Retrieval No.	FOD No.	Leached or Unleached	Anneal Time (hr)	Fractional Release	
				Xe^{135}	Sr^{91}
4000-725	T169(A)SH	L	1		8.8×10^{-4}
			3		2.0×10^{-3}
			5	6.0×10^{-7}	2.9×10^{-3}
4000-725	T169(A)SH	U	1		1.9×10^{-3}
			3		3.7×10^{-3}
			5	3.1×10^{-5}	4.5×10^{-3}
4000-733	T176(B)SL	U	1		2.0×10^{-4}
			3		3.1×10^{-4}
			5	9.2×10^{-4}	8.8×10^{-4}
4000-734	T176(C)SH	U	1		6.7×10^{-4}
			3		6.7×10^{-4}
			5	8.4×10^{-6}	1.1×10^{-3}
4000-737	T213(A)S (No outer PyC layer)	L	1		7.2×10^{-6}
			3		2.4×10^{-5}
			5	2.0×10^{-5}	3.2×10^{-5}
			8		3.7×10^{-5}
4000-737	T213(A)SL	U	1		1.6×10^{-4}
			3		4.8×10^{-4}
			5	5.9×10^{-6}	1.0×10^{-3}
4000-738	T213(B)SL	L	1		2.0×10^{-4}
			3		2.8×10^{-4}
			5	3.3×10^{-6}	3.6×10^{-4}
			8		5.3×10^{-4}
4000-739	T212(B)SL	U	1		1.3×10^{-4}
			3		1.7×10^{-4}
			5	7.7×10^{-7}	5.6×10^{-4}
4000-740	T229(B)SL	L	1		1.4×10^{-4}
			3		1.5×10^{-4}
			5	3.9×10^{-6}	2.5×10^{-4}

TABLE 5-10 (Continued)

Data Retrieval No.	FOD No.	Leached or Unleached	Anneal Time (hr)	Fractional Release	
				Xe^{135}	Sr^{91}
4000-740	T229(B)SL	U	1		1.5×10^{-4}
			3		3.6×10^{-4}
			5	3.8×10^{-5}	5.4×10^{-4}
4000-741	T176(A)SL	L	1		4.8×10^{-4}
			3		6.6×10^{-4}
			5	1.3×10^{-5}	9.3×10^{-4}
4000-741	T176(A)SL	U	1		6.5×10^{-4}
			3		1.4×10^{-3}
			5	7.7×10^{-4}	2.2×10^{-3}
4000-742	T237PBIL(B)SL	U	1		1.1×10^{-4}
			3		2.6×10^{-4}
			5	5.5×10^{-5}	3.2×10^{-4}
4000-750	T253(B)SL	U	1		1.8×10^{-4}
			3		2.7×10^{-4}
			5		4.1×10^{-4}
4000-751	T253(C)SL	U	1		3.6×10^{-4}
			3		8.3×10^{-4}
			5	6.8×10^{-5}	1.2×10^{-3}
4000-752	T253(CL)SL	U	1		3.6×10^{-4}
			3		8.3×10^{-4}
			5	6.8×10^{-5}	1.2×10^{-3}

TABLE 5-11
SUMMARY OF FISSION-PRODUCT RELEASE DATA ON FERTILE PARTICLES USED IN PTE-2

Data Retrieval No.	FOD Batch No.	Coating Type[a]	Fractional Release[b]			
			Xe-135		Sr-91	
			Leached	Unleached	Leached	Unleached
4000-711	T103A	FLHD	1.5×10^{-6}	2.5×10^{-4}	2.6×10^{-5}	9.3×10^{-4}
4000-713	T103C	FLHD	1.6×10^{-6}	--	4.8×10^{-5}	6.5×10^{-4}
4000-715	T105B	FH	2.4×10^{-6}	2.8×10^{-4}	1.5×10^{-3}	1.3×10^{-3}
4000-721	T161B	FLHD	3.3×10^{-6}	4.5×10^{-5}	3.6×10^{-3}	5.5×10^{-4}
4000-725	T169A	FH	6.0×10^{-7}	3.1×10^{-5}	2.9×10^{-3}	4.5×10^{-3}
4000-733	T176BL	FLHD	--	9.2×10^{-4}	--	8.8×10^{-4}
4000-734	T176CH	FH	--	8.4×10^{-6}	--	1.1×10^{-3}
4000-737	T213AL	FLLD	2.0×10^{-5}	5.9×10^{-6}	3.2×10^{-5}	1.0×10^{-3}
4000-738	T213B	FLLD	3.3×10^{-6}	4.4×10^{-5}	3.6×10^{-4}	1.2×10^{-3}
4000-739	T212B	FLLD	--	7.7×10^{-7}	--	5.6×10^{-4}
4000-740	T229B	FLLD	3.9×10^{-6}	3.8×10^{-5}	2.5×10^{-4}	5.4×10^{-4}
4000-741	T176A	FLLD	1.3×10^{-5}	7.7×10^{-4}	9.3×10^{-4}	2.2×10^{-3}
4000-742	T237BL	FLHD	--	5.5×10^{-6}	--	3.2×10^{-4}
4000-750	T253B	FLLD	--	--	--	4.1×10^{-4}
4000-751	T253C	FLLD	--	6.8×10^{-5}	--	1.2×10^{-3}
4000-752	T236BL	FLHD	--	1.8×10^{-4}	--	9.6×10^{-4}

(a) FH = Fertile particle, HTI coating
FLHD = Fertile particle, LTI high-density coating
FLLD = Fertile particle, LTI low-density coating

(b) Total fractional release in 5 hours at 1400°C

Examination of the data in Tables 5-10 and 5-11 shows that all of the sample lots of fertile particles met the metallic fission-product-release specification ($<5 \times 10^{-3}$), but rarely by more than one order of magnitude, and in no case was the release $<1 \times 10^{-4}$ fraction.*

Nine of the fertile particle lots were studied in both the leached and unleached condition. In all but two cases, the leached sample exhibited a lower Sr-91 release fraction, and in one of these cases, the release was essentially the same for both the leached and the unleached samples. The Xe-135 release appears to have been markedly reduced by the leaching process, indicating that significant amounts of uranium were on the surface.

In the discussion of the Sr-91 release characteristics of fissile particles it was pointed out that sample lots with high-temperature isotropic (HTI) coatings generally exhibited higher Sr-91 releases than those with low-temperature isotropic (LTI) coatings. This behavior was also found to be true for the lots of fertile particles used in PTE-2.

---

*The rather high value of the fractional Sr-91 release for fertile particles compared to fissile particles should not be taken as an indication that the fertile particles are of lower quality. Rather, it is a reflection on the manner in which the fractional release is calculated (i.e., Sr-91 released/total Sr-91 produced) and the fact that uranium contamination has been found in the coating of fertile particles. Thus, the fractional number of fissions occurring in the coatings of fertile particles, relative to the number of fissions in the kernel, is heavily weighted by the presence of the high-cross-section uranium in the coating, whereas there is no compensating uranium in the kernel.

6. BONDED FUEL RODS

6.1. REQUIREMENTS AND TYPES OF FUEL RODS

The fuel rods basically consist of columns of both fertile and fissile coated fuel particles packed to a high density and bonded together by a carbon matrix. A bond between the coated particles is desirable to prevent the particles from leaving the element in the event of structural damage to the graphite fuel block. The fuel rod is not bonded to the graphite container wall. In fact, the design of the element calls for a 1- to 2-mil radial gap between the fuel rod and the graphite fuel body wall. The matrix contains carbonized resin binder and carbon filler. In addition to acting as a bonding agent, the carbon matrix also serves to sorb metallic fission products that may escape from the coated particles.

The proof test element design required approximately 994 in. of fuel rod containing a total of 447 g of enriched uranium or 0.45 g of uranium per in. of fuel rod. A total thorium content of approximately 1670 g was also specified, although this number could vary depending on the particle loadings obtained. The fertile coated fuel particles contained all thorium carbide, whereas the fissile particles contained both enriched uranium and thorium carbide with a Th:U ratio of 0.58:1. The design burnup for the fuel rods in the test element after 800 full power days is slightly less than 75,000 MWd/tonne. Capsule irradiation tests of the test-element-type fuel particles have successfully demonstrated the capability of these particles to accommodate both the high burnups at these design temperatures and the fast-neutron dose without loss of integrity (Ref. 17,18). A comparison of PTE-2 fuel rods with other irradiation tests is covered in Section 10. A total of 124 individual fuel rods having nominal lengths of 1.00, 5.93, 11.53, and 14.31 in., were used in the element. The majority (112) of the rods were solid and had a diameter of 0.467 in.; the remaining 12 rods had

an annular design to allow insertion of a thermocouple. These rods had an o.d. of 0.514-in., an i.d. of 0.210 in., and were 5.93 in. long; they contained a graphite tube with a 0.025-in.-thick wall.

The fuel rod composition variables, including four types of coated particles, two types of binder, two types of filler, and two fabrication methods, are listed in Table 6-1.

TABLE 6-1
FUEL ROD VARIABLES

Coated Particle Type:

LTI - Low-Temperature Isotropic pyrolytic carbon outer coating

HTI - High-Temperature Isotropic pyrolytic carbon outer coating

LTI Density:

L - Low density (1.80 to 1.90 g/cm^3)

H - High density (1.90 to 1.98 g/cm^3)

HTI Density:

All HTI particles were high density, 1.90 to 1.98 g/cm^3.

Location of Fuel Rod When Carbonized:

E - Fuel rods carbonized in test element graphite fuel section

S - Fuel rods carbonized in special graphite holders

Fuel Rod Length:

Fuel rods were made in lengths of 1.00, 5.93, 11.53, and 14.31 in.

Fuel Rod Diameter:

Fuel rods were made in diamters of 0.467 and 0.514 in.

All of the FSV initial core fuel was made using LTI Coatings with the LTI outer coating density ranging from 1.60 to 2.00 gm/cm^3. The LTI density of the six-year service limit fuel ranged from 1.70 to 1.90 gm/cm^3. All of the FSV fuel rods were 0.490 in. diam by 1.94 in. long and all were carbonized in alumina in special graphite holders rather than in situ in the fuel block.

6.2. FABRICATION OF BONDED FUEL RODS BY INJECTION MOLDING

There are four main steps to the fuel-rod fabrication injection-molding process:

1. The fissile and fertile coated particles are blended and loaded into the metal mold cavities to form columns of loose, closely packed particles.

2. A thermosetting liquid resin binder mix is injected under pressure into the columns of particles.

3. The thermosetting resin in the mix is then heat-cured to a hard, green state.

4. The green rods are carbonized.

In general, the materials and process outlined in specification X-18-U-7, Issue B, were used in fabricating the rods for PTE-2. The rods were fabricated by both the Fuel Materials Branch (FMB) and the Fuel Operations Division (FOD). The fuel rods fabricated by FOD represent rods made in production fuel manufacturing equipment while the rods fabricated by FMB represent fuel rods made under laboratory conditions.

In the fuel rod fabrication process, a binder formulation is used which, after carbonization, results in a porous matrix material that exhibits partial bonding to the fuel particle surfaces. The partial bonding was intended to reduce the stress imposed on the fuel particle coatings by the matrix material. If, under irradiation, stresses are set up by the shrinkage of the matrix, the particle-to-matrix bond or the matrix material itself should fail before the particle coating. However, this did not prove to be the case, as explained in Section 10.

6.2.1. Molds and Accessories Used in the Process

The green fuel rods are formed in Type 304 stainless-steel molds having six rod cavities in a telephone-dial arrangement. The surface finish in the mold cavities is less than 16 μin., and the cavity bow is less than 0.003 in. per ft.

A schematic diagram of a mold assembly used by the FMB is shown in Fig. 6-1; the detailed assembly illustrated in Fig. 6-2 shows both typical solid rod and annular rod cavities. For the annular rods, graphite tubes of 0.025-in. wall thickness were included as shown in Fig. 6-2. The FOD mold assembly contained six fuel tubes, each of which was 0.464 in. in diameter by 15 in. long as shown in Figs. 6-7 and 6-11.

Other accessories used with the FMB mold include brass ring inserts, for forming a 1/16-in. radius on the rim of the rod at each end, and numbered plastic discs. These discs are inserted in the top of a filled and injected mold cavity to extrude excess binder and to mold the identification number on the top of the rod. Three FMB molds, 1.120, 6.179, and 11.650 in. in length, are shown in Fig. 6-3 along with accessories and completed fuel rods.

Before loading the coated particles, the mold cavities, end caps, and other accessories are coated with a release agent (RAM-225) which is dried for 30 min at 65°C.

A brass insert ring is placed in the bottom of each FMB mold cavity with the radius side facing inward in the hole. The bottom plate with the O-ring in place is assembled and secured. The mold is turned upright and the bottom radius insert ring tamped in place. The mold is now ready to be loaded with the fuel particles. The top plate and radius insert ring are not assembled until the particle loading and injection are complete.

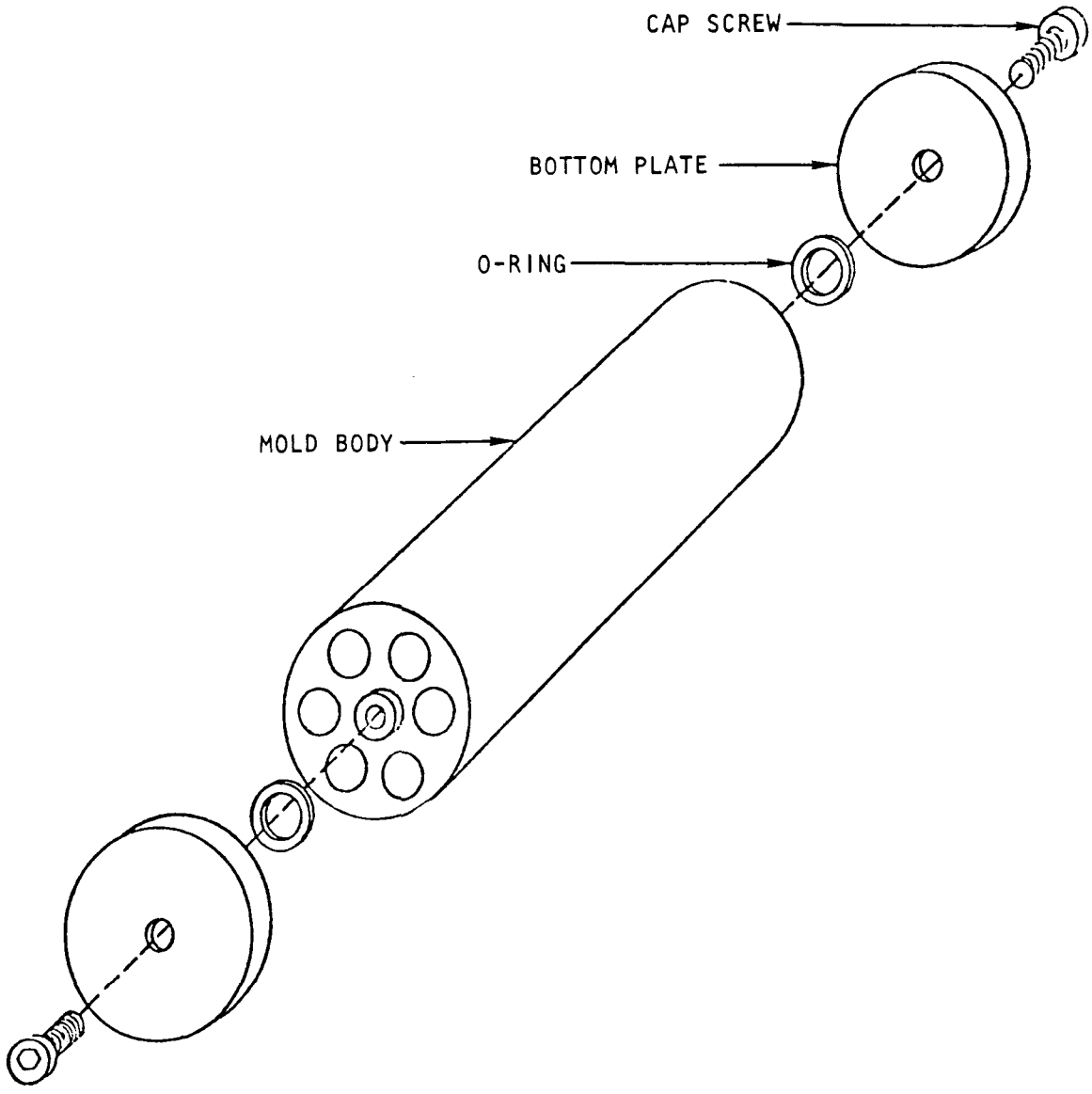

TYPE	MOLD LENGTHS	HOLD DIAM
ROD	0.005 IN.	0.0005 IN.
SOLID	1.120	0.4675
SOLID	5.700	0.4675
ANNULAR	6.179	0.5150
SOLID	11.650	0.4675

SPECIFICATIONS FOR ALL MOLDS

MATERIAL: 304 STAINLESS STEEL

CAVITY FINISH: 16 μIN.

CAVITY BOW PER FT: 0.001 IN.

OUTSIDE DIAMETER: 2-1/2 IN.

Fig. 6-1. Schematic drawing of metal molds for the fabrication of bonded-bed fuel rods by injection molding

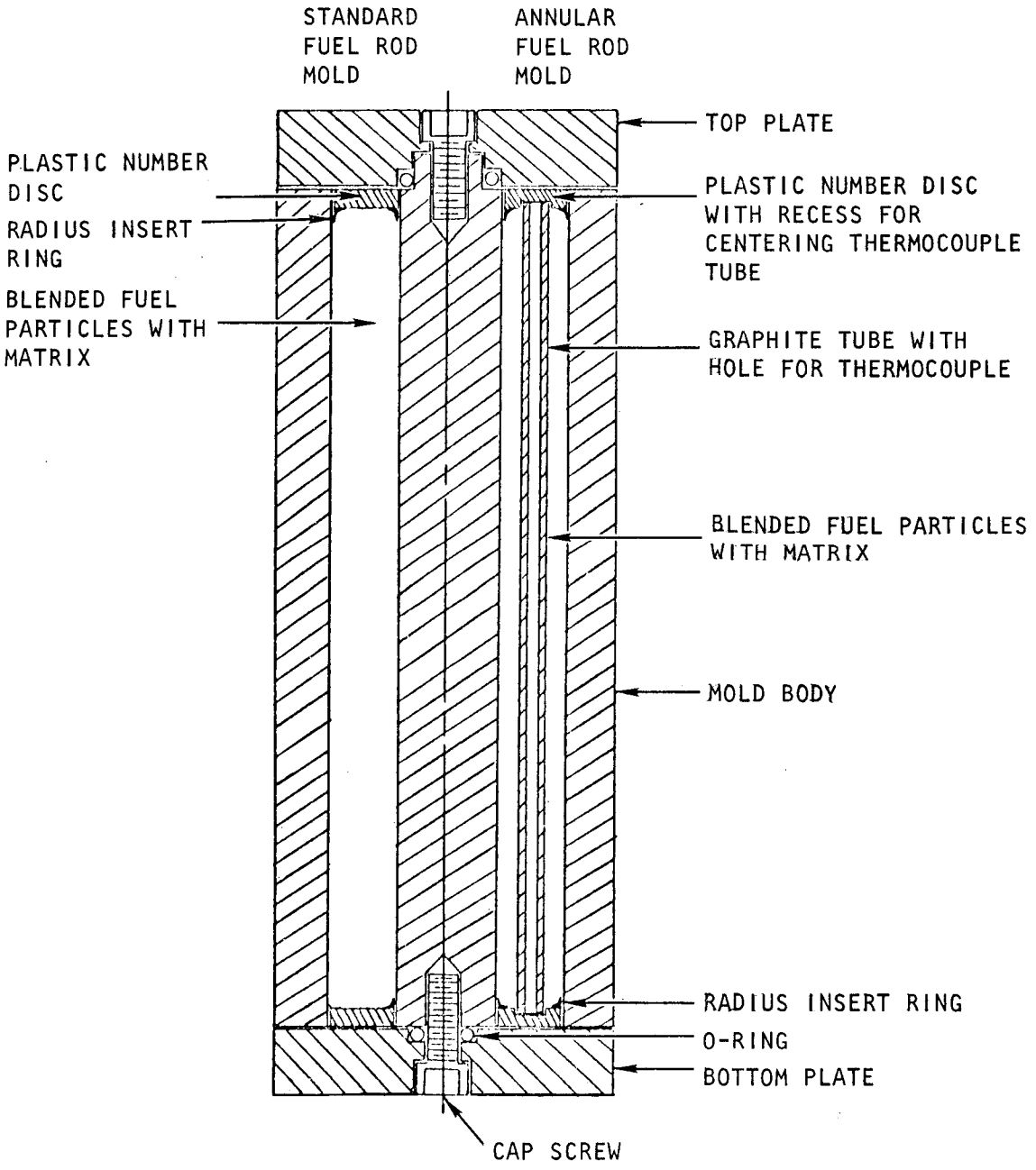

Fig. 6-2. Detail of assembly of mold for the fabrication of bonded-bed fuel rods by injection molding

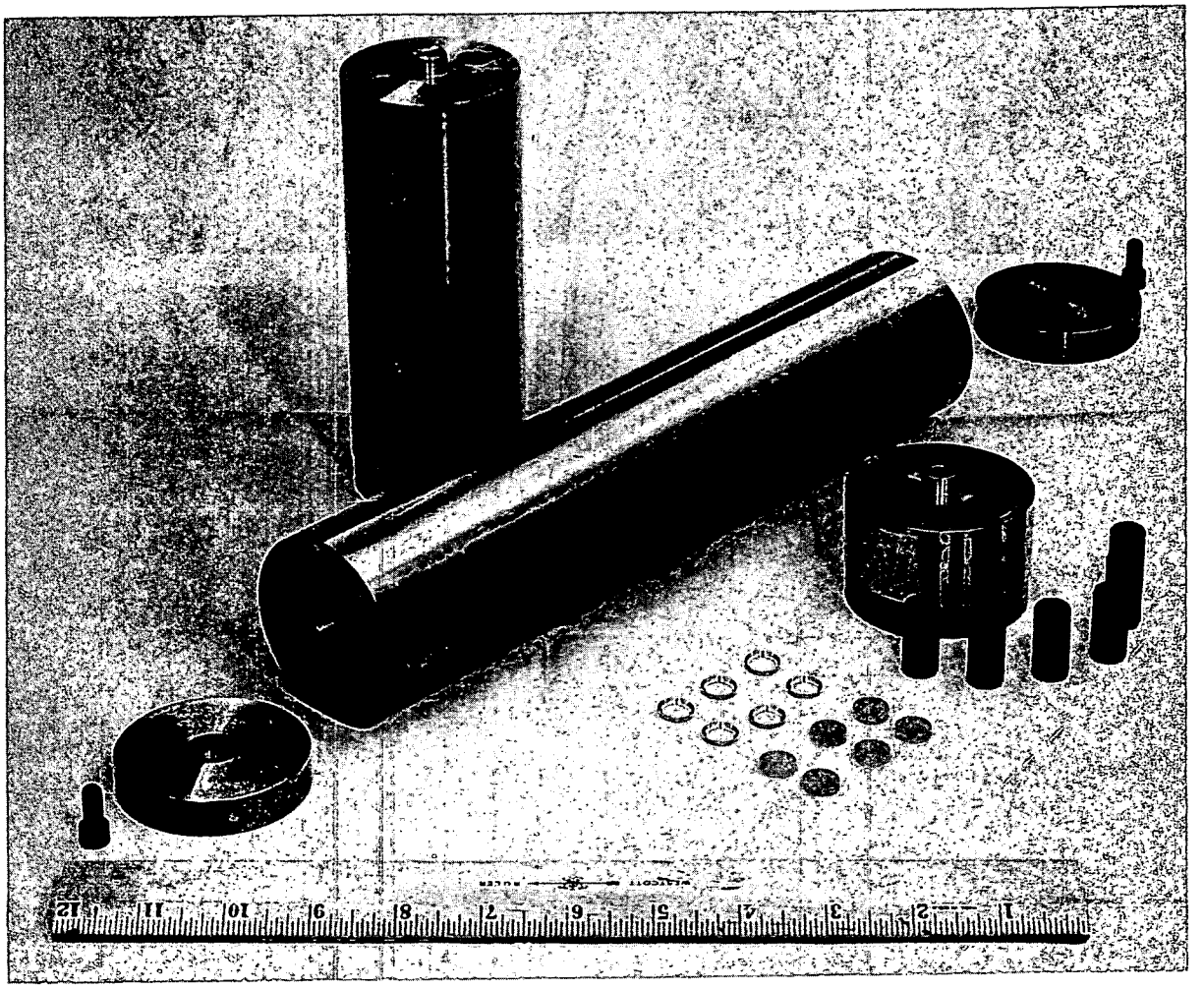

HT59098

Fig. 6-3. Stainless-steel fuel-rod molds and accessories with six cured fuel rods

6.2.2. Blending and Loading of Fuel Particles

The blending and loading of the fissile and fertile particles in the mold cavities are done with a double-hopper - double-orifice metering system. The two types of particles are fed simultaneously through two controlled orifices into a blending funnel and then into the mold cavity. The mold is vibrated to achieve close packing as the particles are loaded.

The double-hopper - double-orifice device, as shown in Fig. 6-4, consists of two triangular cavities with one side of each cavity adjustable to control the orifice opening at the bottom. A micrometer on each side is used to determine the orifice opening. The flow rate through each orifice can be adjusted independently of the other. The orifices are opened and closed simultaneously by a timed, solenoid-operated orifice gate valve. The tapered, conical blending funnel is designed to accept the two streams of flowing particles from each orifice on its wide outer rim, causing the particles to deflect into the tapered lower end of the funnel. Using this technique, an intimate mixture of the two types of particles is obtained with the desired particle distribution.

The lower end of the blending funnel, which is the same diameter as a mold cavity, is aligned with the cavity by means of an adapter plate.

The FMB blending funnel and a mold with the adapter plate attached are shown in Fig. 6-5. The complete FMB loading assembly can be seen in Fig. 6-6. This includes the double-hopper - double-orifice device and the blending funnel with the adapter plate attached to an 11.65-in. mold. The mold is resting on a vibrator. The timer for the solenoid-operated orifice gate valve is also shown. The FOD blending device and mold are shown in Fig. 6-7.

In operating the loading assembly, the required amount of fissile particles for a given uranium loading is weighed and loaded into the hopper;

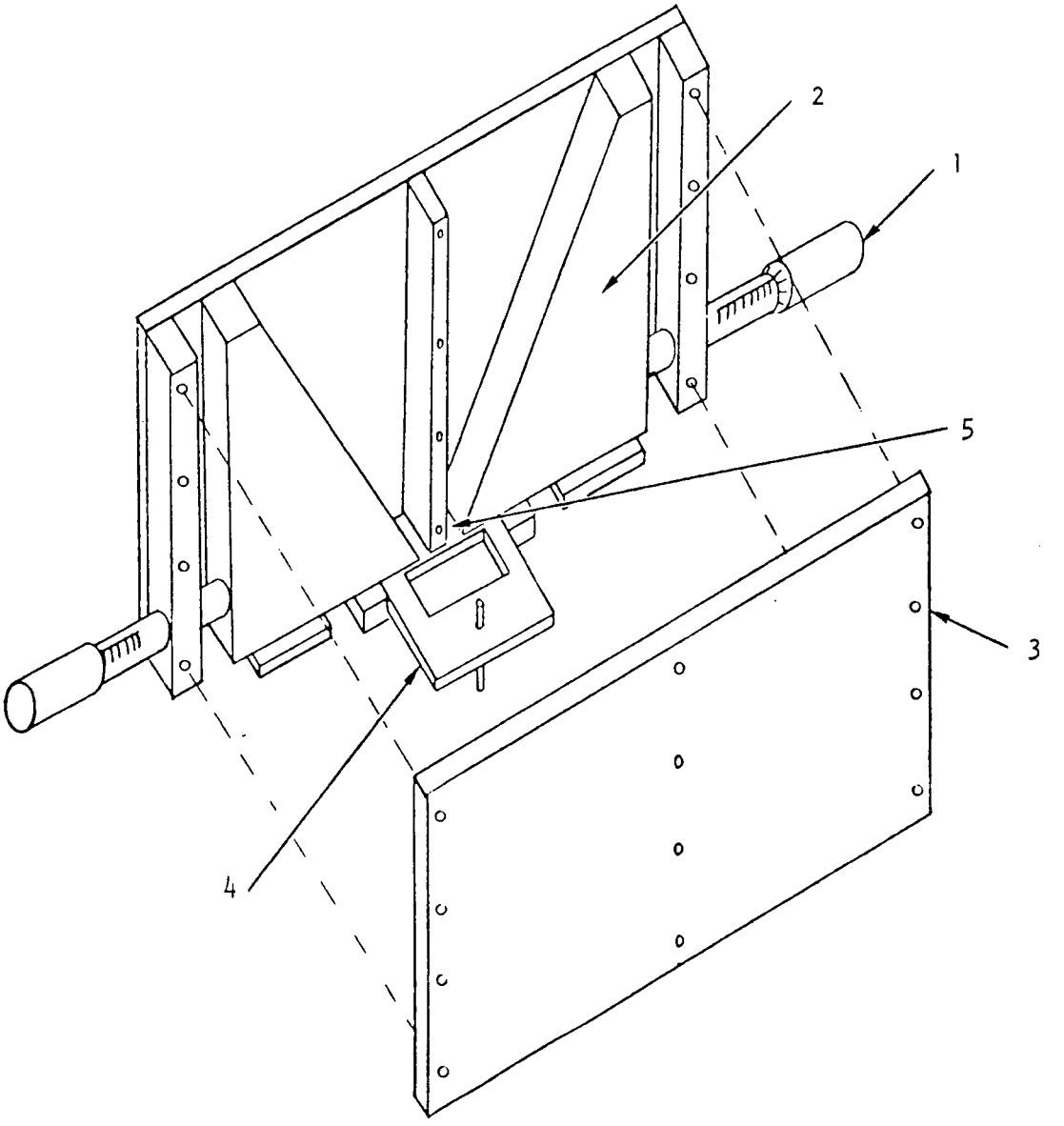

1 HOOPER-ADJUSTING MICROMETER
2 ADJUSTABLE SIDE OF HOPPER
3 HOPPER SIDE PLATE
4 HOPPER SLIDE VALVE
5 ADJUSTABLE ORIFICE OPENING

Fig. 6-4. Detailed assembly of the double-hopper - double-orifice apparatus for the simultaneous metering of fissile and fertile coated fuel particles into the blending funnel

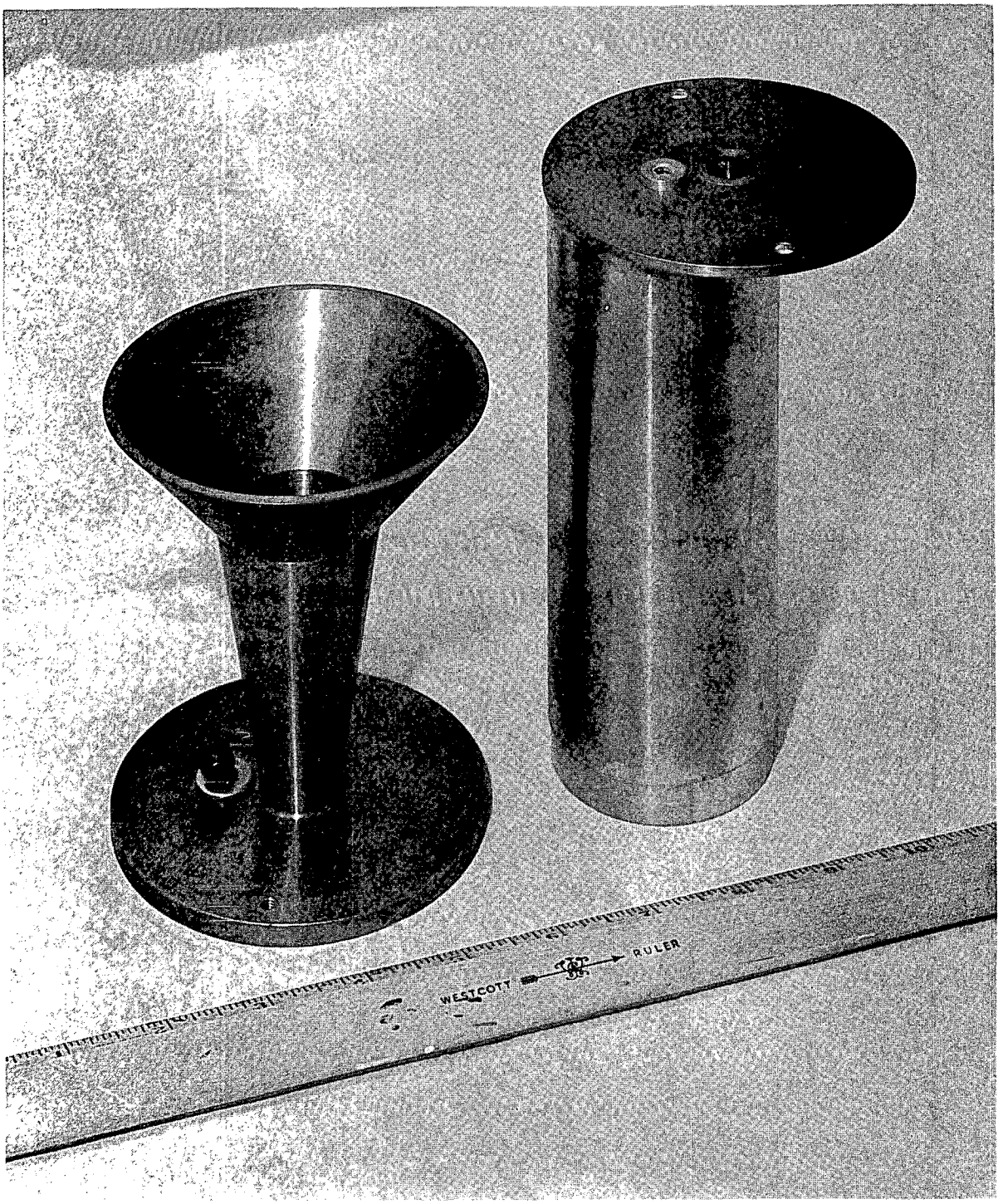

HT59105

Fig. 6-5. Blending funnel for blending and loading fissile and fertile coated fuel particles into a fuel-rod mold; a mold with adaptor plate attached is also shown

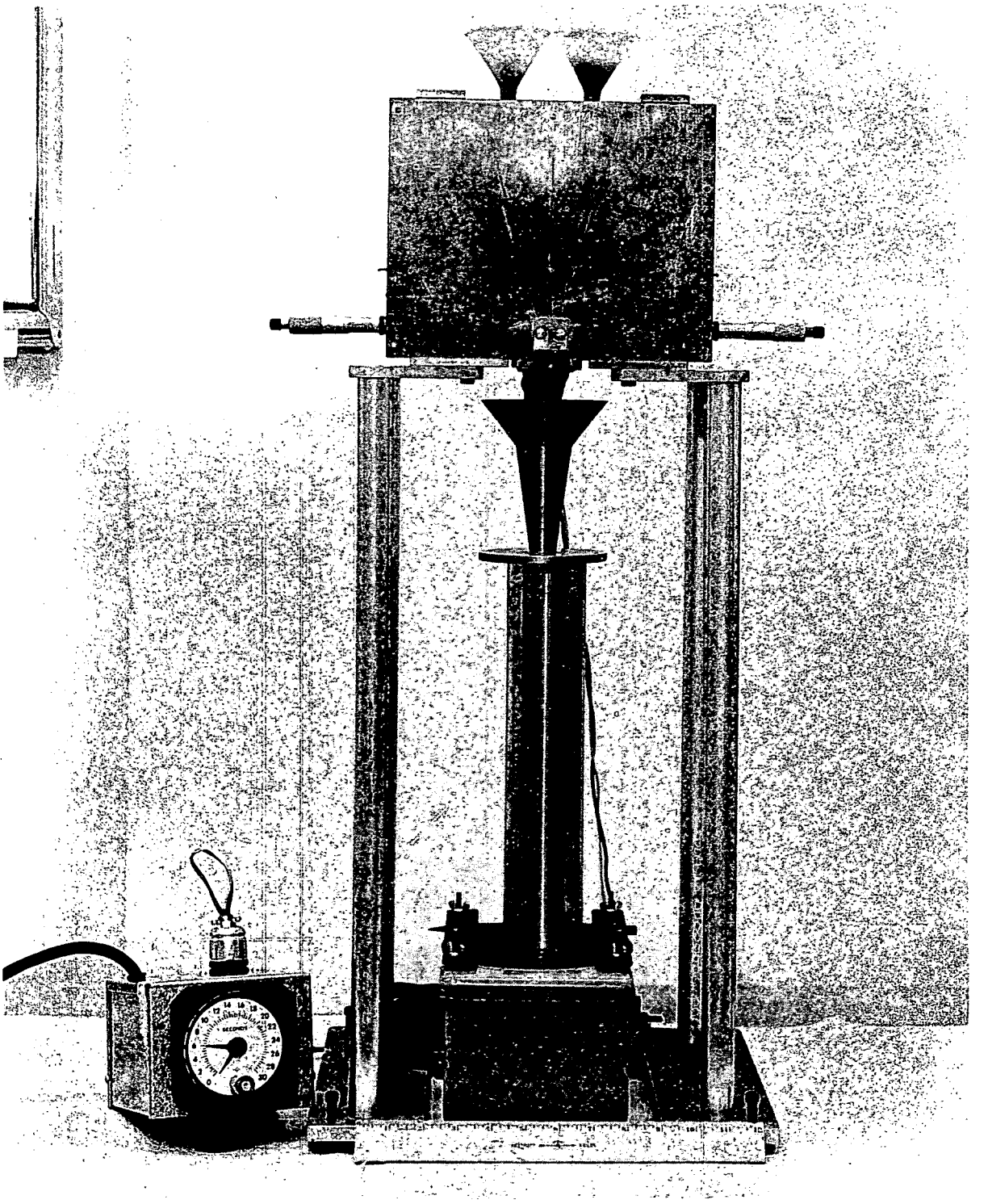

HT59103

Fig. 6-6. Complete fissile and fertile coated-particle metering, blending, and loading assembly with fuel-rod mold

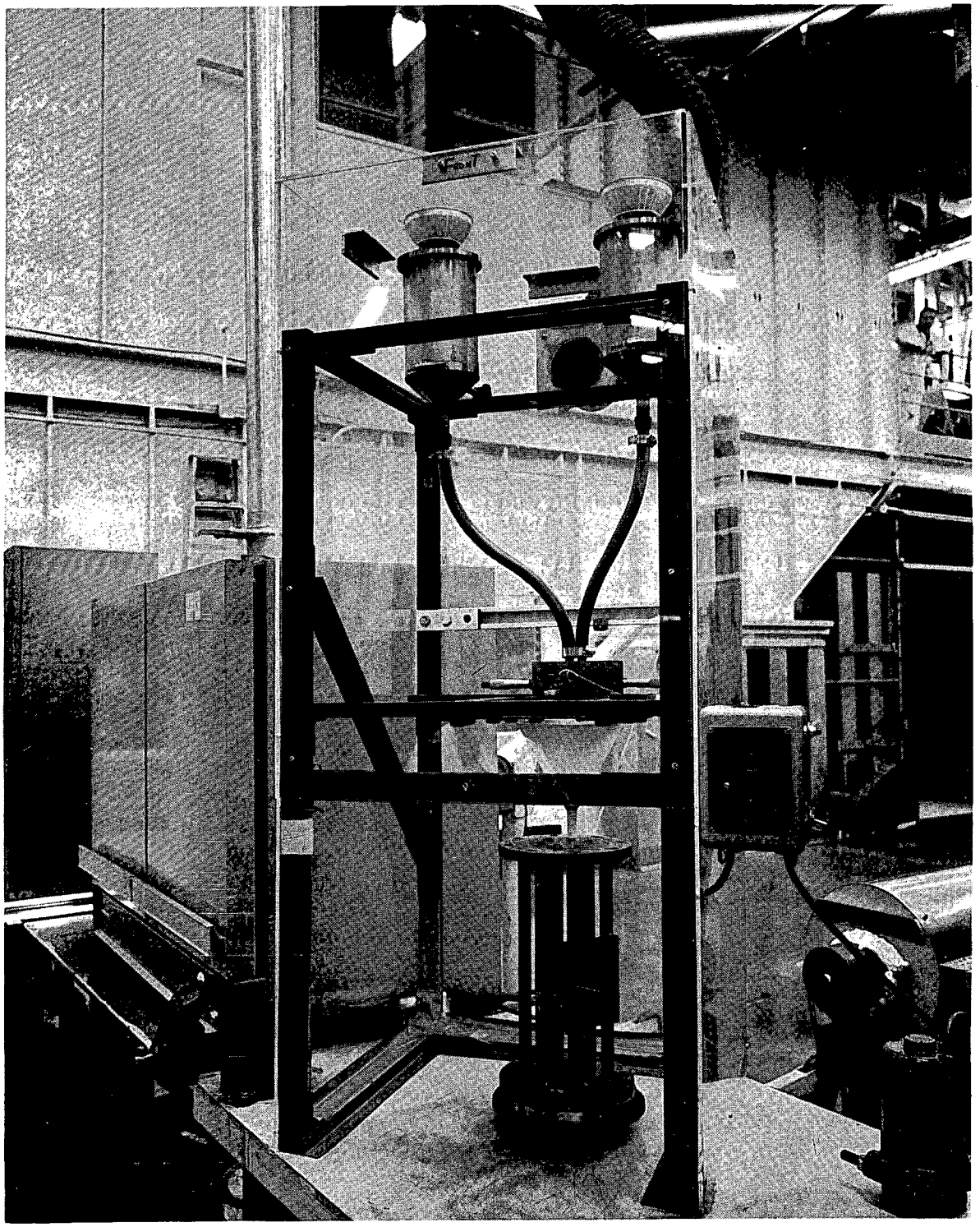

HT63548

Fig. 6-7. FOD PTE-2 particle blending device and fuel-rod mold

the total flow time through the orifice is then measured. (In setting the flow rate, usually about 2 g/sec, orifice openings of less than 3 particle diameters should not be used because of the possibility of particle bridging.) The required amount of fertile particles is then loaded into the other hopper and this orifice adjusted to give a total flow time equal (to within 0.1 sec) to that of the fissile particles. Once the settings are determined, weighed amounts of both types of particles can be loaded into each cavity without making changes. As the particles fall into the mold cavity, a high packing fraction (60 to 65 vol %) is obtained by vibrating the mold. An FMB mold with two cavities filled with loose particles and the blending funnel are shown in Fig. 6-8.

From earlier developmental work, this method of blending and loading the fuel particles was determined to be the most successful and resulted in particle distributions which deviated from the ideal by only ±4% maximum (Ref. 1).

Three basic types of TRISO coated particles were used in the fuel rods. These were particles with HTI coatings, LTI low-density coatings, and LTI high-density coatings. The particles used consisted of blends of several batches of the same type as described in Section 5. As indicated in Section 6.1, the FSV initial core was made entirely from TRISO coated LTI fuel particles, with the pyrolytic outer coating ranging from 1.60 to 2.00 gm/cm^3.

6.2.3. Formulation and Injection of Matrix Mix

One type of matrix mix formulation was used for all of the rods in the proof test element. This liquid thermosetting mix consisted of the following:

47.4 wt % Rezolin R-72S phenolic resin
15.8 wt % Maleic anhydride
15.8 wt % Nadic methyl anhydride
21.0 wt % GP-38 graphite powder sized to <30 microns

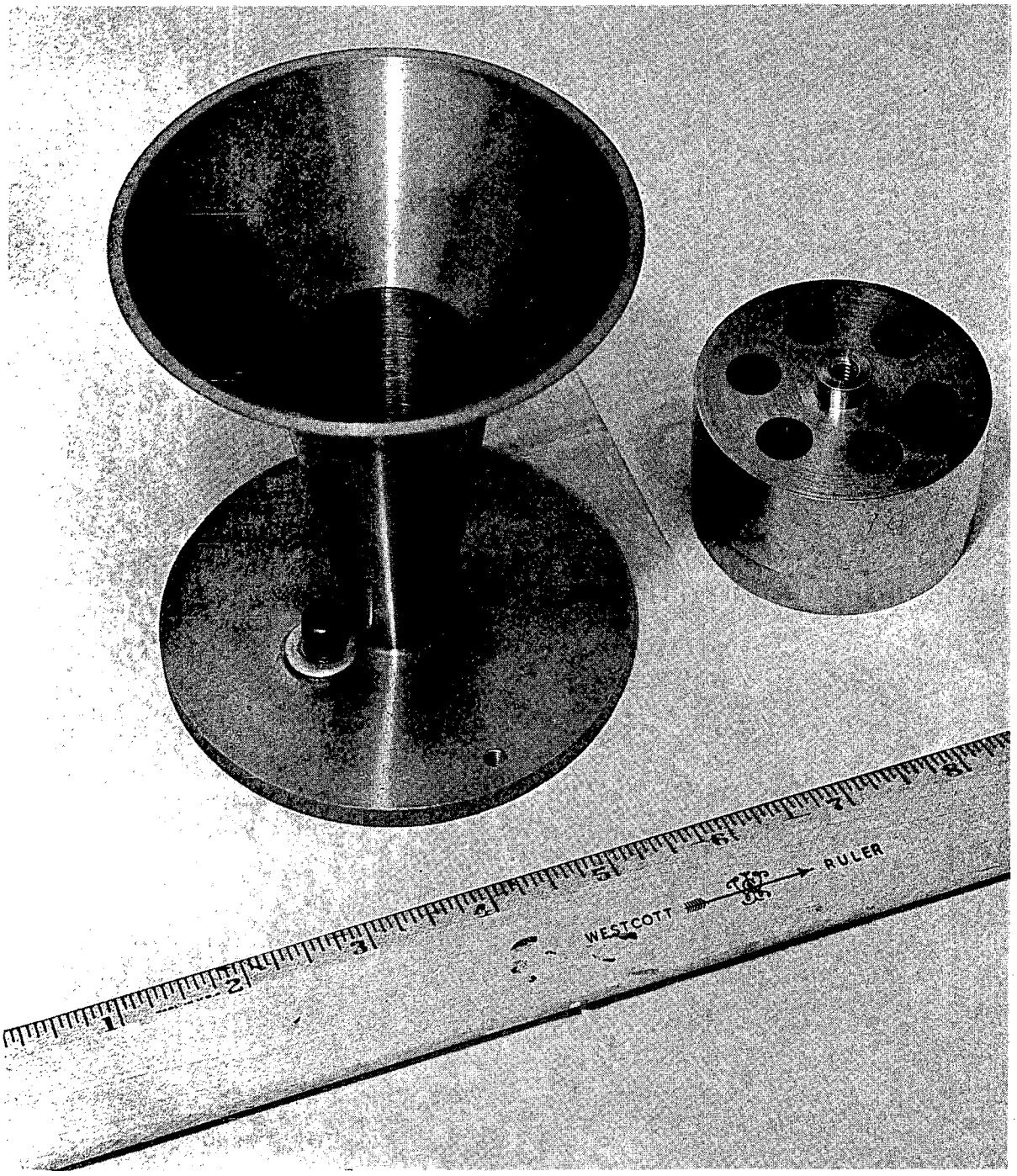

HT59113

Fig. 6-8. Blending funnel and fuel-rod mold with two cavities containing loose fissile and fertile coated fuel particles

In blending the preweighed components, the maleic anhydride was first dissolved in the nadic methyl anhydride with heating (approximately 100°C). The anhydride mix was cooled to room temperature and the phenolic resin added. The graphite powder was then stirred and the whole mix thoroughly blended with a motor-driven stirrer. The green matrix was used within 4 hr after mixing. As indicated in Section 10, this matrix was not used in FSV. Rather, a pitch-bonded, natural graphite flour matrix was eventually chosen for use.

For FMB matrix injection, the liquid mix is loaded into the reservoir of the grease-gun injection apparatus. This apparatus consists basically of a liquid mix reservoir, a pressure chamber with two check valves to direct the flow of the matrix, a double-acting air cylinder to develop injection pressures of up to 1280 psi, a set of multiple-injection loading orifices with a mold seal surface, and a mold support structure. A schematic diagram of this apparatus is shown in Fig. 6-9. The whole assembly and a 6-in.-long mold being loaded are shown in Fig. 6-10. After the reservoir is filled with matrix mix, the mold containing the loose coated particles is placed in the mold support structure and the top tightened against the mold seal surface. The double-acting air cylinder is then activated and cycled to begin pumping the matrix mix down through the column of particles. The multiple-loading injection-molding orifices allow all six cavities of a mold to be injected simultaneously. Completion of the injection is indicated by a stopping of the air cylinder action and the appearance of matrix mix at the edge of the bottom-end mold plate. After injection is completed and the mold removed from the apparatus, the top brass ring inserts and plastic discs are put in place. The top mold plate is assembled and tightened down to force the rings and discs into place; this also displaces any excess matrix remaining at the top of the mold cavity.

The process used to fabricate fuel rods by FOD was to fill the die (mold) cavity with the specified fissile and fertile particles using the double-orifice blending device. Adjustment for the specified length was made by using spacers in the die cavity. Six 14.31-in. fuel rods could be

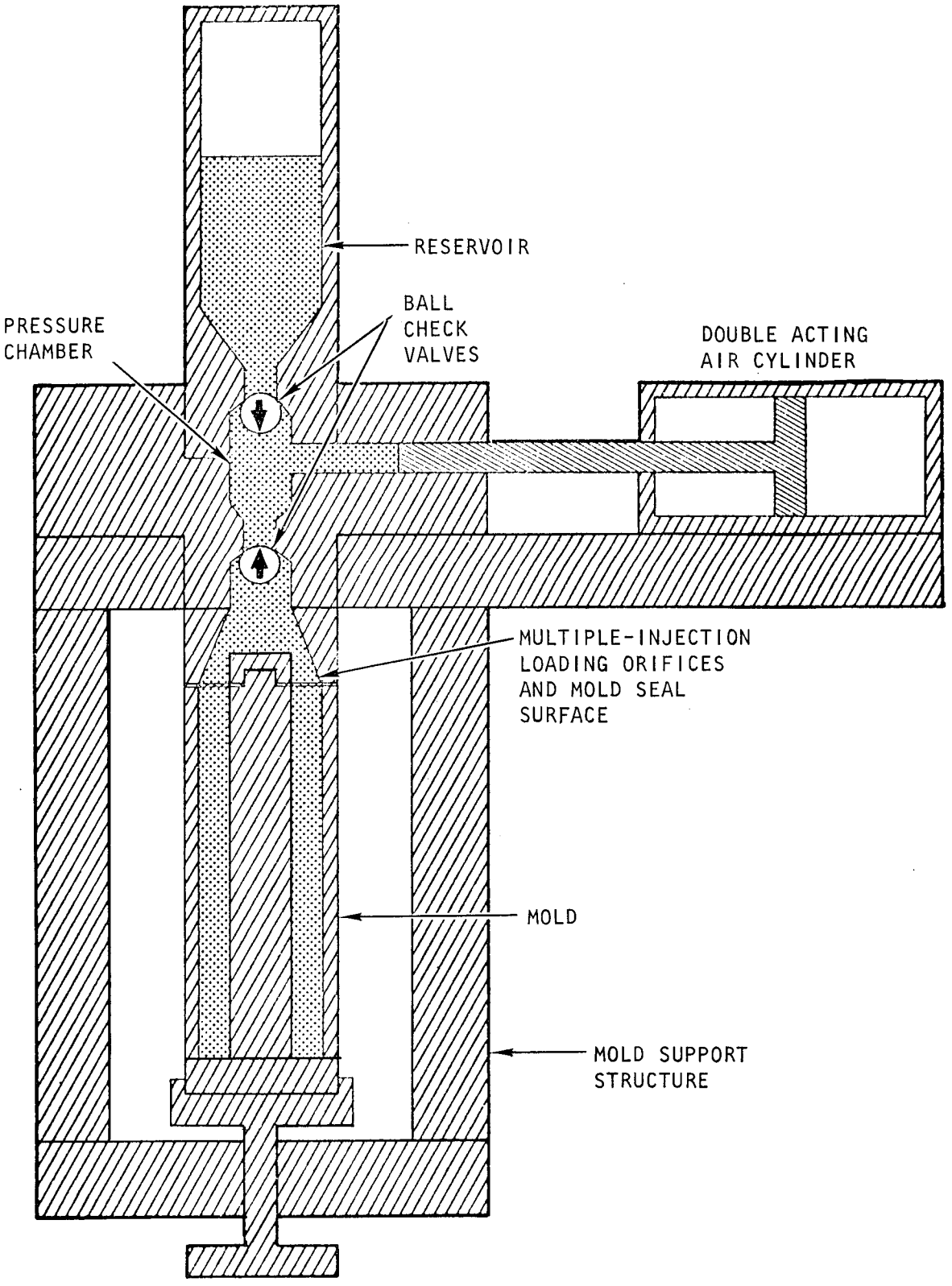

Fig. 6-9. Fuel-rod injection-molding apparatus (grease gun)

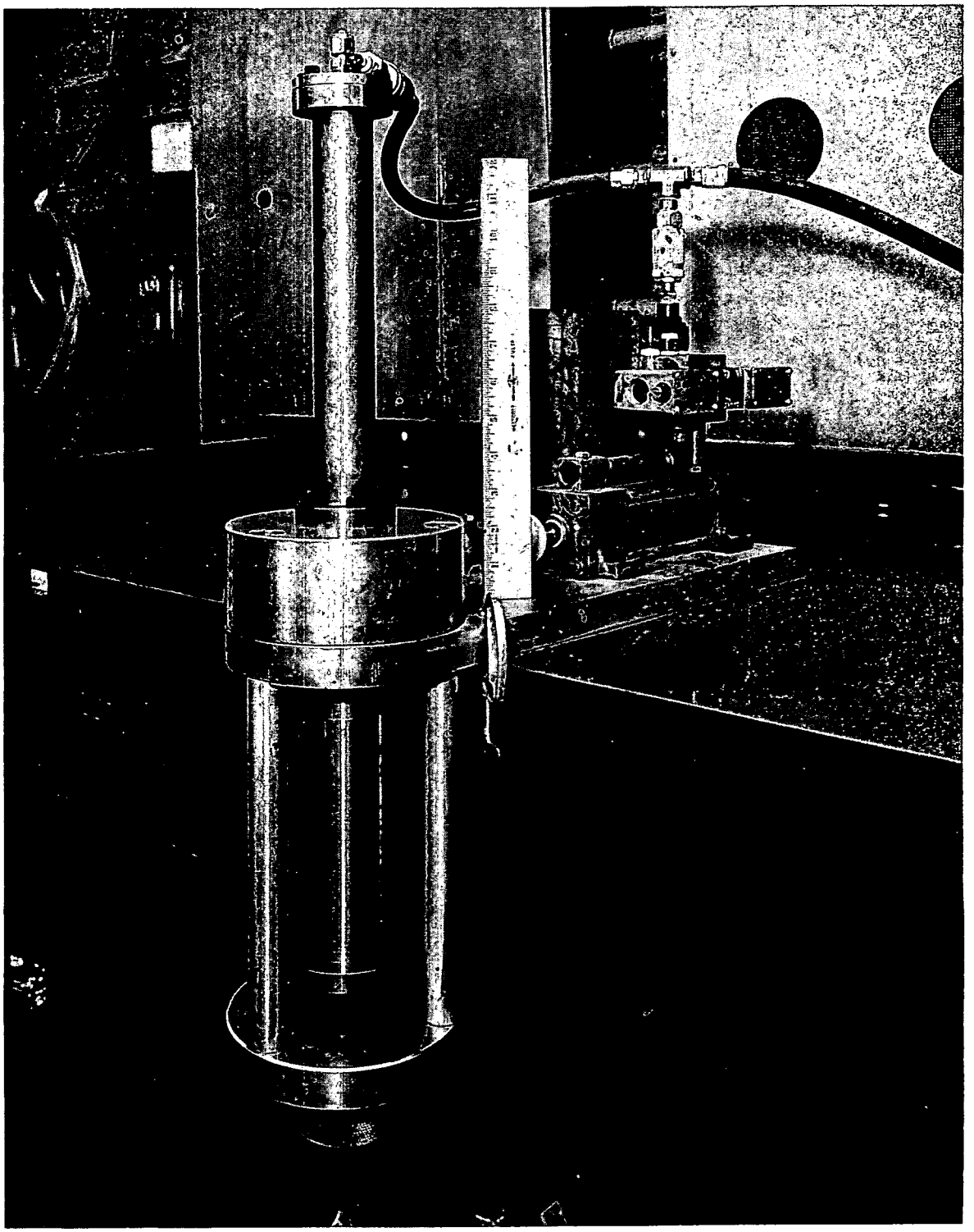

HT59111

Fig. 6-10. Complete assembly of fuel-rod injection-molding apparatus (grease gun) with 6-in. mold in place

made at one time; however, for this proof test element, five fuel rods were made to the specified length and a 1-in. rod was made in the sixth cavity for fission-product-release measurements.

Figure 6-11 shows an FOD die being injected with binder mix (center of Fig. 6-11) whereby 1200-psi pressure is applied on the matrix binder in an auxiliary die attached to the fuel rod die. After the fuel rod die is injected, it is sealed and heated to 100°C for 1 hr and cooled to room temperature. The rods are then easily ejected from the die. Some fuel rods, as they appear coming out of the die, are shown on the left side of Fig. 6-11.

6.2.4. Curing and Carbonization of the Fuel Rods

To cure the phenolic resin and harden the FMB fuel rods, the loaded molds were placed in a circulating-air oven at 105°C for 1 hr. This completed the green or thermosetting cure. The mold was then disassembled and the green cured rods, which were quite strong at this stage, were pushed out, examined, and measured. They were then placed loosely in a graphite container for carbonization. The container used for many of the rods was the actual graphite test element section. Carbonization of the FMB fuel rods was accomplished in a resistance-heated furnace with nitrogen purge using the following heating cycle:

Temperature (°C)	Total Heating Time (hr)	Heating Rate (°C/hr)
Room (250)	3	100
250 to 500	10	25
500 to 1000	5	100
Hold at 1000	1	--

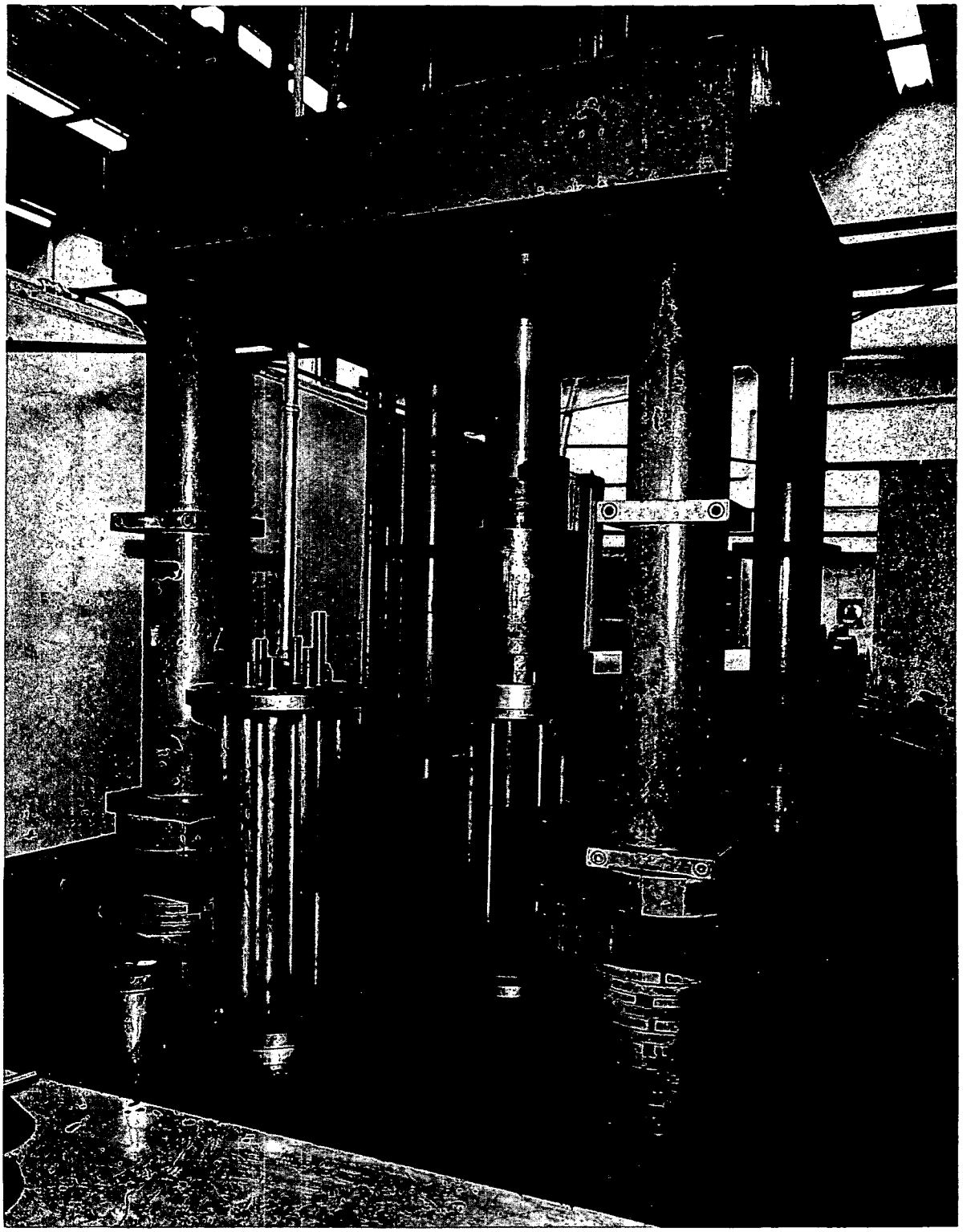

HT63545

Fig. 6-11. FOD mold being injected with matrix binder mix

The carbonization furnace, used for both FMB and FOD fuel rods, is shown in Fig. 6-12. Carbonization of the FOD fuel rods was also performed in a resistance-heated furnace with nitrogen purge using the following heating cycle:

Temperature (°C)	Total Heating Time (hr)
Room (200)	3
200 to 500	9
500 to 1000	6
Hold at 1000	1

These programs were designed to give the slowest heating rate while the maximum amount of volatile material was being released from the rods. After carbonization and cooldown, the rods were removed and again examined and measured. They were then stored until gamma scanning and final assembly were performed.

6.3. EVALUATION OF FUEL RODS PRODUCED FOR PTE-2

A total of 97 solid rods 1.00 in. long, 24 annular rods 5.93 in. long, and 70 solid rods 11.53 in. long were fabricated by the FMB for PTE-2 using three basic types of fuel particles. A total of 17 solid 1.00-in.-long and 79 solid 14.31-in.-long fuel rods were made by FOD for PTE-2. These rods were evaluated by visual inspection (for broken particles on the surface and general rod integrity), dimensional measurements, metallography, gamma scanning, and fission product release testing. The FMB and FOD rods that were rejected because of broken particles on the surface and high fission-product release are listed in Table 6-2 by particle type. The FMB and FOD rods selected for insertion in the element are listed by particle type, batch number, and rod identification number in Tables 6-3 and 6-4 respectively. The FMB and FOD fuel rods used in each fuel zone are shown in the fuel zone

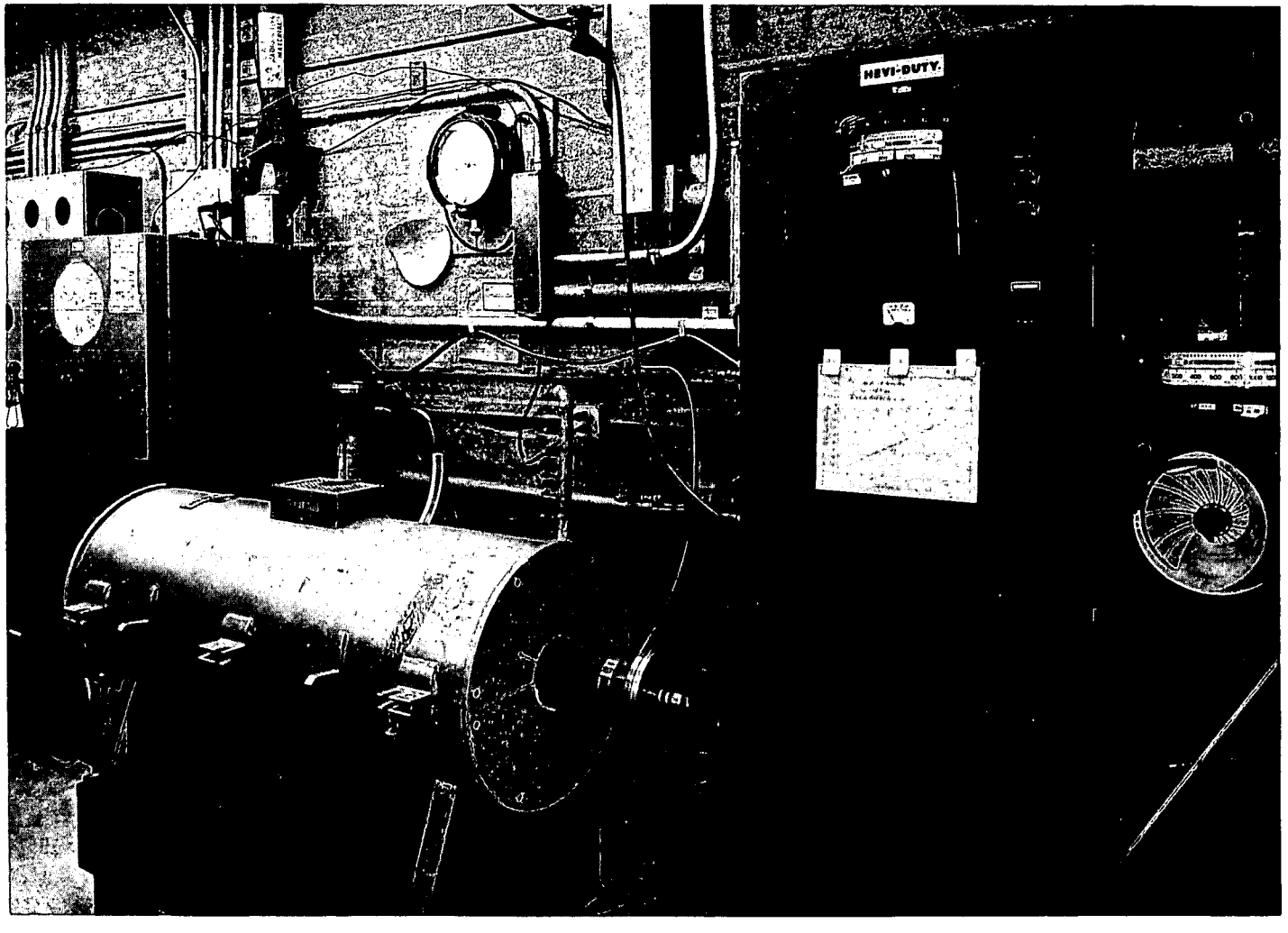

HT59106

Fig. 6-12. Resistance-heated furnace and atmosphere tube for carbonizing fuel rods (note furnace controls and cam for giving programmed heat-up cycle)

TABLE 6-2
FUEL RODS PRODUCED FOR PTE-2 ACCEPTED AND REJECTED

Type of Fuel Particles in Rods	HTI Coatings		LTI Low-Density Coatings					LTI High-Density Coatings			
Length of Fuel Rods (in.)	1.00	11.53	1.00		5.93	11.53	14.31	1.00		11.53	14.31
Rods made by	FMB	FMB	FMB	FOD	FMB	FMB	FOD	FMB	FOD	FMB	FOD
Total number of rods fabricated	48	30	23	8	24	12	40	26	9	28	39
Number of rods required for element	24	12	11	0	12	6	22	10	0	11	16
Number of rods accepted for use in element[a]	32	22	14	0	14	12	23	14	0	17	19
Number of rods rejected because of broken particles	--	2	1	0	4	--	4	1	0	9	13
Number of rods rejected because of high FPR[b]	11	6	5	0	6	--	13	5	0	2	7
Number of rods used in FPR[b] test	5	--	3	8	--	--	0	6	8	--	0

[a] Some rods were accepted which did not meet all of the FPR requirements and some were accepted which initially had one or two visible broken particles which were subsequently removed.

[b] Fission product release

TABLE 6-3
IDENTIFICATION NUMBERS OF FMB RODS SELECTED FOR INSERTION IN PTE-2

Type of Coated Fuel Particles	Fissile Particle Batch No.	Fertile Particle Batch No.	Fuel Rod Length (in.)	Identification Numbers of Rods Used in PTE-2
HTI	ET170B-170A2	T169A-105B	1.00	2A, 4A, 823, 824, 825 826, 827, 828, 829, 830, 831, 832, 833, 841, 842, 843, 844, 845, 846, 847, 848, 850, 851, 852
HTI	ET170B-170A2	T169A-105B	11.53	7A, 9A, 835, 836, 838, 840, 853, 854, 855, 856, 857, 858
LTI Low density	ET171C	T-213B,229B 176A	1.00	919, 920, 922, 931, 932, 935
LTI Low density	ET171C	T213B,229B 176A	5.93 (annular)	49, 51, 53, 54, 55, 56, 57, 58
LTI Low density	ET171C	T-213B,229B 176A	11.53	925
LTI Low density	ET-255A	T212B,253B 253C	1.00	943, 944, 945, 946, 948
LTI Low density	ET-255A	T212B,253B 253C	5.93 (annular)	61, 62, 63, 64
LTI Low density	ET-255A	T212B,253B 253C	11.53	937, 938, 940, 941, 942
LTI High density	ET170C,171B	T103A,103C 161B	1.00	890, 892, 894, 902, 903, 904, 905, 906
LTI High density	ET170C,171B	T103A,103C 161B	11.53	907, 908, 909, 910, 911,912
LTI High density	ET170C,171B	T-237B	1.00	949, 952
LTI High density	ET170C,171B	T-236B	11.53	19A, 20A, 21A, 22A, 23A

TABLE 6-4
IDENTIFICATION NUMBERS OF FOD RODS SELECTED FOR INSERTION IN PTE-2

Type of Coated Fuel Particles	FOD Load No.	Fissile Particle Batch No.	Fertile Particle Batch No.	Fuel Rod Length (in.)	Identification No. of Rods used in PTE-2
LTI High density	2	ET-170C-171B	T-103A-103C-161B	14.31	526, 568, 464, 556
	3	ET-170C-171B	T-103A-103C-161B	14.31	560, 562, 553
	4	ET-170C-171B	T-103A-103C-161B	14.31	566
	5	ET-170C-171B	T-176B	14.31	549, 552
	6	ET-170C-171B	T-237B	14.31	551, 584, 586, 546
LTI Low density	7	ET-171C	T-213B-229B-176A	14.31	582, 587, 573, 577, 578
	8	ET-171C	T-213B-229B-176A	14.31	571, 572, 585, 583, 579
	9	ET-171C	T-213B-229B-176A	14.31	581, 588, 574, 576, 575
	10	ET-171C	T-213B-229B-176A	14.31	983, 985, 9-chipped 978, 980
	11	ET-255A	T-212B-253B-253C	14.31	986, 996
LTI High density	16	ET-170C-171B	T-236B	14.31	960, 957

assembly drawings listed in Section 8 and in Tables 6-5, 6-6, 6-7, and 6-8 which correlate the representative TRIGA fission-product release rods with the fuel rods inserted into PTE-2.

All of the 14.31-in.-long fuel rods used in PTE-2 were fabricated by FOD, while all of the 1.00-, 5.93-, and 11.53-in.-long fuel rods were made by FMB. (FOD did make some 1.00-in.-long rods which were used as fission gas samples and not placed into PTE-2.) There was no significant difference between the methods used by the two groups in fabricating the PTE-2 fuel rods. There were thirty-eight 14.31-in.-long fuel rods finally used in PTE-2 and this represents 55% of the total fuel in PTE-2. All of these rods were placed in fuel zones 2 and 3 where both the flux and temperature are maximum. All of the remaining fuel in PTE-2 (45%) was fabricated by FMB.

6.3.1. Dimensional Measurements of Fuel Rods

The dimensional requirements for the different types of fuel rods are shown in Table 6-9. After final carbonization, dimensional measurements were made on a large, representative number of rods by both Metallurgy and Quality Assurance personnel. The rod diameter was measured in six places: two at the top, middle, and bottom, each 90 deg from the other. One length measurement was made. All measurements were recorded in engineering log books. The group of rods which were carbonized in place in the actual graphite test element section were left undisturbed. All of the measured rods selected for insertion in the element met the dimensional requirements.

The FOD fuel rods were carbonized in their respective fuel blocks and data for representative carbonized fuel rods are shown in Table 6-10. These fuel rods were not, however, used in the test element.

TABLE 6-5
CORRELATION BETWEEN TRIGA ROD NUMBERS AND RODS USED IN PTE-2, ZONE 1

Representative TRIGA Rod No.	PTE-2, Zone 1 Rod Numbers			
	14.31-in. Rods	11.53-in. Rods	5.93-in. Rods	1.00-in. Rods
889	None			890 892 894
24A		19A 22A 20A 23A 21A		
936		925		931 932 935
947		937 941 938 942 940	64 63	
924				919 920 922
953				952 949

TABLE 6-6
CORRELATION BETWEEN TRIGA ROD NUMBERS AND RODS USED IN PTE-2, ZONE 2

Representative TRIGA Rod No.	PTE-2, Zone 2 Rod Numbers			
	14.31-in. Rods	11.53-in. Rods	5.93-in. Rods	1.00-in. Rods
456	526			
	556			
	568			
	464			
550	549			
	552			
849		856		845
		857		848
		853		847
		858		842
				851
				852
				843
				841
				850
				846
				844
834				823
				825
				829
				824
				831
				830
				833
				832
3A		7A		2A
		9A		4A
924			56	
			57	
			58	
901				905
				904
570	551			
	586			
	584			
	546			
	960			
	957			

TABLE 6-6 (Continued)

Representative TRIGA Rod No.	PTE-2, Zone 2 Rod Numbers			
	14.31-in. Rods	11.53-in. Rods	5.93-in. Rods	1.00-in. Rods
947		None	61 62	None
559	566 560			
569	562 553			

TABLE 6-7
CORRELATION BETWEEN TRIGA ROD NUMBERS AND RODS USED IN PTE-2, ZONE 3

Representative TRIGA Rod No.	PTE-2, Zone 3 Rod Numbers			
	14.31-in. Rods	11.53-in. Rods	5.93-in. Rods	1.00-in. Rods
979	575	None		
	581			
	574			
	588			
	576			
580	582			
	577			
	587			
	578			
	573			
924			55	
			54	
			53	
			51	
			49	
947				948
				946
				943
				945
				944
977	9-chipped			
	978			
	983			
	980			
	985			
589	571			
	583			
	572			
	585			
	579			
994	986			
	996			

TABLE 6-8
CORRELATION BETWEEN TRIGA ROD NUMBERS AND RODS USED IN PTE-2, ZONE 4

Representative TRIGA Rod No.	PTE-2, Zone 4 Rod Numbers			
	14.31-in. Rods	11.53-in. Rods	5.93-in. Rods	1.00-in. Rods
834	None	835	None	826
		836		828
		838		
		840		
849		854		
		855		
901		911		903
		909		902
		907		906
		910		
		908		
		912		
3A				5A

TABLE 6-9
DIMENSIONAL REQUIREMENTS OF PTE-2 FUEL RODS

Type of Rod	Diameter (in.)	Length (in.)
Solid	$0.467^{+0.001}_{-0.003}$	1.00 ± 0.05
Annular	$0.514^{+0.001}_{-0.003}$ 0.210 ± 0.002 (inside diameter)	5.93 ± 0.05
Solid	$0.467^{+0.001}_{-0.003}$	11.53 ± 0.07
Solid	$0.467^{+0.001}_{-0.003}$	14.31 ± 0.07

TABLE 6-10
DIMENSIONAL CHANGES DUE TO CARBONIZATION OF FUEL RODS

Loading	Fuel Rod	Length	Weight (gm)			Diameter					
			Gross	Fissile	Fertile	0°	90°	0°	90°	0°	90°
4 after cure	555	14.325	105.8	29.32	57.98	0.464	0.465	0.464	0.464	0.464	0.464
After carbonization		14.367	96.0			0.464	0.464	0.464	0.463	0.463	0.463
4 after cure	557	14.324	106.0	29.32	57.98	0.464	0.465	0.465	0.464	0.464	0.464
After carbonization		14.372	96.2			0.464	0.464	0.464	0.463	0.464	0.464

6.3.2. Fuel Rod Metallography

Metallographic sections were made of several representative FMB and FOD 1.00-in.-long rods. Three samples representing the three basic particle types (HTI, LTI high-density, and LTI low density) are shown in Figs. 6-13, 6-14, and 6-15. All of the samples showed a generally homogeneous matrix with a large amount of porosity. There also appeared to be a fairly substantial amount of bonding of matrix to the particle surface. A few cracks in the outer PyC layer of the low-density LTI particles could be noted in that sample, but these were estimated to be less than 1%. No cracked or broken coatings were noted in the other samples. The fissile-fertile particle distribution appeared to be good.

6.3.3. Fuel Rod Gamma Scanning

The total enriched uranium content and loading variations of a number of representative fuel rods were checked by a gamma-scanning technique. The rods were positioned in the apparatus in a rotating and indexing fixture modified to accept dual detector probes located diametrically opposite each other. Glass tubes were used to contain the rods for counting to prevent any possible damage to the rods and cross-contamination. The apparatus was calibrated with standards of known enriched uranium content for 14.31-, 11.53-, and 1.00-in.-long fuel rods, and the uranium loading in the rods determined from the counts from each rod. The loadings from 5.93-in.-long rods were not compared to any standard since none is available for this type. Uranium loadings listed are deviations from the average count of all the rods in this group.

All but 18 of the 124 rods loaded into the element were scanned. All of these met the total uranium requirement of ±5% of the nominal loading.

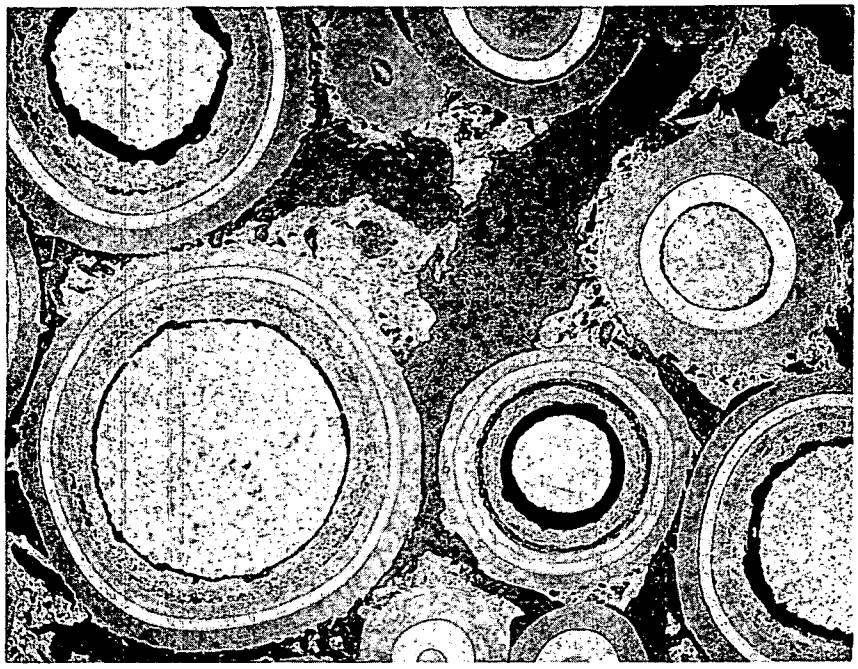

M31819-1

Fig. 6-13. Fuel rod No. 6A, 1.00 in. long; TRISO HTI coated fissile and fertile particles in an injection molded fuel rod with a 79% phenolic resin binder-21% graphite powder filler matrix

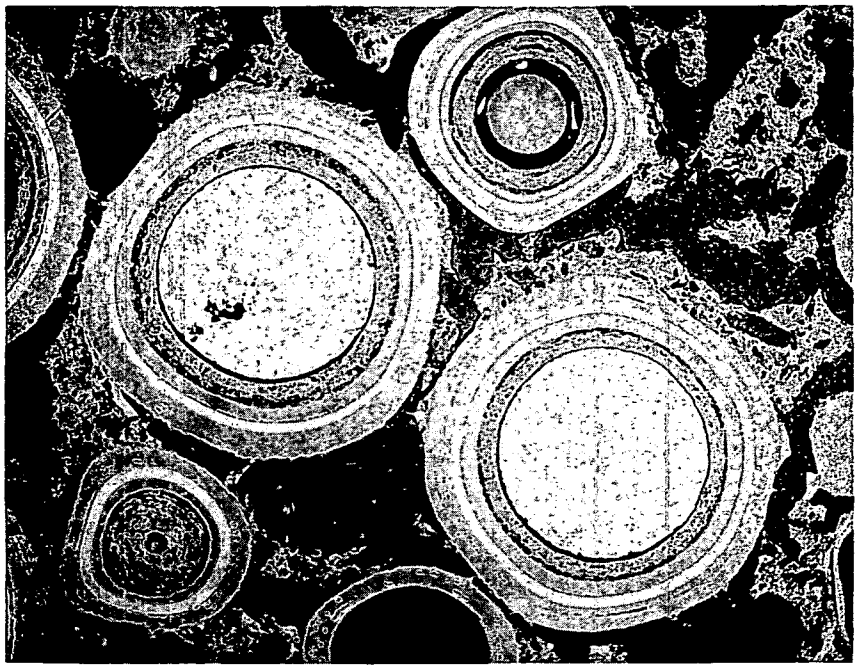

M31817-1

Fig. 6-14. Fuel rod No. 933, 1.00 in. long; TRISO low-density LTI coated fissile and fertile particles in an injection molded fuel rod with a 79% phenolic resin binder-21% graphite powder filler matrix

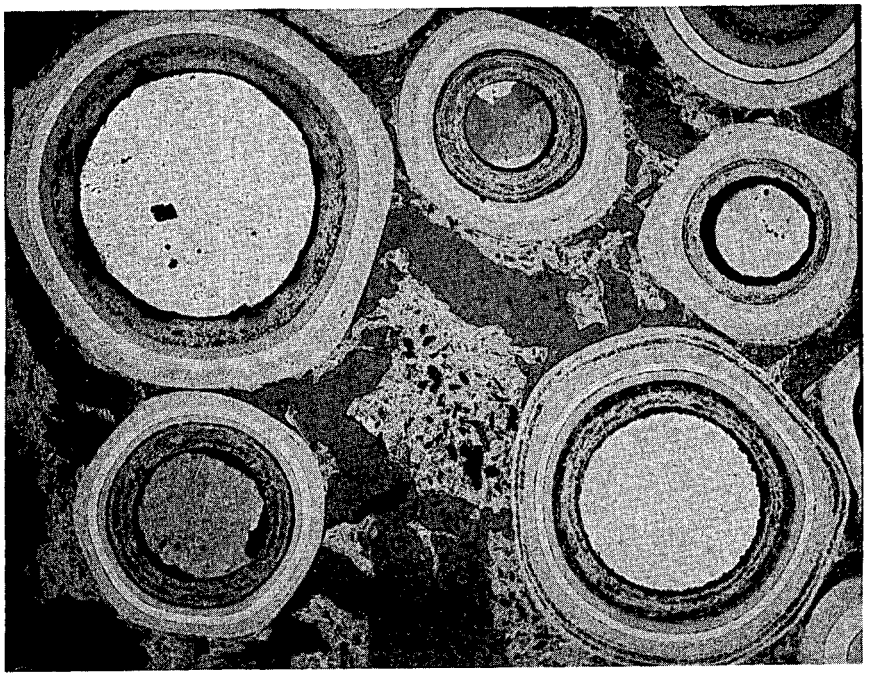

M31818-1 75X

Fig. 6-15. Fuel rod No. 891, 1.00-in. long; TRISO high-density LTI coated fissile and fertile particles in an injection molded fuel rod with a 79% phenolic resin binder-21% graphite powder filler matrix

Ninety of the 122 rods met the ±10% per in. requirement. The data are in Table 6-11 and the results obtained from the PTE-2 fuel rods are given in Table 6-12.

Tables 6-13 and 6-14 list the fuel rods made by FOD for PTE-2. These tables give the percentage of uranium loading deviation, as compared to standards. In some cases, the ±10% homogeneity requirement was not met in the last 1 in. of the numbered end. This was to be expected because all rods were loaded with particles in a manner such that, when the die cavity was filled, the fertile particles were to flow a fraction of a second longer than the fissile particles.

Differences in the total uranium loading from the exact nominal value can be attributed to two possible causes: the first would be an error in the chemical analysis of the particles in the standard rod or the particles in the production rod; the second would be an error in the gamma-counting equipment which could cause it to read unreproducibly.

The requirement of ±10% U/in. was not met in 32 of the 122 rods. In all cases the deviation was at the top end of the rod, as fabricated, and in the -10% direction, that is, less than nominal uranium. This deviation is not unexpected since in rod fabrication the loading process is designed to avoid an excess of uranium at the top end.

6.3.4. Fission-Product-Release Evaluation

Measurement of the release of inert fission gases from fuel rods during irradiation in the TRIGA King furnace facility was adopted as a quality control procedure during fabrication of fuel rods for the PTE-2. Since both BISO and TRISO coatings are excellent barriers to the release of fission gases, the measured fractional releases (R/B)* from fuel rods are a measure of the amount of exposed uranium in the fuel rods. This exposed uranium may be present:

*R/B is the ratio of the release rate to the birthrate from each isotope. It is the instantaneous value of the fractional release normally measured under steady-state conditions.

TABLE 6-11
RESULTS OF GAMMA-SCANNING OF FUEL RODS
USED IN TEST ELEMENT

	Rod Length (in.)				
	1.00	5.93	11.53	14.31	Total
No. of rods fabricated	45	12	29	38	124
No. of rods meeting the total uranium requirement, ±5%	44[a]	12[b]	29	37[c]	122
No. of rods meeting the uranium per inch requirement, ±10%	44[a]	7[b]	23	16[c]	90

[a] Rod No. 5A not counted.

[b] There were no standards available for this evaluation. Values indicate that 12 and 7 rods were within 5% and 10% of the average for those 12 rods.

[c] Rod No. 464 not counted.

TABLE 6-12
PTE-2 FUEL ROD GAMMA SCAN RESULTS

Rod No.	Nominal Length Fuel Rod (in.)	Percent Uranium Loading Deviation
526	14.31	-2.7
546	14.31	+0.8
549	14.31	-3.6
551[(a)]	14.31	-0.1
552	14.31	-4.1
553[(a)]	14.31	-2.8
556	14.31	-3.5
560[(a)]	14.31	-3.6
562[(a)]	14.31	-2.9
566[(a)]	14.31	-1.8
568[(a)]	14.31	-2.3
571	14.31	+2.3
572	14.31	+2.0
573	14.31	+2.7
574[(a)]	14.31	+3.7
575[(a)]	14.31	+2.9
576[(a)]	14.31	+3.1
577	14.31	+3.6
578	14.31	+4.1
579	14.31	+2.7
581[(a)]	14.31	+2.1
582	14.31	+4.0
583[(a)]	14.31	+3.6
584[(a)]	14.31	+0.3
585	14.31	+3.5
586[(a)]	14.31	+0.2
587	14.31	+3.0
588[(a)]	14.31	+3.6
957[(a)]	14.31	-4.9
960[(a)]	14.31	-4.3
978[(a)]	14.31	+2.9
980[(a)]	14.31	+3.1

TABLE 6-12 (Continued)

Rod No.	Nominal Length Fuel Rod (in.)	Percent Uranium Loading Deviation
983[a]	14.31	+3.3
985[a]	14.31	+3.6
986	14.31	+2.3
996	14.31	+2.4
9-chipped[a]	14.31	+3.7
7A[a]	11.53	+1.5
9A	11.53	+1.5
19A[a]	11.53	-1.3
20A	11.53	+1.8
21A[a]	11.53	-0.4
22A	11.53	+2.7
23A[a]	11.53	+1.0
925	11.53	+3.4
937	11.53	+1.0
938	11.53	+1.3
940	11.53	+2.0
941	11.53	+0.8
942	11.53	-0.2
49	5.93	+0.3
51	5.93	0.0
53	5.93	+0.1
54	5.93	+1.9
55	5.93	-0.3
56[a]	5.93	+1.8
57[a]	5.93	0.0
58[a]	5.93	+1.2
61[a]	5.93	+0.6
62	5.93	-0.4
63[a]	5.93	+1.3
64	5.93	-0.6
2A	1.00	-0.9
4A	1.00	0.0

TABLE 6-12 (Continued)

Rod No.	Nominal Length Fuel Rod (in.)	Percent Uranium Loading Deviation
890	1.00	-2.9
892	1.00	-2.9
894	1.00	-2.0
902	1.00	-2.5
903	1.00	-2.9
904	1.00	-3.0
905	1.00	-2.4
906	1.00	-2.5
823	1.00	+0.1
824	1.00	+0.7
825	1.00	+0.7
826	1.00	+1.3
828	1.00	+1.9
829	1.00	+1.0
830	1.00	+0.4
831	1.00	-0.2
832	1.00	+1.7
833	1.00	+1.6
841	1.00	+0.6
842	1.00	+1.2
843	1.00	+0.2
844	1.00	+1.2
845	1.00	+1.7
846	1.00	+0.1
847	1.00	-0.5
848	1.00	+0.5
850	1.00	+0.4
851	1.00	-0.1
852	1.00	
919	1.00	+0.3
920	1.00	+2.9
922	1.00	+3.8

TABLE 6-12 (Continued)

Rod No.	Nominal Length Fuel Rod (in.)	Percent Uranium Loading Deviation
931	1.00	+1.7
932	1.00	+2.8
935	1.00	+1.2
943	1.00	+0.3
944	1.00	+3.4
945	1.00	+2.9
946	1.00	+3.6
948	1.00	+3.5
949	1.00	-1.4
952	1.00	-1.5
The following PTE-2 fuel rods were not gamma scanned:		
464	14.31	
835	11.53	
836	11.53	
838	11.53	
840	11.53	
853	11.53	
854	11.53	
855	11.53	
856	11.53	
857	11.53	
858	11.53	
907	11.53	
908	11.53	
909	11.53	
910	11.53	
911	11.53	
912	11.53	
5A	1.00	

[a]The last 1 in. of the numbered end did not meet the ±10% homogeneity requirement.

TABLE 6-13
FUEL OPERATIONS LTI HIGH-DENSITY RODS
USED IN PTE-2

Loading	Fuel Rod	% U Loading Deviation
2	526	-2.7
	568	-2.3
	556	-3.5
	464	--
3	560	-3.6
	562	-2.9
	553	-2.8
4	566	-1.8
5	549	-3.6
	552	-4.1
6	551	-0.1
	584	+0.3
	586	+0.2
	546	+0.8
16	957	-4.9
	960	-4.3

TABLE 6-14
FUEL OPERATIONS LTI LOW-DENSITY RODS
USED IN PTE-2

Loading	Fuel Rod	% U Loading Deviation
7	582	+4.0
	587	+3.0
	573	+2.7
	577	+3.6
	578	+4.1
8	571	+2.3
	572	+2.0
	585	+3.5
	583	+3.6
	579	+2.7
9	581	+2.1
	588	+3.6
	574	+3.7
	576	+3.1
	575	+2.9
10	983	+3.3
	985	+3.6
	9--[a]	+3.7
	978	+2.9
	980	+3.1
11	986	+2.3
	996	+2.4

[a] Fuel rod chipped, last two digits unknown.

1. On the surface of the coatings of the fuel particles

2. Within a recoil distance of the surface of the coating (approximately 15 μm)

3. In the carbonized matrix

4. In particles cracked or broken during rod fabrication

The specification for PTE-2 fuel rods (Ref. 19) lists the following maximum acceptable steady-state release values (R/B) for the fission gas nuclides:

Xe-139	1×10^{-6}
Xe-138	3×10^{-6}
Kr-89	4×10^{-6}
Kr-88	3×10^{-5}
Kr-87	2×10^{-5}
Kr-85m	4×10^{-5}

These values were based on data obtained from the GAIL IV irradiation capsule and were used to calculate expected activity levels in the Fort St. Vrain plant. It was therefore one of the objectives of PTE-2 to equal the performance expected of the Fort St. Vrain fuel.

Thirty-one fuel rods, 16 from the Fuel Operations Division (FOD) and 15 from the Fuel Materials Branch (FMB), were irradiated in the King furnace, and the fission gas release rate was measured as part of a quality control program to evaluate fabrication techniques and to determine the acceptability of the fuel rods for use in Fort St. Vrain PTE-2. These 31 test rods represent one sample from each production lot of fuel rods.

The rods were irradiated at approximately 10^{14} fissions for 1 hr at 1000°C and the fission gases were collected and counted as described previously (Ref. 20).

Corrections to compensate for the nonattainment of steady-state (Ref. 20) conditions for the longer-lived nuclides were not applied to the experimental data.* These corrections, which had been used in earlier studies, were found to be inapplicable to the current measurements. The corrections are based on a model which assumes that the gas release from the fuel particles is a diffusion-controlled process which would be expected to show a marked dependence on the half-life of the nuclide. Detailed studies, reported elsewhere (Ref. 21), have shown that this half-life dependence was absent and that under the test conditions of the TRIGO King furnace experiment, the release of fission gases is primarily due to recoils from contamination in the PyC coating rather than being a diffusion-controlled process. A recoil-controlled phenomenon should not be half-life dependent.

The data obtained for specimen rods fabricated by FOD are given in Table 6-15 and for those fabricated by FMB in Table 6-16.

The fuel rods tested were fabricated from LTI low-density, LTI high-density, or HTI particles. (All particles were of the TRISO-II design.) Eight of the 16 rods fabricated by FOD were made from LTI high-density particles, of which seven exceeded the specified release value for the short-lived isotopes. Four of the remaining eight FOD rods, fabricated from LTI low-density particles, met all the release specifications (Ref. 19). Only five of the 16 rods fabricated met the release specification for all the short-lived isotopes; all but one rod met the release specification for the longer-lived krypton isotopes. Of the 11 batches of fuel rods (represented by sample fuel rods No. 456, 569, 559, 550, 570, 958, 580, 587, 979, 977, and 994) used in PTE-2, six did not meet some part of the release specification - generally the shorter lived X3-138 and Xe-139 limits. All 11 batches met the Kr-85m specification. In the FSV initial core, the only release specification to be met was the Kr-85m specification. The six batches not meeting the specification were used because no additional batches could be fabricated in time to meet the scheduled date of PTE-2 insertion into the Peach Bottom reactor.

---

*Kr-85m, Kr-88, Kr-87, and Xe-138 do not reach a steady state in 1 hr.

TABLE 6-15
FISSION GAS RELEASE FROM PROOF TEST FUEL RODS FABRICATED BY
THE FUEL OPERATIONS DIVISION

Sample No.	Release Fraction					
	Kr^{85m}	Kr^{88}	Kr^{87}	Kr^{89}	Xe^{138}	Xe^{139}
LTI High Density						
Sample 1 Loading 1	3×10^{-6}	4×10^{-6}	4×10^{-6}	1×10^{-5}(a)	1×10^{-5}(a)	7×10^{-6}(a)
456 Loading 2	2×10^{-6}	3×10^{-6}	3×10^{-6}	3×10^{-6}	3×10^{-6}	9×10^{-7}
569 Loading 3	3×10^{-6}	4×10^{-6}	4×10^{-6}	3×10^{-6}	5×10^{-6}(a)	3×10^{-6}(a)
559 Loading 4	3×10^{-6}	3×10^{-6}	1×10^{-6}	3×10^{-6}	2×10^{-6}	3×10^{-6}(a)
550 Loading 5	2×10^{-6}	3×10^{-6}	2×10^{-6}	3×10^{-6}	3×10^{-6}	2×10^{-6}(a)
570 Loading 6	4×10^{-6}	7×10^{-6}	3×10^{-6}	5×10^{-6}(a)	5×10^{-6}(a)	2×10^{-6}(a)
963 Loading 15	2×10^{-5}	3×10^{-5}	2×10^{-5}	3×10^{-5}(a)	3×10^{-5}(a)	1×10^{-5}(a)
958 Loading 16	2×10^{-6}	4×10^{-6}	2×10^{-6}	7×10^{-6}	6×10^{-6}(a)	3×10^{-6}(a)
LTI Low Density						
580 Loading 7	2×10^{-6}	1×10^{-6}	7×10^{-7}	1×10^{-6}	1×10^{-6}	1×10^{-6}
589 Loading 8	3×10^{-6}	3×10^{-6}	2×10^{-6}	3×10^{-6}	2×10^{-6}	1×10^{-6}
979 Loading 9	3×10^{-5}	3×10^{-5}	2×10^{-5}	9×10^{-6}(a)	1×10^{-5}(a)	4×10^{-6}(a)
977 Loading 10	5×10^{-6}	6×10^{-6}	3×10^{-6}	3×10^{-6}	3×10^{-6}	4×10^{-7}
994 Loading 11	3×10^{-6}	3×10^{-6}	1×10^{-6}	2×10^{-6}	2×10^{-6}	6×10^{-7}
976 Loading 12	3×10^{-5}	3×10^{-5}	3×10^{-5}(a)	2×10^{-5}(a)	2×10^{-5}(a)	5×10^{-6}(a)
993 Loading 13	2×10^{-5}	2×10^{-5}	2×10^{-5}	2×10^{-5}(a)	2×10^{-5}(a)	5×10^{-6}(a)
972 Loading 14	9×10^{-5}(a)	7×10^{-5}(a)	7×10^{-5}(a)	6×10^{-5}(a)	6×10^{-5}(a)	2×10^{-5}(a)
Fuel Rod Leaching Experiment						
25A	4×10^{-6}	4×10^{-6}	3×10^{-6}	5×10^{-6}	6×10^{-6}	5×10^{-6}
33A	3×10^{-6}	4×10^{-6}	3×10^{-6}	3×10^{-6}	3×10^{-6}	4×10^{-6}

(a) Denotes value exceeds specification.

TABLE 6-16
FISSION GAS RELEASE FROM PROOF TEST FUEL RODS FABRICATED BY
THE FUEL MATERIALS BRANCH

Sample No.	Release Fraction					
	Kr^{85m}	Kr^{88}	Kr^{87}	Kr^{89}	Xe^{138}	Xe^{139}
LTI High Density						
877	1×10^{-5}	1×10^{-5}	1×10^{-5}	7×10^{-6}(a)	7×10^{-6}(a)	4×10^{-6}(a)
889	2×10^{-6}	2×10^{-6}	8×10^{-7}	1×10^{-6}	2×10^{-7}	3×10^{-7}
901	2×10^{-6}	3×10^{-6}	1×10^{-6}	1×10^{-6}	6×10^{-7}	9×10^{-7}
918	2×10^{-6}	1×10^{-6}	3×10^{-7}	3×10^{-7}	2×10^{-7}	2×10^{-7}
953	2×10^{-6}	2×10^{-6}	1×10^{-6}	2×10^{-6}	2×10^{-6}	1×10^{-6}
24A	5×10^{-7}	6×10^{-7}	3×10^{-7}	3×10^{-7}	3×10^{-7}	3×10^{-7}
LTI Low Density						
924	1×10^{-6}	2×10^{-6}	1×10^{-6}	2×10^{-6}	9×10^{-7}	8×10^{-7}
936	6×10^{-6}	6×10^{-6}	6×10^{-6}	3×10^{-6}	3×10^{-6}	2×10^{-6}(a)
947	2×10^{-6}	2×10^{-6}	3×10^{-7}	2×10^{-7}	3×10^{-7}	5×10^{-7}
13A	2×10^{-5}	2×10^{-5}	2×10^{-5}	2×10^{-5}(a)	2×10^{-5}(a)	1×10^{-5}(a)
HTI						
834	2×10^{-6}	3×10^{-6}	1×10^{-6}	3×10^{-6}	3×10^{-6}	1×10^{-6}
849	2×10^{-6}	3×10^{-6}	1×10^{-6}	3×10^{-6}	3×10^{-6}	4×10^{-7}
870	9×10^{-6}	7×10^{-6}	8×10^{-6}	6×10^{-6}(a)	5×10^{-6}(a)	2×10^{-6}(a)
3A	3×10^{-6}	3×10^{-6}	2×10^{-6}	5×10^{-6}(a)	4×10^{-6}(a)	2×10^{-6}(a)
51A	4×10^{-6}	6×10^{-6}	3×10^{-6}	4×10^{-6}	3×10^{-6}	2×10^{-6}(a)

(a) Denotes value exceeds specification.

Of the 15 FMB rods tested, six were fabricated from LTI high-density particles, four from LTI low-density particles, and five from HTI particles. Six of the 15 rods exceeded the maximum acceptable release values; one of the six was fabricated from LTI high-density, two from LTI low-density, and three from HTI particles. In none of the cases did the release for the longer-lived krypton isotopes exceed specifications. Since both FMG and FOD used the same fuel-particle batches in rod fabrication, it appears that fuel rods fabricated by FMB are of a slightly higher quality than those fabricated by FOD. Of the 10 batches of fuel rods (represented by sample fuel rods 889, 901, 953, 24A, 924, 936, 947, 834, 849, and 3A) used in PTE-2, two did not meet the release specification. Again, all 10 batches did meet the Kr-85m specification which was the only specification used for the FSV initial core fuel rods. The two batches not meeting the specification were also used because no additional batches could be fabricated in time to meet the date of PTE-2 insertion into the Peach Bottom reactor.

7. PIGGYBACK IRRADIATION SPECIMENS

Piggyback samples of various fuel and graphite materials were prepared for irradiation in the Fort St. Vrain Proof Test Element No. 2 (PTE-2) so that the behavior of the component materials can be compared with that of the composite fuel rods and graphite elements. Also, the performance of these materials can be determined in an HTGR flux spectrum rather than in a water test reactor spectrum.

The samples being tested are:

1. Loose coated particles from each of the 14 batches or blends being used in the fuel rods

2. HTI PyC and SiC coating structures, both restrained and unrestrained.

3. Matrix material of the type being used in the fuel rods

4. Graphite samples of interest to HTGR

7.1. DESCRIPTION OF SPECIMENS

7.1.1. Coated Particles

Coated particle samples from each of the 14 batches used in the proof test element fuel rods are being tested in piggyback locations as loose particles contained in individual graphite crucibles. Eight samples were taken from individual batches and the remaining six were taken from composite blends of 15 individual batches, just as they were used in the element. Descriptions of the samples are given in Table 7-1. Photographs of the loaded crucibles are in Fig. 7-1.

TABLE 7-1
DESCRIPTION OF COATED-PARTICLE SAMPLES BEING TESTED AS PIGGYBACK SAMPLES IN PTE-2[a]

Batch Number (Data Retrieval)	Coating								Particle	
	Buffer		Inner Isotropic Thickness[b] (μm)	SiC Thickness (μm)	Outer Isotropic			Total Thickness (μm)		
	Thickness[b] (μm)	Density (g/cm^3)			Thickness (μm)	Density (g/cm^3)	BAF		Type	Diam. (μm)
4000-701	44	1.16	17	21	33	1.93	1.01	112	$(Th,U)C_2$	194
-703	44	1.25	17	20	32	1.97	1.11	108	$(Th,U)C_2$	194
-745	43	1.20	29	20	27	1.83	1.08	112	$(Th,U)C_2$	194
-744	44	1.31	16	21	33	1.87	1.12	108	$(Th,U)C_2$	194
-748	46	1.03	18	21	28	1.89	1.12	109	$(Th,U)C_2$	194
-704	43	1.08	19	22	43	1.91	1.06	123	ThC_2	393
-702	43	1.15	24	20	44	1.93	1.06	128	ThC_2	432
-707	44	1.01	23	21	37	1.86	1.05	118	ThC_2	378
-706	45	1.12	20	19	45	1.88	1.08	127	ThC_2	408
-733	40	1.12	25	19	36	1.98	1.03	122	ThC_2	471
-734	40	1.12	25	19	44	1.91	1.02	128	ThC_2	471
-737	46	1.12	18	20	44	1.91	(c)	119	ThC_2	392
-752	43	1.13	25	17	37	1.93	1.10	119	ThC_2	374
-742	49	1.05	28	19	37	1.97	1.12	128	ThC_2	374

[a] In many cases the values in this table are average values. Complete details on coated particles may be found in Section 5.

[b] Seal coats included. Density and BAF not determined.

[c] Not determined.

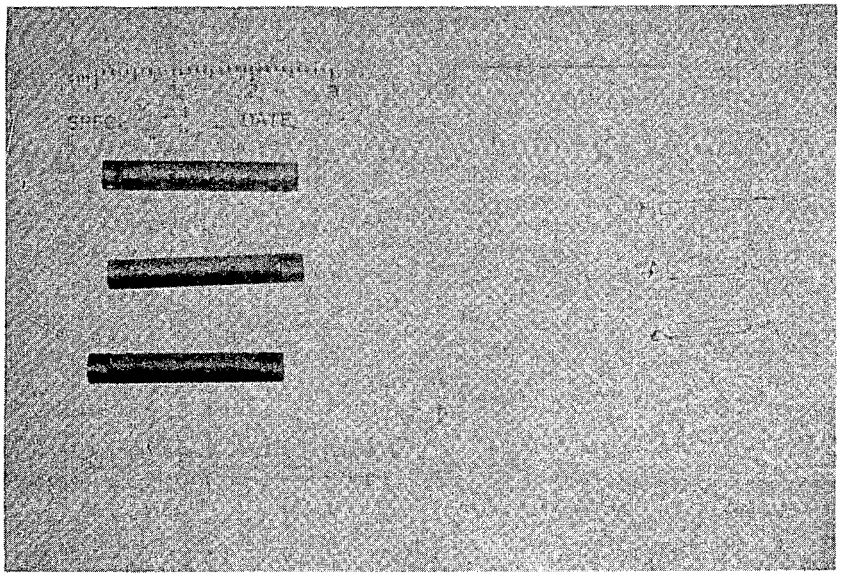

MC38570-10

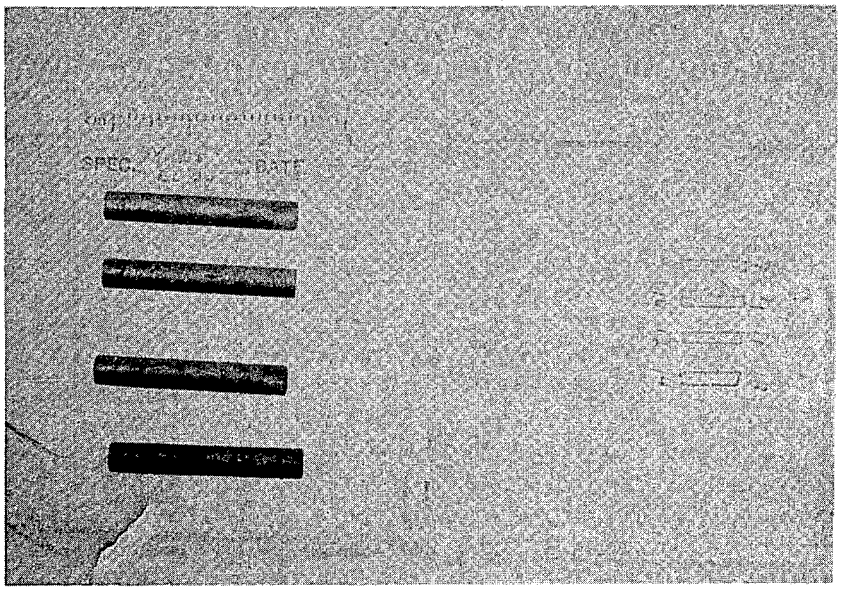

MC38570-9

Fig. 7-1. Photographs of loose coated particle piggyback samples (in graphite crucibles) included in PTE-2. Fissile coated particle samples are contained in crucibles 1 through 5; fertile coated particle samples are contained in crucibles 6 through 14

7.1.2. Pyrolytic carbon and Silicon Carbide Strips

Pyrolytic carbon (HTI) and SiC coating structures are included as piggyback samples in the proof test element. The HTI-PyC coatings are being tested as both restrained and unrestrained samples, while the SiC coatings are being tested as unrestrained strips only. A description of these samples is given in Table 7-2. Figure 7-2 contains a photograph of the loaded crucibles.

7.1.3. Matrix Material

Four samples of the matrix material used in PTE-2 fuel rods are being tested as piggyback specimens. The samples were all made by the injection-molding process using matrix formulation D-38 (Described in Section 6). A description of the samples is given in Table 7-3. Figure 7-3 contains a photograph of the four specimens.

7.1.4. Graphite Samples

Five graphites of interest to HTGR (H-327B, RC4, TS688, TS814, and 9567) are being tested as piggyback samples. Samples cut from both the parallel and perpendicular extrusion directions are being tested for dimensional change information. The samples are located in zone three of the element (See Section 7.2 below). The samples in fuel hole 7, within fuel rods 54 and 55, are rods approximately 1/8 in. in diameter and 1/2 in. long; those in the other fuel holes are discs approximately 1/2 in. in diameter and 1/8 in. thick. A detailed description of the graphite samples is given in Table 7-4. Photographs of representative samples of each of these two specimen types are contained in Fig. 7-4..

7.2. LOCATION OF SPECIMENS

The piggyback samples are located in several fuel holes in zone three of the proof test element. The majority of the samples are in fuel hole 7

TABLE 7-2
DESCRIPTION OF PyC AND SiC STRIPS BEING TESTED AS PIGGYBACK SAMPLES WITH PTE-2

Specimen Number	Coating Run Number	Density (g/cm^3)	BAF	Remarks
R-1	4174-137	1.55	1.18	Restrained HTI PyC specimens
R-2	4174-137	1.55	1.18	
R-3	4174-137	1.55	1.18	
1	4174-137	1.55	1.18	HTI-PyC strips, 40-mil wide
2	4174-137	1.55	1.18	
3	4174-137	1.55	1.18	
---	3662-111	--	--	8 SiC strips, 40-mil wide

TABLE 7-3
DESCRIPTION OF MATRIX MATERIALS BEING TESTED AS PIGGYBACK SAMPLES WITH PTE-2

Sample Number	Matrix[(a)]	Diameter (in.)	Length (in.)	Weight (g)	Method of Manufacture
GA3963-60-2 (2-60)	D-38	0.1510 - 0.1512	0.4910	0.1488	Injection molded
GA3963-60-4 (4-60)	D-38	0.1513 - 0.1517	0.4895	0.1508	Injection molded
GA3963-60-5 (5-60)	D-38	0.1510 - 0.1513	0.4930	0.1521	Injection molded
GA3963-60-6 (6-60)	D-38	0.1502 - 0.1503	0.4850	0.1496	Injection molded

[(a)] D-38 formulation: 21.0 w/o <30 μm GP38 graphite
47.4 w/o rezolin R-72S phenolic resin
15.8 w/o maleic anhydride
15.8 w/o nadic methyl anhydride

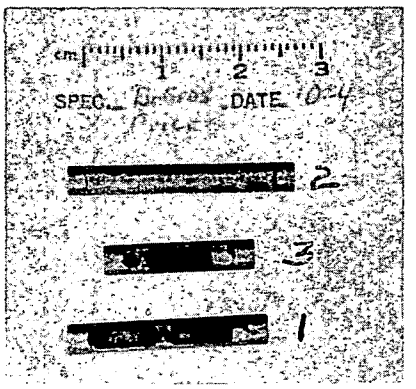

MC38570-8

Fig. 7-2. Photograph of pyrocarbon and silicon carbide piggyback samples in graphite crucibles included in PTE-2. The top crucible contains unrestrained PyC and SiC strips and the other two crucibles contain restrained PyC samples

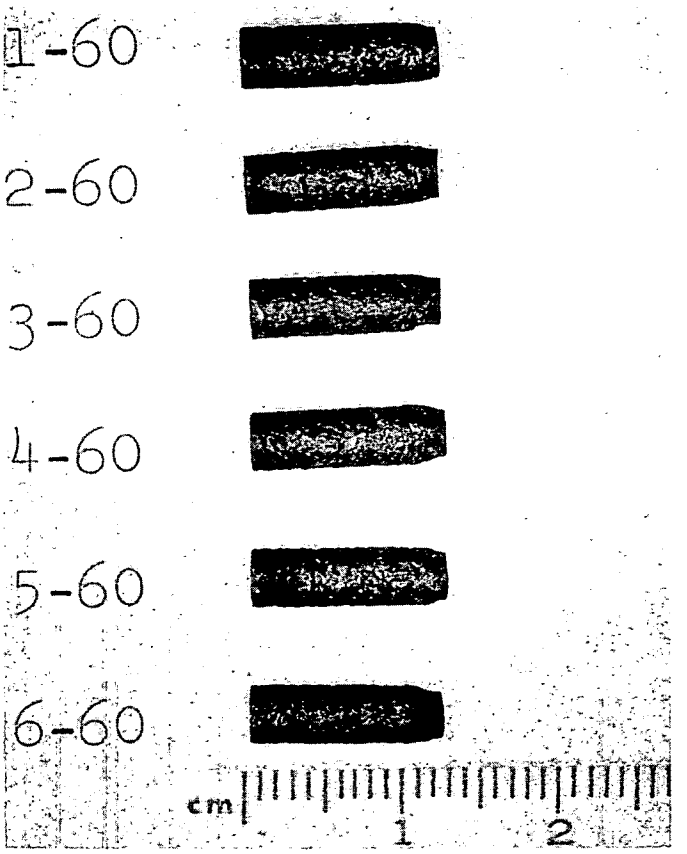

M27453-1

Fig. 7-3. Photograph of fuel rod matrix piggyback samples included in PTE-2. Four specimens (numbers 2-60, 4-60, 5-60, and 6-60) were used in the element; two specimens (numbers 1-60 and 3-60) were held as control samples

TABLE 7-4
DESCRIPTION OF GRAPHITE SAMPLES BEING TESTED AS PIGGYBACK SAMPLES WITH PTE-2

Specimen Number[a]	Extrusion Direction	Type of Graphite	Weight (g)	Diameter (in.)	Thickness (in.)
Rod 1	Perpendicular	9567	0.2321	0.1465	0.5005
Rod 2	Perpendicular	TS814	0.2546	0.1456	0.5150
Rod 3	Perpendicular	H327	0.2255	0.1457	0.4608
Rod 4	Perpendicular	TS688	0.2207	0.1460	0.4767
Rod 5	Perpendicular	H327	0.2306	0.1460	0.4613
Rod 6	Perpendicular	TS814	0.2482	0.1456	0.5034
Rod 7	Perpendicular	9567	0.2283	0.1456	0.5021
Rod 8	Perpendicular	TS814	0.2316	0.1461	0.4740
Rod 9	Perpendicular	H327	0.2172	0.1458	0.4346
Rod 10	Perpendicular	TS688	0.2337	0.1456	0.5049
Rod 11	Perpendicular	H327	0.2307	0.1460	0.4696
Rod 12	Perpendicular	TS814	0.2542	0.1455	0.5240
Disk F	Parallel	H327	0.5733	0.4409	0.1292
Disk I	Parallel	TS688	0.5524	0.4410	0.1299
Disk H	Perpendicular	H327	0.5687	0.4410	0.1289
Disk J	Parallel	TS688	0.5520	0.4409	0.1293
Disk B	Parallel	RC4	0.5554	0.4401	0.1287
Disk N	Parallel	9567	0.5659	0.4405	0.1291
Disk P	Perpendicular	9567	0.5626	0.4403	0.1285
Disk A	Parallel	RC4	0.5569	0.4401	0.1286
Disk D	Perpendicular	RC4	0.5540	0.4401	0.1286

[a] Rod samples are in zone 3, fuel rods numbered 54 and 55. Disk samples are in zone 3, bottom of fuel holes 2-6 and 9-12 (samples replaced push plugs).

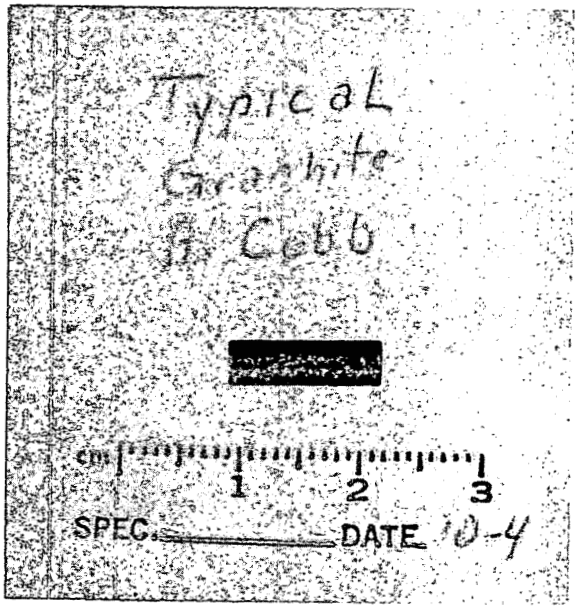

K97778

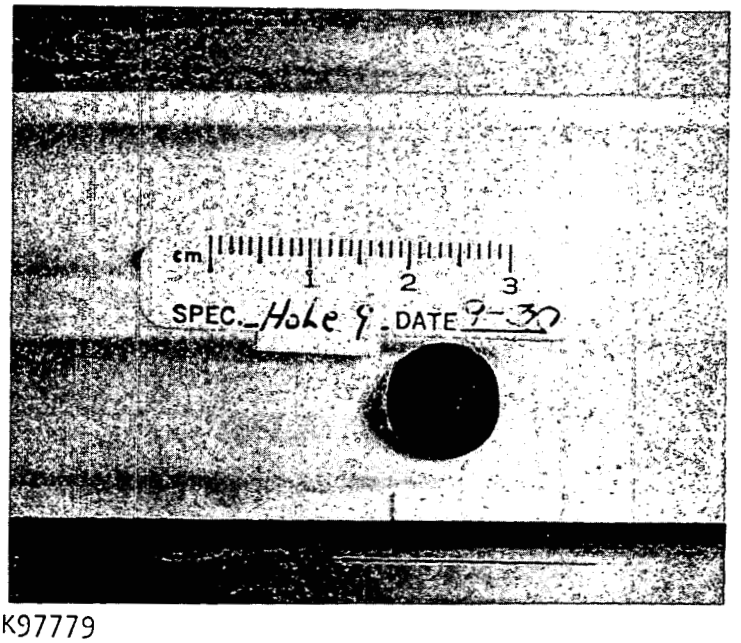

K97779

Fig. 7-4. Photographs of typical graphite rod samples (top) and typical graphite disc samples (bottom) included in PTE-2

and are located in the center of annular fuel rods. This fuel hole contains all four types of samples described above. The samples are 1/8 in. in diameter and occupy a total length of 17 in. They will be irradiated at a temperature of 1150 to 1200°C, which will be monitored by a nearby thermocouple, and they will receive a fast-neutron dose of about 1.3×10^{21} n/cm^2 (E > 0.18 MeV). A loading map of samples in this hole is given in Fig. 7-5.

The piggyback samples in other fuel holes in zone three (numbers 2, 3, 4, 5, 6, 9, 10, 11, and 12) are graphite discs inserted in the bottom of the holes, in place of the standard graphite push plugs. These discs are made of the various graphites described in Section 7.1.4 above, and each is nominally 1/2 in. in diameter and 1/8 in. thick. They will be irradiated at approximately the same temperature and to the same fast dose as those in fuel hole 7.

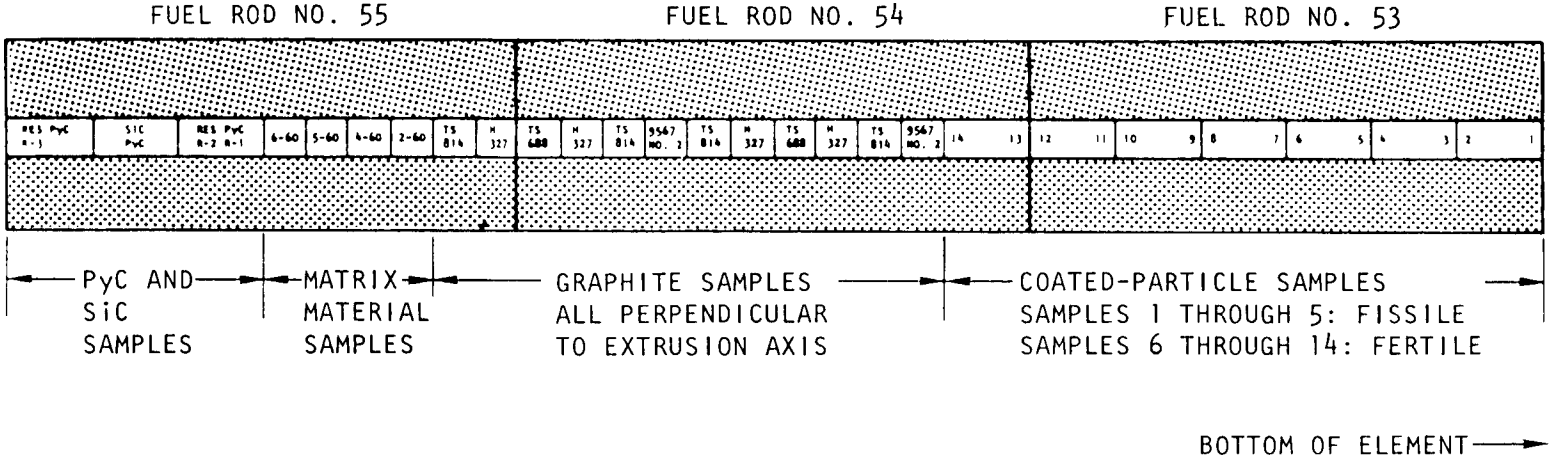

Fig. 7-5. Loading map for piggyback samples contained in zone three, Fuel Hole No. 7 of PTE-2

8. LOADING AND ASSEMBLY

The Capsule Group of the Fuels and Materials Division was responsible for the detail assembly procedure, design and manufacture of jigs, fixtures, and on-site shipping containers, procurement of all parts listed on the test element drawings, complete assembly of fuel bodies and test elements, and delivery to the Office of Nuclear Materials Control facility for insertion in a shipping container.

8.1. IDENTIFICATION OF FUEL SECTIONS

Each element has an identification number imprinted on the top reflector. Also a horizontal orientation groove from the center coolant hole to the corner of the hex is machined on the top face of the top reflector. The groove is aligned with the type B thermocouple. The groove is facing reactor north after installation, as shown on Fig. 3-1. In addition, on each of the four fuel zones, on the top reflector, bottom reflector, and bottom connector, the digit 2 has been engraved adjacent to the orientation groove. The top and bottom reflectors and the bottom connector have been marked at the top end of each section, while the four fuel zones are marked at the bottom of each section. In Fig. 8-4 the digit 2 is shown on the top reflector.

8.2. FUEL LOADING

To preclude handling damage to the fuel rods two initial ground rules were established regarding the loading of the fuel: (1) holes would be loaded only when the entire fuel hole loadings were available, and (2) the fuel rods would not be handled unless absolutely necessary. For this latter reason, two double troughs of the required height to slip-feed a fuel rod into its hole were made. A handling sequence was also adopted to minimize the possibility of accidentally dropping or otherwise damaging the

fuel rods. Several areas were prepared with a masslin cloth covering to handle the enriched fuel. The uncarbonized (green) fuel rods were emptied from the glass tubes in which they were received by sliding them directly into the troughs. Selected green rods were then identified by sticking a numbered tag containing the rod number molded into each fuel rod onto the trough alongside the fuel rod. Once identified, the trough with the fuel was moved to a masslin-covered pan and positioned for photography. Entire fuel rods were not photographed since the intention was to photograph the worst end and to include a representative surface condition. Table 8-1 lists the green fuel rods that were photographed; examples of these rods are shown in Fig. 8-1. After the fuel rod was photographed, the trough was moved to another masslin-covered table prepared for loading the fuel rod into the test element.

Each fuel hole within the graphite sections was visually examined and then cleaned with a special adapter attached to a portable vacuum cleaner.

A flat area, 1/4 in. wide by 2 in. long to be used as an orientation mark for hole numbering, was made by filing away a selected point between two flats of the hexagonal configuration of the graphite fuel zone. At the end opposite of this mark, 3/16-in. by 3/16-in. flats were filed in suitable numbers to denote the zone number. Cutoff marks were scribed circumferentially for posttest separation of the zones in the Hot Cell Facility. Two cuts will be required, one to open up the holes at the bottom of each fuel stack and the other above each fuel stack.

As each zone was prepared for loading, the pertinent drawing illustrating the kind of rod makeup required was posted on the wall. The numbers of the fuel rods and their materials were listed and published as the rods were made up. The numbers from these lists were assigned to the proper positions by locating them on the drawing.

Before each fuel rod was loaded, a graphite pusher plug approximately 0.250 in. long was inserted in each of the fuel rod holes. The ultimate use of this plug is to assist in the removal of the fuel rods for post-irradiation examination.

TABLE 8-1
LISTING OF THE PTE-2 FUEL RODS IN THE UNCARBONIZED (GREEN) CONDITION THAT WERE PHOTOGRAPHED

Fuel Zone No.	Hole No.	Fuel Rod No. Photographed
1	6	894, 21A
	10	920, 941
2	6	568, 552
	10	857, 830, 832, 831, 833, 562
3	3	576, 983
	6	582, 572
	10	577, 585, 943
	12	9--[a]
4	11	855
	12	912, 906

[a] Fuel rod chipped, last two digits unknown.

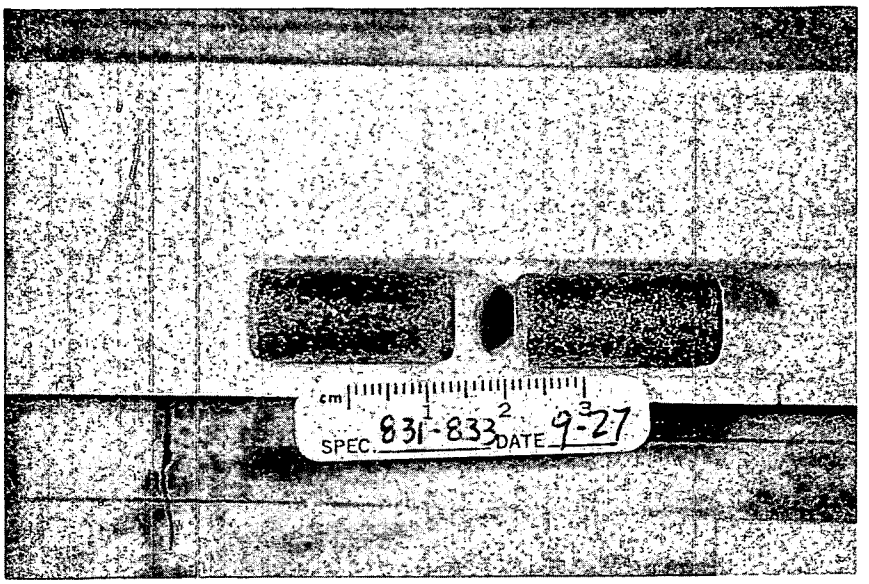

MC38570-5

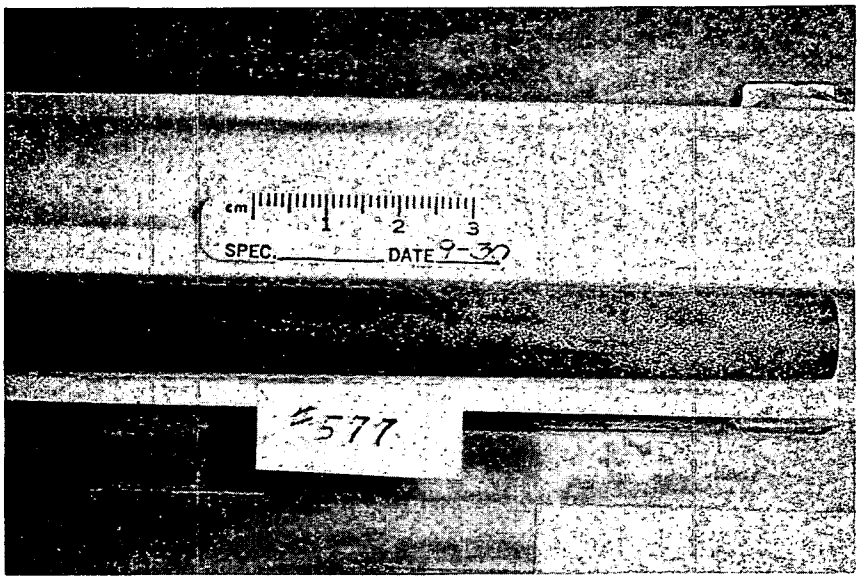

MC38570-4

Fig. 8-1. Typical examples of green fuel rods. One-in.-long fuel rods No. 831 and 833 were placed in fuel zone two, hole 10; 14.31-in.-long fuel rod No. 577 was placed in fuel zone three, hole 10

The loading of a fuel rod into its assigned place was performed by one individual and witnessed by another. As each rod was inserted in place, the rod number was written on the drawing to document the loading. An arrow was placed adjacent to the rod number and pointed to the direction in which the numbered end of the fuel-rod face was inserted into the fuel zone graphite. Figures 8-2, 8-3, 8-4, and 8-5 locate each fuel rod within each of the four fuel zones and indicate the orientation of each fuel rod. The void-space gap above each fuel stack is also indicated on these drawings.

All of the holes, with the exception of the 12 annular fuel rods in fuel zones one, two, and three and the 1.00-in.-long fuel rod in hole 11 of fuel zone four, were loaded with green fuel rods. All of the rods were then carbonized in place within the fuel zone as discussed in Section 6.2.4.

After carbonization, selected fuel rods were carefully pushed out of each fuel zone and photographed. Again, entire fuel rods were not photographed--only the worst end and a section to represent the general surface condition. Table 8-2 lists the carbonized fuel rods that were photographed. Examples of these rods are shown in Fig. 8-6.

After the postcarbonization photographs were taken, the selected fuel rods were returned to their respective fuel zones.

The annular fuel rods, above the termination point of the thermocouple, were loaded with the piggyback samples described in Section 4. After each hole was fully loaded, a polyethylene foam plug was fitted in the void between the fuel-rod stack and the graphite top plug. The top plugs were cemented in place with carbon cement Grade P-514.* Any excess cement was carefully removed. A typical view of a fuel zone with the fuel hole plugs cemented in place is shown in Fig. 8-7.

---

*Great Lakes Carbon Corporation.

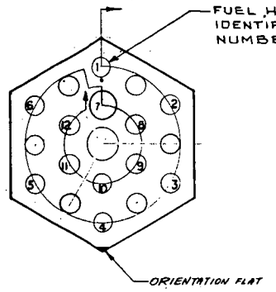

TOP VIEW

REFERENCE DIAMETERS

FUEL HOLE NUMBER	FUEL HOLE DIAMETER	FUEL ROD DIAMETER
1	.474 ± .001	.467 ± .003
2		
3		
4		
5		
6	.321 ± .001	.314 ± .003
7		
8	.474 ± .001	.467 ± .003
9		
10		
11		
12		

LOADING TABULATION
TABLE-ONE

FUEL ROD COMPOSITION	QUANTITY	REF ROD LENGTH	TYPE	TOTAL LENGTH
LHE	5 .5	11.53 1.00	SOLID	62.65
LHS	2	5.93	ANNULAR	11.86
LLE	6 6	11.53 1.00	SOLID	75.18

ROD COMPOSITION CODING	
FIRST LETTER TYPE OF OUTER COATING ON PARTICLE	L = LOW TEMP ISOTROPIC PYROCARBON H = HIGH TEMP ISOTROPIC PYROCARBON
SECOND LETTER DENSITY OF OUTER COATING ON PARTICLE	L = LOW DENSITY H = HIGH DENSITY
THIRD LETTER LOCATION OF FUEL ROD WHEN CARBONIZED	E = FUEL RODS CARBONIZED IN TEST ELEMENT GRAPHITE FUEL SECTION S = FUEL RODS CARBONIZED IN SPECIAL GRAPHITE HOLDERS

NOTES:
(1) ALL PARTICLES ARE TRISO TYPE II.
(2) ALL FUEL RODS UTILIZED A BINDER WITH 79 W/o BASE RESIN MIX AND 21 W/o GP 38 GRAPHITE FLOUR (SEE BELOW FOR BASE RESIN MIX FORMULATION.)
(3) ALL FUEL RODS WERE FABRICATED USING THE INJECTION MOLDING PROCESS.
(4) ALL FUEL RODS WERE CARBONIZED IN NITROGEN AT 1000°C.

— BASE RESIN MIX FORMULATION —
47.4 PARTS REZOLIN R 725
15.8 PARTS MALEIC ANHYDRIDE
15.8 PARTS NADIC METHYLANHYDRIDE

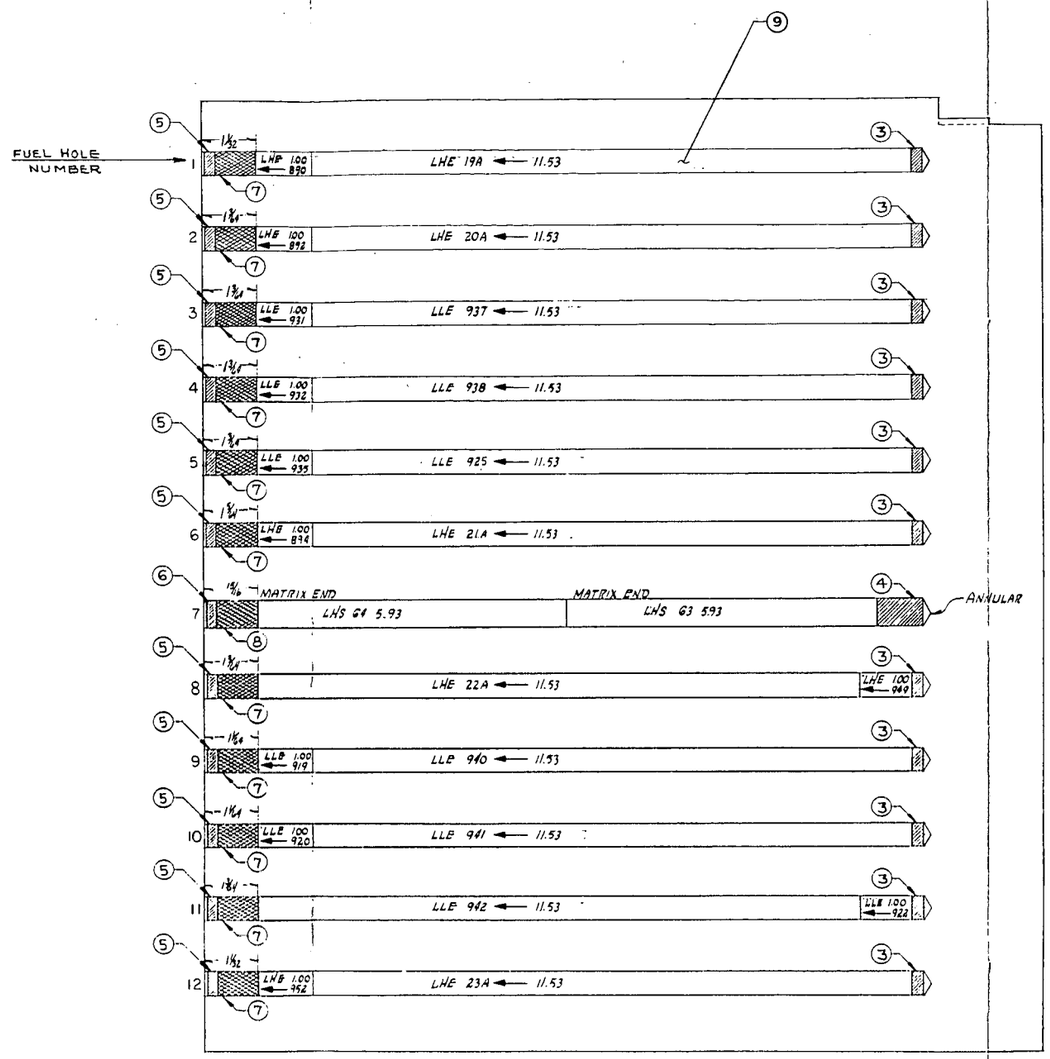

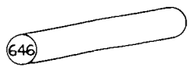

TYPICAL IDENTIFICATION OF FUEL RODS

ARROW INDICATES THE NUMBERED END OF THE FUEL ROD.

NOTES:
1- SEE DWG. 90/SK-1976 FOR DIMENSIONS.
2- THE GRAPHITE PLUGS ARE TO BE CEMENTED INTO PLACE WITH P-514 GRAPHITE CEMENT.

REQUIRED	ITEM	PART NO.	DESCRIPTION	MATL	MATL SPEC
			LIST OF MATERIAL		
AR	9		FUEL RODS	SEE TABLE ONE	
1	8		SPACER 0.5103 x 1912 x .29	POLYETHYLENE	—
11	7		SPACER 0.4430 x AR.	POLYETHYLENE	—
1	6		PLUG .5 900 x .3310 x 0.25	GRAPHITE	H-327
11	5		PLUG .471 DIA. X 0.25	↓	↓
1	4		PUSHER 0.507 0.22 x .3610 x .092		
11	3		PUSHER 0.460 DIA X 0.25		
1	2	90-SK-1976	FUEL SECTION ONE	GRAPHITE	H-327
	1		ASSEMBLY		

Fig. 8-2. Fuel zone one assembly

3

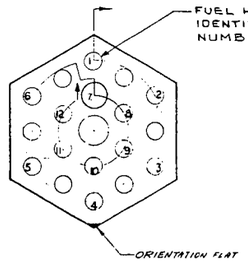

TOP VIEW

REFERENCE DIAMETERS

FUEL HOLE NUMBER	FUEL HOLE DIAMETER	FUEL ROD DIAMETER
1	.476 ± .001	.427 ± .001 .003
2		
3		
4		
5		
6		
7	.552 ± .001	.514 ± .001
8	.474 ± .001	.436 ± .001 .003
9		
10		
11		
12		

LOADING TABULATION
TABLE-ONE

FUEL ROD COMPOSITION	QUANTITY	PER ROD LENGTH	TYPE	TOTAL LENGTH
LHE	16	14.31	SOLID	230.96
	2	1.00		
LLS	5	5.93	ANNULAR	29.65
WHB	6	11.53	SOLID	90.8
	21	1.00		

ROD COMPOSITION CODING	
FIRST LETTER TYPE OF OUTER COATING ON PARTICLE	L = LOW TEMP ISOTROPIC PYROCARBON H = HIGH TEMP ISOTROPIC PYROCARBON
SECOND LETTER DENSITY OF OUTER COATING ON PARTICLE	_ = LOW DENSITY H = HIGH DENSITY
THIRD LETTER LOCATION OF FUEL ROD WHEN CARBONIZED	E = FUEL RODS CARBONIZED IN TEST ELEMENT GRAPHITE FUEL SECTION S = FUEL RODS CARBONIZED IN SPECIAL GRAPHITE HOLDERS

NOTES:
(1) ALL PARTICLES ARE TRISO TYPE II.
(2) ALL FUEL RODS UTILIZED A BINDER WITH 79% BASE RESIN MIX AND 21 W/o G.P. 38 GRAPHITE FLOUR (SEE BELOW FOR BASE RESIN MIX FORMULATION.)
(3) ALL FUEL RODS WERE FABRICATED USING THE INJECTION MOLDING PROCESS.
(4) ALL FUEL RODS WERE CARBONIZED IN NITROGEN AT 1000°C.

— BASE RESIN MIX FORMULATION —
47.4 PARTS REZOLIN R 725
15.8 PARTS MALEIC ANHYDRIDE
15.8 PARTS NADIC METHYLANHYDRIDE

NOTES
1. SEE DWG. 90/SK-1977 FOR DIMENSIONS.
2. THE GRAPHITE PLUGS ARE TO BE CEMENTED INTO PLACE WITH GRAPHITE CEMENT

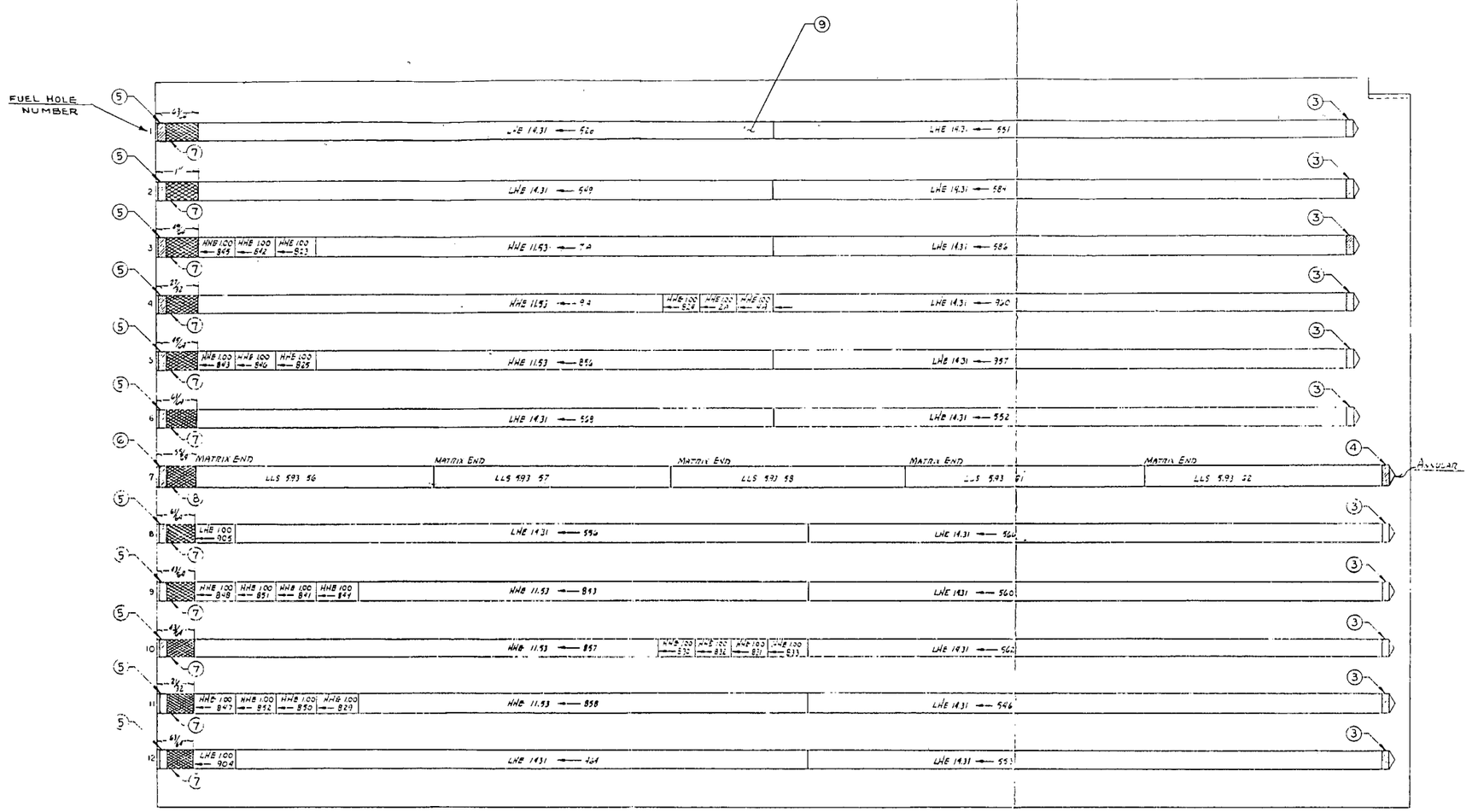

686

TYPICAL IDENTIFICATION OF FUEL RODS

ARROW INDICATES THE NUMBERED END OF THE FUEL ROD.

REQUIRED	ITEM	PART NO.	DESCRIPTION	MATL	MATL SPEC
			LIST OF MATERIAL		
AR	9		FUEL RODS	SEE TABLE ONE	
1	8		SPACER .500 O.D. x .250 I.D.	POLYETHYLENE	—
11	7		SPACER .500 O.D. x .A.R.	POLYETHYLENE	—
1	6		PLUG .500 O.D. x .A.R.	GRAPHITE	H-327
11	5		PLUG .471 O.D. x .25	↓	↓
1	4		PUSHER .500 O.D. x .A.R.	↓	↓
11	3		PUSHER .460 O.D. x .10	↓	H-327
1	2	90/SK-1977	FUEL ZONE TWO	GRAPHITE	9547
	1		ASSEMBLY		

Fig. 8-3. Fuel zone two assembly

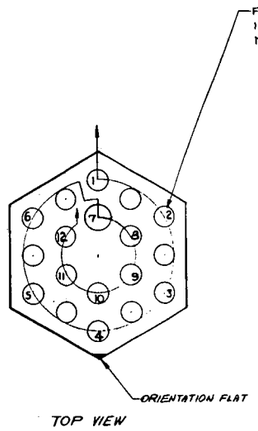

TOP VIEW

FUEL HOLE NUMBER

NOTES
1. SEE DWG. 90/SK-1978 FOR DIMENSIONS
2. THE GRAPHITE PLUGS ARE TO BE CEMENTED INTO PLACE WITH P-514 GRAPHITE CEMENT.

FUEL HOLE NUMBER	
1	LLE 14.31 — 575 / LLE 14.31 — 978
2	LLE 14.31 — 574 / LLE 14.31 — 980
3	LLE 14.31 — 576 / LLE 14.31 — 983
4	LLE 14.31 — 581 / LLE 14.31 — 985
5	LLE 14.31 — 588 / LLE 14.31 — 571
6	LLE 14.31 — 582 / LLE 14.31 — 572
7	MATRIX END LLS 5.93 55 / MATRIX END LLS 5.93 54 / MATRIX END LLS 5.93 53 / MATRIX END LLS 5.93 51 / MATRIX END LLS 5.93 49 — ANNULAR
8	LLE 1.00 — 940 / LLE 14.31 — 587 / LLE 14.31 — 579
9	LLE 14.31 — 573 / LLE 1.00 — 946 / LLE 14.31 — 583
10	LLE 14.31 — 577 / LLE 14.31 — 585 / LLE 1.00 — 943
11	LLE 14.31 — 578 / LLE 14.31 — 986 / LLE 1.00 — 944
12	LLE 14.31 — 9_ _ / LLE 14.31 — 996 / LLE 1.00 — 945

PVC & SiC SAMPLES; FOUR BERIA SAMPLES; TWO GRAPHITE SAMPLES; TEN GRAPHITE SAMPLES; TWO FERTILE PARTICLE BEDS; SEVEN FERTILE PARTICLE BEDS; FIVE FISSILE PARTICLE BEDS

REFERENCE DIAMETERS

FUEL HOLE NUMBER	FUEL HOLE DIAMETER	FUEL STICK DIAMETER
1	.474 ± .001	.467 +.001 −.003
2		
3		
4		
5		
6		
7	.572 ± .001	.374 +.001 −.003
8	.474 ± .001	.467 +.001 −.003
9		
10		
11		
12		

LOADING TABULATION
TABLE-ONE

FUEL ROD COMPOSITION	QUANTITY	REF. ROD LENGTH	TYPE	TOTAL LENGTH
LLE	22 5	14.31 1.00	SOLID	319.82
LLS	5	5.93	ANNULAR	29.65

"ROD" COMPOSITION CODING

FIRST LETTER TYPE OF OUTER COATING ON PARTICLE	L = LOW TEMP ISOTROPIC PYROCARBON H = HIGH TEMP ISOTROPIC PYROCARBON
SECOND LETTER DENSITY OF OUTER COATING ON PARTICLE	L = LOW DENSITY H = HIGH DENSITY
THIRD LETTER LOCATION OF FUEL ROD WHEN CARBONIZED	E = FUEL RODS CARBONIZED IN TEST ELEMENT GRAPHITE FUEL SECTION S = FUEL RODS CARBONIZED IN SPECIAL GRAPHITE HOLDERS

NOTES:
(1) ALL PARTICLES ARE TRISO TYPE II
(2) ALL FUEL RODS UTILIZED A BINDER WITH 79 W/O BASE RESIN MIX AND 21 W/O GP-38 GRAPHITE FLOUR (SEE BELOW FOR BASE RESIN MIX FORMULATION)
(3) ALL FUEL RODS WERE FABRICATED USING THE INJECTION MOLDING PROCESS
(4) ALL FUEL RODS WERE CARBONIZED IN NITROGEN AT 1000°C

LLE FUEL RODS — BASE RESIN MIX FORMULA:
47.4 PARTS REZOLIN R725
15.8 PARTS MALEIC ANHYDRIDE
15.8 PARTS NADIC METHYLANHYDRIDE
LLS FUEL RODS — BASE RESIN MIX FORMULA:
47.4 PARTS REZOLIN R725
15.8 PARTS MALEIC ANHYDRIDE
15.8 PARTS NADIC METHYLANHYDRIDE

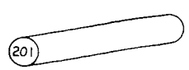

TYPICAL IDENTIFICATION OF FUEL RODS

ARROW INDICATES THE NUMBERED END OF THE FUEL ROD

REQUIRED	ITEM	PART NO.	DESCRIPTION	MATL	MATL SPEC
9	11		SPEC. SAMPLE PUSH .440 DIA. x .124	GRAPHITE	VARIOUS
1	10		PUSHER .507 OD x .160 ID x .25	GRAPHITE	H-327
3	9		DISK .507 DIA X 0.10	GRAPHITE	H-327
AS	8		FUEL RODS	SEE TABLE ONE	
11	7		SPACER .51 DIA X A.R.	POLYETHYLENE	—
11	6		SPACER .46 DIA X A.R.	POLYETHYLENE	—
11	5		PLUG .519 DIA X .25	GRAPHITE	H-327
11	4		PLUG .471 DIA X .25	↑	↑
2	3		PUSHER .460 DIA X .10	↑	↑
1	2	90-5K-1978	FUEL SECTION THREE	GRAPHITE	H-327
	1		ASSEMBLY		

LIST OF MATERIAL

Fig. 8-4. Fuel zone three assembly

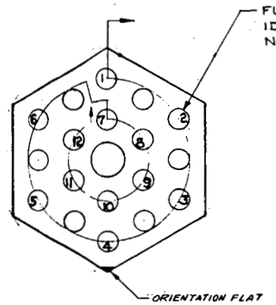

TOP VIEW

REFERENCE DIAMETERS

FUEL HOLE NUMBER	FUEL HOLE DIAMETER	FUEL ROD DIAMETER
1	.471 ±.001	.467 +.001 −.003
2		
3		
4		
5		
6		
7		
8		
9		
10		
11		
12		

LOADING TABULATION
TABLE-ONE

FUEL ROD COMPOSITION	QUANTITY	REF. ROD LENGTH	TYPE	TOTAL LENGTH
LHE	6 3	11.53 1.00	SOLID	72.18
HHE	6 2	11.53 1.00	SOLID	71.18
HHS	1	1.00	SOLID	1.00

ROD COMPOSITION CODING

FIRST LETTER TYPE OF OUTER COATING ON PARTICLE	L = LOW TEMP ISOTROPIC PYROCARBON H = HIGH TEMP ISOTROPIC PYROCARBON
SECOND LETTER DENSITY OF OUTER COATING ON PARTICLE	L = LOW DENSITY H = HIGH DENSITY
THIRD LETTER LOCATION OF FUEL ROD WHEN CARBONIZED	E = FUEL RODS CARBONIZED IN TEST ELEMENT GRAPHITE FUEL SECTION S = FUEL RODS CARBONIZED IN SPECIAL GRAPHITE HOLDERS

NOTES:
(1) ALL PARTICLES ARE TRISO TYPE II
(2) ALL FUEL RODS UTILIZED A BINDER WITH 79 W/O BASE RESIN MIX AND 21 W/O GP-38 GRAPHITE FLOUR (SEE BELOW FOR BASE RESIN MIX FORMULATION)
(3) ALL FUEL RODS WERE FABRICATED USING THE INJECTION MOLDING PROCESS.
(4) ALL FUEL RODS WERE CARBONIZED IN NITROGEN AT 1000°C

—BASE RESIN MIX FORMULA:—
47.4 PARTS REZOLIN R 725
15.8 PARTS MALEIC ANHYDRIDE
15.8 PARTS NADIC METHYLANHYDRIDE

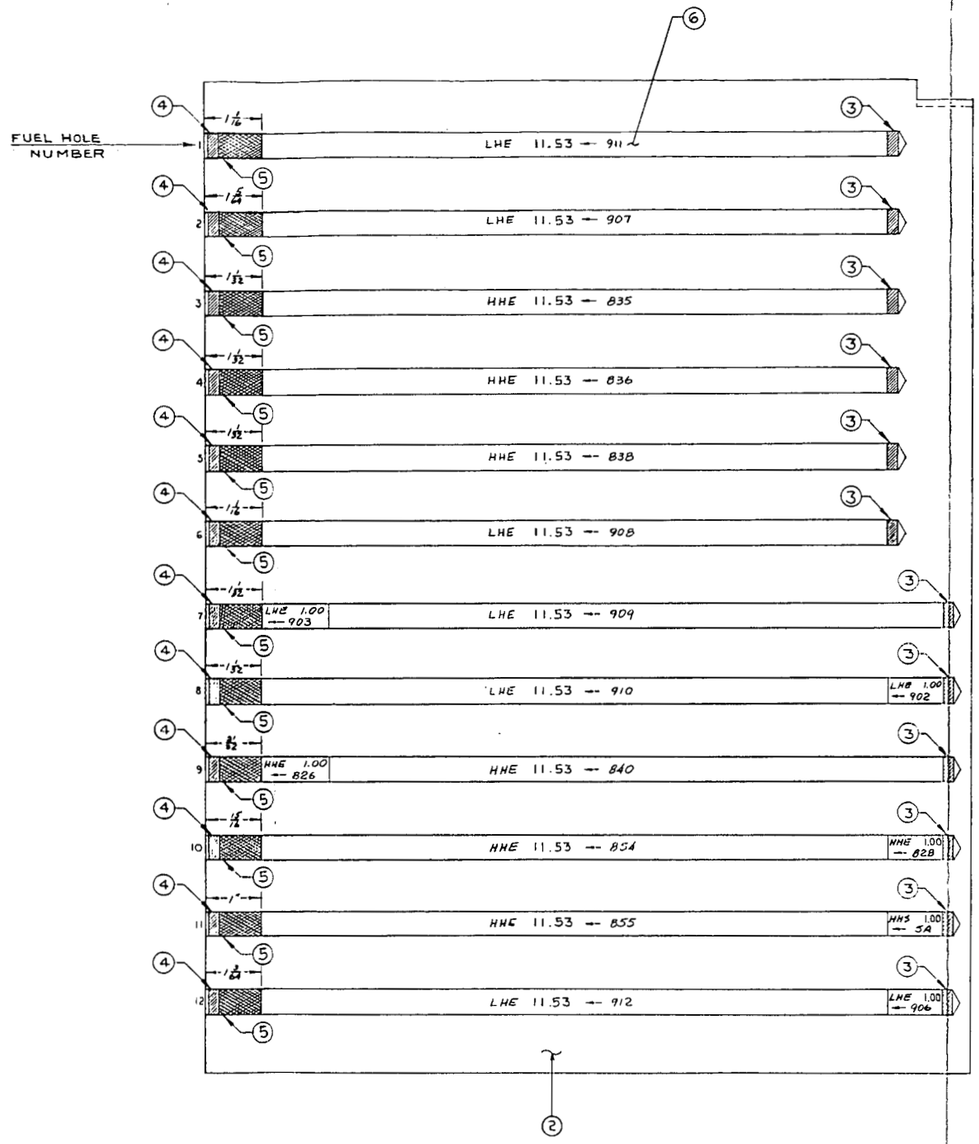

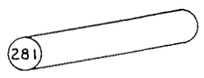

TYPICAL IDENTIFICATION OF FUEL RODS

ARROW INDICATES THE NUMBERED END OF THE FUEL ROD.

NOTES:
1- SEE DWG. 90/SK-1979 FOR DIMENSIONS.
2- THE GRAPHITE PLUGS ARE TO BE CEMENTED INTO PLACE WITH P-514 GRAPHITE CEMENT.

REQUIRED	ITEM	PART NO.	DESCRIPTION	MATL	MATL SPEC
AR	6		FUEL RODS	SEE TABLE ONE	
12	5		SPACER .46 DIA X A.R	POLYETHYLENE	—
12	4		PLUG .471 DIA X .25	GRAPHITE	H-327
12	3		PUSHER .460 DIA X .25	GRAPHITE	H-327
1	2	90-SK-1979	FUEL ZONE FOUR	GRAPHITE	H-327
	1		ASSEMBLY		

LIST OF MATERIAL

Fig. 8-5. Fuel zone four assembly

TABLE 8-2
LISTING OF THE PTE-2 FUEL RODS IN THE CARBONIZED CONDITION THAT WERE PHOTOGRAPHED AND DIMENSIONED PRIOR TO IRRADIATION

Fuel Zone No.	Hole No.	Fuel Rod No. Photographed
1	6	894, 21A
	7	64, 63
	10	920,[a] 941[a]
2	6	568, 552
	7	56, 57, 58, 61, 62
	10	857, 830, 832, 831, 833, 562
3	3	576, 983
	6	582, 572
	7	55, 54, 53, 51, 49
	10	577, 585, 943
4	1	911
	2	907
	3	835
	4	836
	5	838
	6	908
	7	903, 909
	8	910, 902
	9	826, 840
	10	854, 828
	11	855, 5A
	12	912, 906

[a] Rod 920 and 941 were photographed but not dimensioned. In addition, rod 940 in hole 9 of fuel zone 1 was dimensioned but not photographed.

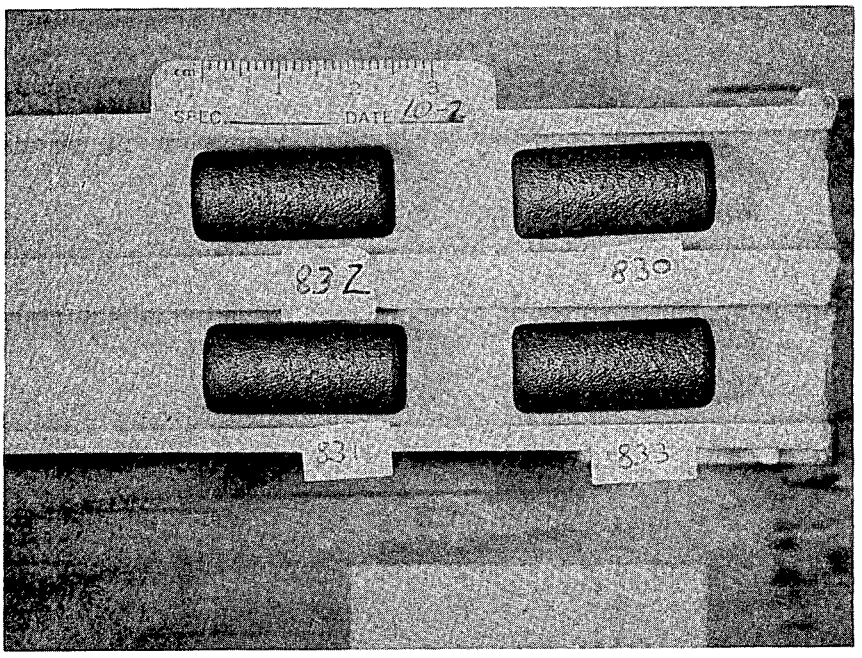

MC38570-3

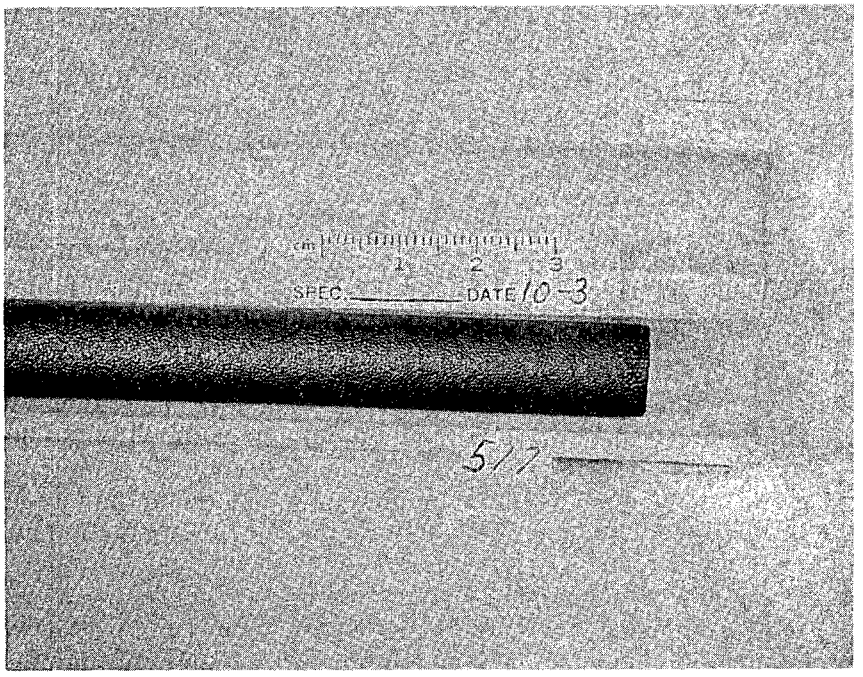

MC38570-2

Fig. 8-6. Typical examples of carbonized fuel rods; one-in.-long fuel rods No. 830, 831, 832, and 833 were placed in fuel zone two, hole No. 10; 14.31-in.-long fuel rod No. 577 was placed in fuel zone three, hole 10

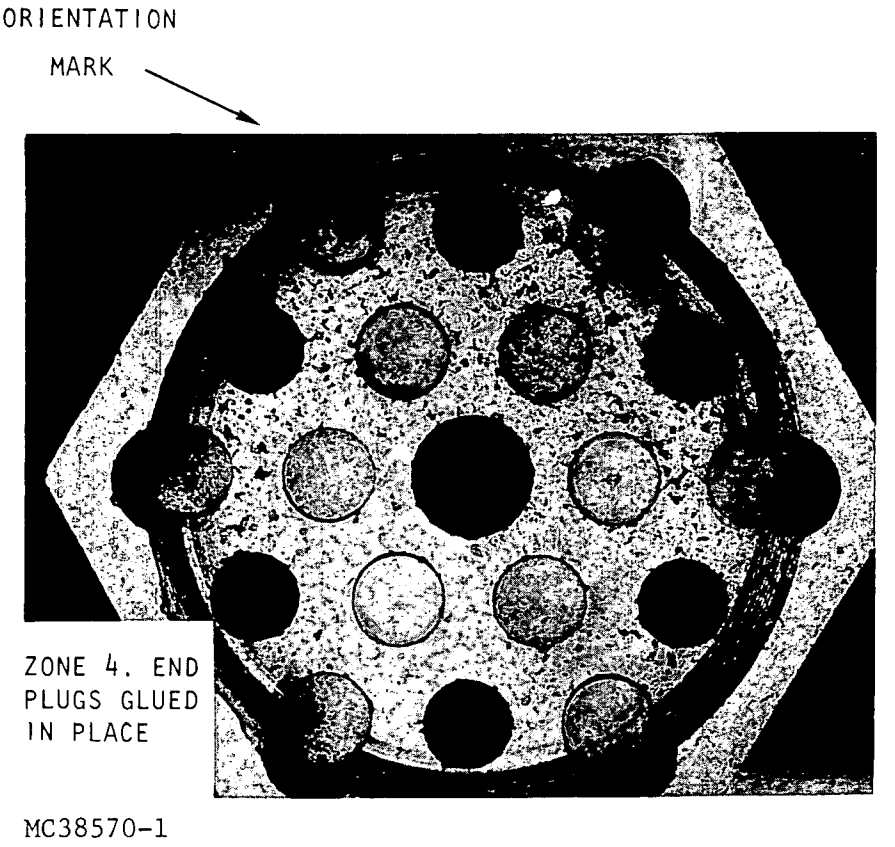

Fig. 8-7. End view of fuel zone four with the fuel hole plugs cemented in place

8.3. PTE-2 ASSEMBLY

Immediately prior to assembly of the element, the handling-tool lifting block was placed on the top of the bottom connector. When all of the zones had been loaded with fuel and capped off by cementing the plugs in place, the threaded portions of the graphite element components were brushed and vacuum cleaned to remove dust and particles. All of the threads were coated with primer, and P-514 cement was applied to both male and female threads just prior to assembling the individual sections. Immediately after assembling any two sections together, a wooden dowel with a cheesecloth-covered end was passed through the gas holes of each joint to remove any cement that had extruded into them. The gas passages were then examined visually as each section was added. The thermocouple holes were checked for alignment after each addition was made by inserting a rod of approximately the same diameter as the thermocouple.

The assembly was started by joining the bottom connector to the bottom reflector and was continued by using the assembly fixture (Dwgs. No. 90-SK-2071 and 90-SK-2209) until fuel zones one, two, and three were in place. At that point, the tungsten-3% rhenium/tungsten-25% rhenium and Chromel/Alumel thermocouples were installed in the element. Thermocouple response, resistance, and thermoelement identification were determined prior to installation. The installation was made so that the positive and negative leg of the elements aligned with the proper contacts. Joining of the thermoelements and the contacts was made by tungsten inert-gas welding. The screws holding the contact assembly were firmly seated and tack-welded to prevent loosening. The bottom of the element, together with the thermocouple contactor assembly, is shown in Fig. 8-8. The element area at the thermocouple hot junction was gently heated with a heated-air blower and the thermocouple response checked with a potentiometer. After ensuring that both thermocouples were operating properly, fuel zone four and the top reflector were added to complete the unit. The completely assembled PTE-2 is shown in Fig. 8-9.

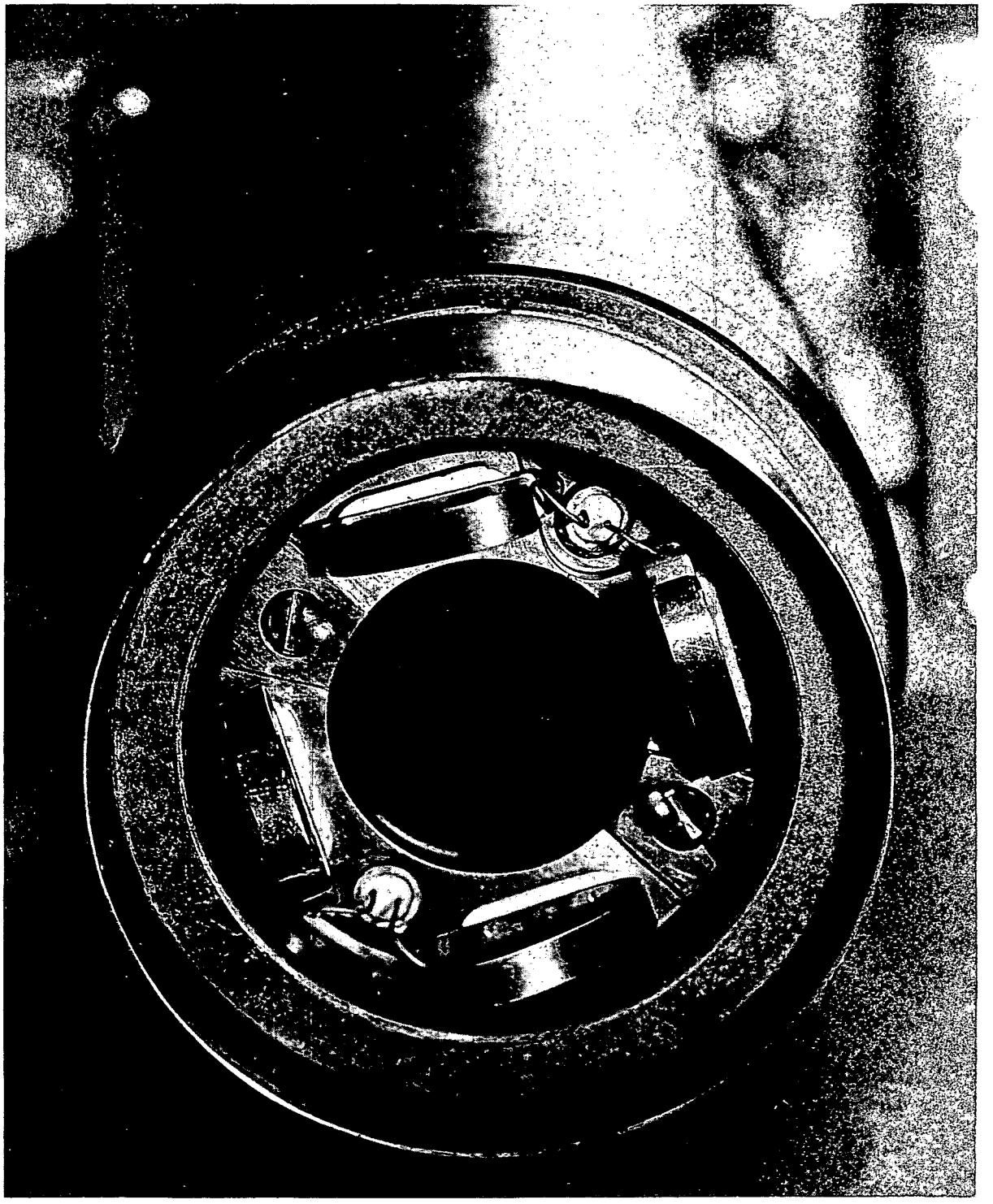

HT66523

Fig. 8-8. View of the bottom of PTE-2 showing the thermocouple contactor assembly

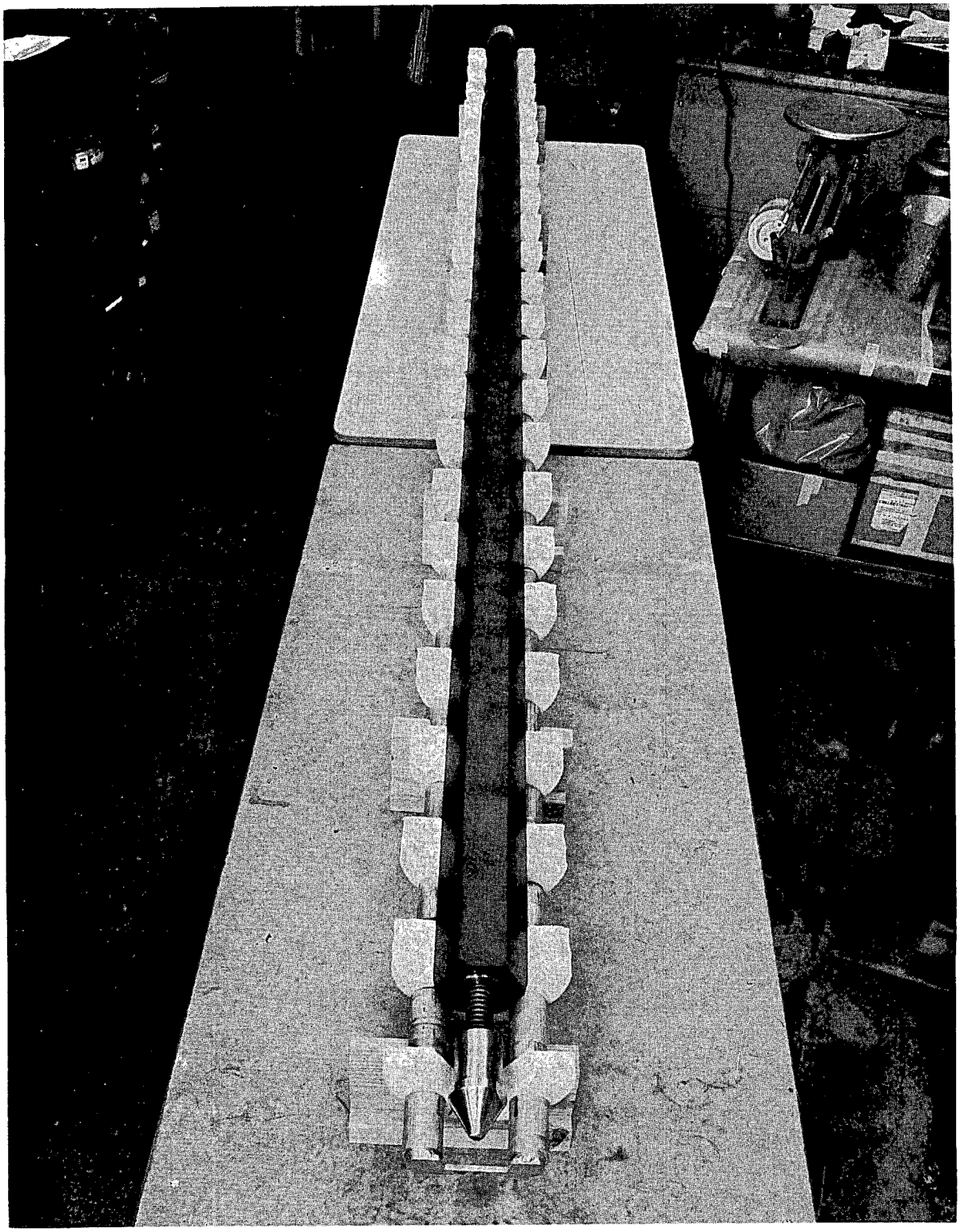

HT66524

Fig. 8-9. Completed assembly of PTE-2

8.4. CEMENTED JOINT CURING

The cement recommended for assembly of the proof test element sections was Grade P-514 carbon cement. The recommended curing to 260°F at increases of 15°F/hr could not be applied because the polyethylene plugs inserted on top of each of the fuel-rod stacks as a motion restrainer lose their integrity at a temperature of 210°F. Thus, the curing cycle used for PTE-2 was limited to 175°F at gradual increments of 15°F/hr. The 175°F temperature was held for 1/2 hr. Final cure and carburization of the cement will occur when the element reaches operating temperature in the reactor.

8.5. LOADING OF PTE-2 INTO SHIPPING CONTAINER

The foam shipping support for PTE-2 consisted of four lengths of 1-in. aluminum Schedule 40 pipe equipped with 3-1/4-in.-long aluminum spacers made of 1-1/4-in. Schedule 40 pipe. Polyethylene foam pads die cut to the proper configuration were inserted between the spacers. The support was constructed in two halves. One half of the foam shipping support (Dwg. No. 90-SK-2354) was positioned to receive the element. The handling tool, as shown in Fig. 8-10, was inserted into the element and latched. The element was then lifted by four individuals and placed in this cradle. A protective cap (Dwg. No. 90-SK-2314) was placed over the thermocouple contact points and secured to the cradle with glass-reinforced tape. The second half of the cradle was placed in position and the two halves were bound together with glass-reinforced tape. PTE-2 contained within the shipping support cradles is shown in Fig. 8-11.

The shipping container (Dwg. No. 90-SK-2309) is constructed from a piece of 8-in. Schedule 40 pipe that is threaded on both ends and equipped with fork-lift brackets, supports, and eye bolts for horizontal and vertical lifting. The PTE-2 shipping container is shown in Fig. 8-12.

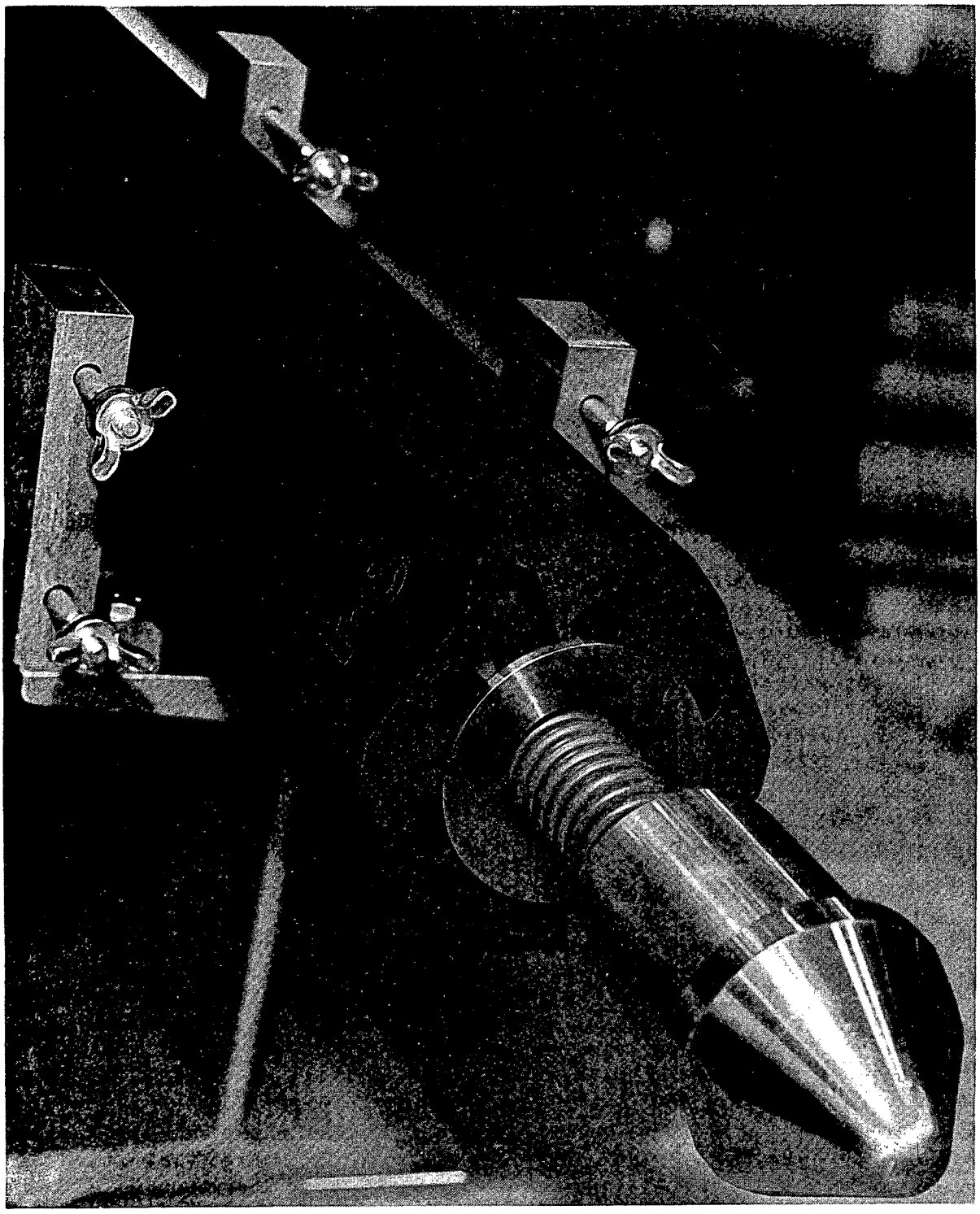

HT66522

Fig. 8-10. Handling tool latched within PTE-2

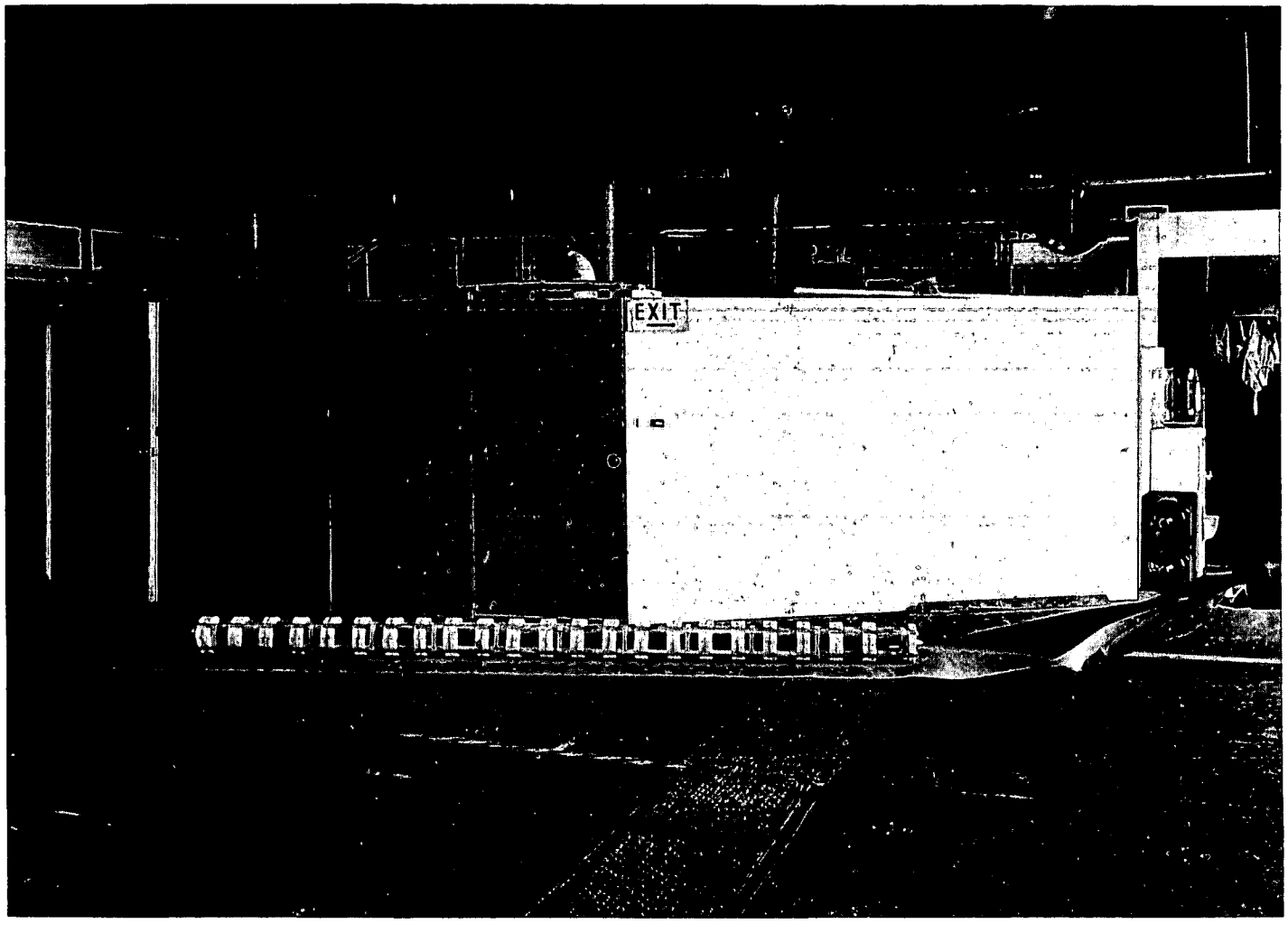

HT66519

Fig. 8-11. PTE-2 contained within the foam shipping support cradles

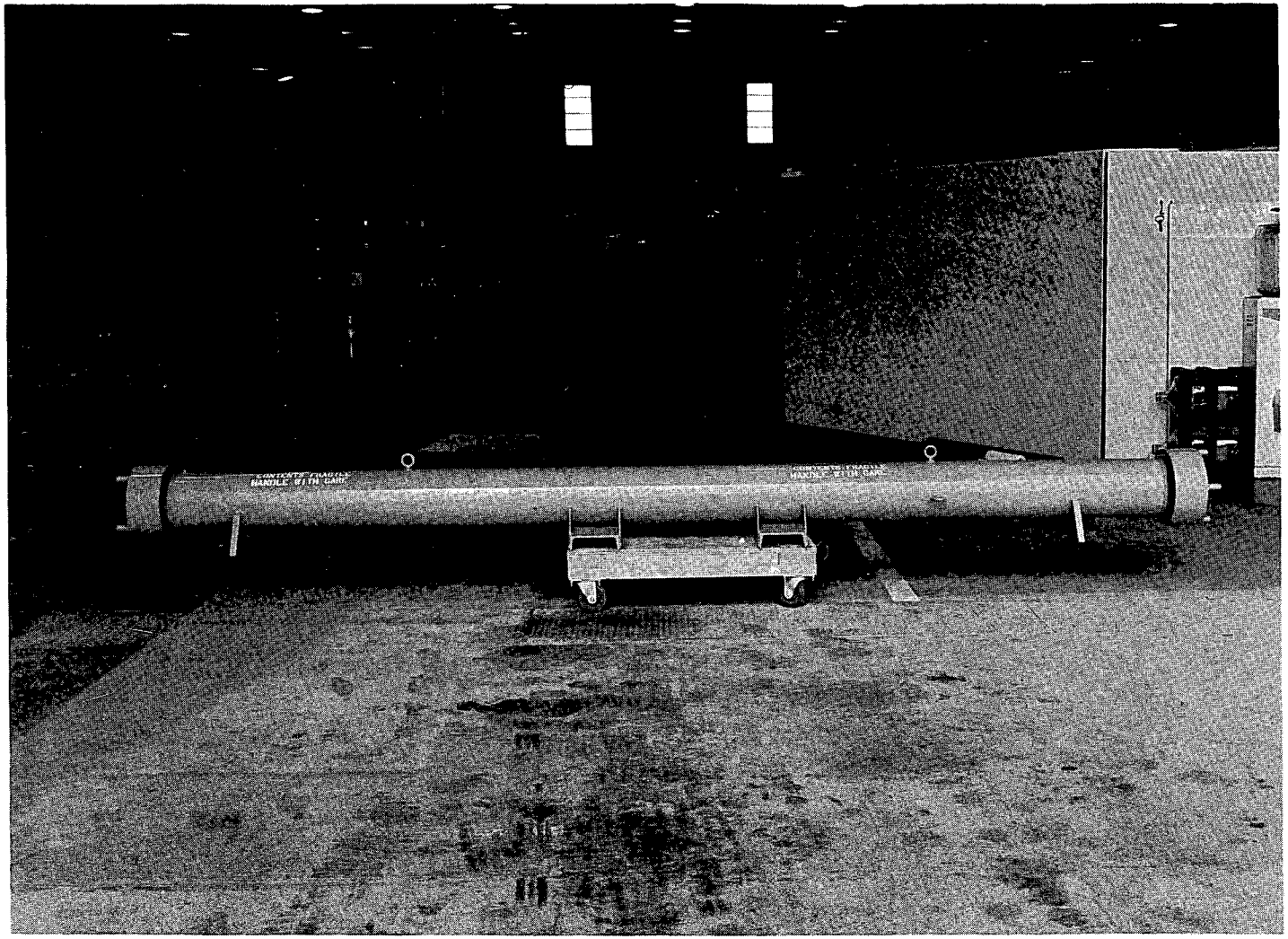

HT66520

Fig. 8-12. PTE-2 shipping container

A length of 3-ft-wide Kraft paper was fed through the 8-in. pipe and an equal length was allowed to extend out one end. The element, in its foam support, was wrapped in the protruding piece of paper. When all was ready, one individual pulled on the Kraft paper at one end of the 8-in. pipe while four individuals lifted and slid the cradle into the pipe at the other end.

Once the element was in place, the excess paper was removed and discarded, the padded pipe caps were attached, wire-lock holes were drilled, and the caps were wire-locked in place. Both ends of the pipe were enclosed with a polyethylene bag and sealed with tape.

9. QUALITY ASSURANCE

Quality Assurance Plan 90-48 describes the QA tasks to be accomplished to assure that requirements of the drawings and specifications for PTE-2 are met.

Standard Peach Bottom materials and parts were used, whenever available, and modified to conform to PTE-2 requirements. Certifications were obtained on these materials for the PTE-2 QA file.

All of the piece parts were inspected to PTE-2 drawings and the deviations approved by the Fuel Element Design Branch. The hex flats on the reflectors and fuel sections were checked in numerous locations and the dimensions recorded for evaluation of expansion characteristics during the postirradiation examination.

Fuel particle evaluation data were obtained and compared from FOD and FMB. Each deviation was carefully weighed and final acceptance was made by FMB. This final acceptance hinged to a large extent on the metallic fission product release values furnished by the Fuel Chemistry Branch. The threshhold acceptance values of the fission-product-release tests were somewhat arbitrarily selected from previous irradiation tests. It is not known how valid these choices are.

Fuel rods were made by both FOD and FMB and were dimensionally inspected by them. One sample from each mold run was evaluated by the Fuel Chemistry Branch for gaseous fission-product release. Due to schedule pressures, steady-state corrections were inferred on many of the results; therefore, the same comments apply here as for the fuel particles.

Specific data were unavailable for the thermocouples used in PTE-2. Typical data on similar thermocouples sent to GGA were supplied by Continental Sensing and used to evaluate expected performance for the thermocouples used.

The assembly was made and tested to the FSV Proof Test Element Assembly Specification X-18-U-8. Specific data were recorded in the Engineering Log Book. Checklists were formulated and used by QA to assure that all the checks called for in X-18-U-8 were performed. These lists as well as all other pertinent QA data obtained for PTE-2 will be retained in the PTE-2 QA file.

10. COMPARISON OF PTE-2 WITH OTHER IRRADIATION TESTS

Fuel rods of the type contained in PTE-2 have been tested in a series of GGA capsule irradiation experiments. These irradiation tests commenced at about the same time as PTE-2, however, because of the accelerated nature of capsule tests, the irradiation results became available at a much earlier date. A brief summary of these irradiation results is presented below.

A total of 15 phenolic-resin bonded fuel rods were irradiated in four GGA capsule tests to peak exposures of up to 5.3×10^{21} n/cm^2 (E > 0.18 MeV) at 1175°C. These capsule experiments were FR-1, FR-2, FR-3, and P23 (Refs. 21, 22). Fuel rods irradiated in these experiments were 0.50 in. in dia. x 1.0 in. long and all rods were fabricated using the cold-injection molding technique. The rod matrix was composed of a phenolic resin binder and GP-38 graphite filler. Filler contents were varied between 18 and 24 wt % GP-38. Coated particle types were $(Th,U)C_2$ TRISO fissiles and ThC_2 TRISO fertiles. Coating variables were similar to those tested in PTE-2. Both HTI and LTI isotropic pyrolytic coatings were investigated, and outer PyC densities in the range of 1.74 to 1.95 gm/cm^3 were included. Sections 5 and 6 of this report give detailed descriptions of PTE-2 samples.

A summary of the capsule fuel rod samples is presented in Table 10-1. Postirradiation examinations showed that this type of rod remained reasonably intact up to the peak exposure of these tests. Rods irradiated in capsules FR-2, FR-3, and P23 to $\leq 2 \times 10^{21}$ n/cm^2 were in good condition and were determined to have shrunk both radially and axially. The measured shrinkages correlated with the temperature fluence conditions of the irradiations. The higher exposure rods irradiated in capsule FR-1 were intact, however, their conditions were fragile and they began to crumble when handled during

TABLE 10-1
DESCRIPTION AND POSTIRRADIATION EXAMINATION OF COLD-INJECTED FUEL RODS TESTED IN GGA CAPSULES

Capsule Number	Rod Number	Particle		Coating			Fuel Rod[d] Matrix Filler Wt-%	Fissile Burnup (% FIMA)	Irradiation Conditions				Postirradiation Condition				Macro Examination Remarks[g]
					Outer Isotropic				Temperature (°C)			Fast Fluence ($\times 10^{21}$ n/cm^2)	Dimensional Change (%)		Met. Exam. (% Fail)		
		Lot Number	Type[a]	Type[h]	Density (g/cm^3)	BAF[c]			Average	Maximum	EOL[g]		Length	Diameter	Fissile[f]	Fertile[f]	
FR-1	01-1A-C018	3923-87E	Fissile	TRISO LTI	1.95	1.01	21	21	1100	1300[i]	1300[i]	5.0	+1.2	+1.4	74	94	Intact, fragile Matrix & coating cracks visible Burn: 0.3% SiC coatings failed
		4000-711[h]	Fertile		1.90	1.01											
FR-1	01-2A-0019	3923-149E	Fissile	TRISO HTI	1.86	1.03	21	22	1200[i]	1330[i]	1100[i]	5.3	+2.3	+1.6	100	100	Intact, fragile Matrix & coating cracks visible, some particles debonded Burn: 0.8% SiC coatings
		4000-712[h]	Fertile		1.95	1.01											
FR-1	01-3A-C020	3923-149E	Fissile	TRISO HTI	1.86	1.03	18	22	1140[i]	1280	1000[i]	5.3	(h)	+1.2	100	100	Partially damaged during disassembly, fragile Matrix and coating cracks visible Burn: 0.5% SiC coatings failed
		4000-712[h]	Fertile		1.95	1.01											
FR-1	01-4A-C021	3923-87E	Fissile	TRISO LTI	1.95	1.01	21	20	1120[i]	1290	1030[i]	4.8	+2.1	+1.6	65	100	Intact, fragile Pitted-matrix & coating cracks visible, some debonding of particles Burn: 0.4% SiC coatings failed
		4000-711[h]	Fertile		1.90	1.01											
FR-1	01-5A-C022	3923-87E	Fissile	TRISO LTI	1.95	1.01	24	16	1160	1300	1115	3.8	+1.6	+1.0	9	100	Intact, good condition Matrix & coating cracks visible Burn: not performed
		4000-711[h]	Fertile		1.90	1.01											
FR-2	02-1A-C036	4000-889[h]	Fissile	TRISO LTI	1.92	1.07	21	5.5	900	920	910	0.87	-0.8	-0.8	15	80	Intact, good condition
		4000-711[h]	Fertile		1.90	1.01											
FR-2	02-2A-C039	3923-111E	Fissile	TRISO HTI	1.89	0.92	21	6.5	1210	1280	1280	0.95	-0.9	-1.0	(j)	(j)	Intact, good condition
		4000-734[h]	Fertile		1.91	1.02											
FR-2	02-3A-C068	4000-889E[h]	Fissile	TRISO LTI	1.92	1.07	21	6.5	1230	1250	1245	1.00	-1.1	-1.4	(j)	(j)	Intact, good condition
		4273-145	Fertile		1.96	1.04											
FR-2	02-4A-C043	4000-889E[h]	Fissile	TRISO LTI	1.92	1.07	24	6.0	1230	1240	1240	0.91	-1.0	-1.0	(j)	(j)	Intact, good condition
		4000-139[h]	Fertile		1.86	1.19											
FR-2	02-5A-C053	4000-889E[h]	Fissile	TRISO LTI	1.92	1.07	21	4.5	605	625	630	0.68	-0.3	-0.4	(j)	(j)	Intact, good condition
		4000-711[h]	Fertile		1.90	1.01											
FR-3	03-1A-C052	3923-111E	Fissile	TRISO HTI	1.84	1.01	21	7.0	905[i]	910	905[i]	1.1	-0.8	(e)	(j)	(j)	Intact, good condition
		4000-138[h]	Fertile		1.84	1.09											
FR-3	03-2A-C048	4000-889E[h]	Fissile	TRISO LTI	1.92	1.07	21	8.5	1225	1250	1250	1.3	-0.9	-0.3	30	80	Intact, slight amount of surface pitting
		4000-711[h]	Fertile		1.90	1.01											
FR-3	03-3A-C070	3923-111E	Fissile	TRISO HTI	1.84	1.01	21	8.5	1230	1260	1250	1.3	-1.6	-1.7	(j)	(j)	Intact, good condition
		4273-149	Fertile		1.74	(j)											
FR-3	03-5A-C046	3592-35E	Fissile	TRISO LTI	(j)	(j)	21	6.0	1045	1265	1260	0.92	-0.7	-0.8	(j)	(j)	Intact, good condition
		4000-733[h]	Fertile		1.98	1.03											
P-23	23-5A-C034	4000-889E	Fissile	TRISO LTI	1.92	1.07	21	8	1170	1200	1190	1.4	-0.8	-1.0	35	50	Intact, very good condition Slight matrix cracking visible
		4000-711	Fertile		1.90	1.01											

[a] Fissile particle kernels are $(Th,U)C_2$; fertile particle kernels are ThC_2

[b] TRISO particles have a silicon carbide diffusion barrier coating. LTI denotes low-temperature isotropic outer pyrolytic carbon, and HTI denotes high-temperature isotropic outer pyrolytic carbon coating.

[c] Bacon anisotropy factor (BAF)

[d] All fuel rods are approximately 1 in. in length and 0.5 in. in diameter. Rods fabricated using cold-injection molding technique. Matrix had phenolic resin binder and GP 38 graphite filler.

[e] End of life temperature

[f] Cracked outer isotropic PyC coatings only

[g] Burn indicates a piece of the rod was oxidized in order to determine the percent broken silicon carbide shells

[h] Coated particles produced in production scale coaters

[i] Estimated, thermocouple failed during the test

[j] Not determined

the postirradiation examination. These rods were irradiated to fluences of 3.8 to 5.3 x 10^{21} n/cm^2 at approximately 1175°C. All of the FR-1 rods expanded both radially and axially and expansions of up to 2% were measured for the rods with the highest exposure.

Metallographic examination of rods from each of these tests revealed a high percentage of the outer PyC coatings had failed, even at the lowest exposures. It was observed that a very strong bond existed between the matrix and the outer PyC coatings. Also the phenolic resin GP-38 matrix shrank considerably under irradiation. This combination of conditions resulted in the outer PyC coatings being broken-off from the particles. With increasing exposure, the broken coatings were distorted by adhering matrix which apparently caused the slight expansions observed in the high-exposure rods from capsule FR-1. It should be noted, that although there was complete failure of the outer PyC coatings in many of the rods, a maximum of 0.8% SiC coatings were observed to have failed. Most of these were on the larger fertile particles.

Considerable improvements have been made in fuel rod matrices since these tests. Extensive irradiation testing of rods with pitch-natural flake graphite matrices have demonstrated their excellent irradiation stability to exposure conditions which exceed those in the FSV reactor (Refs. 23, 24). This type of matrix has been selected for the Fort St. Vrain rods (Ref. 25).

11. DRAWINGS AND SPECIFICATIONS FOR PTE-2

The following is a complete list of all drawings used for PTE-2.

Drawing No.	Title
90-SK-1972	Fuel Element Assembly
90-SK-1971	Comparative Views of Peach Bottom and PSC Proof Test Fuel Elements
90-SK-1970	Proof Test Element in Peach Bottom Core
90-SK-2003	Radial Thermocouple Location
90-SK-2004	Radial Reference Dimensions
90-SK-1974	Proof Test Bottom Connector
90-SK-1975	Bottom Reflector
90-SK-1976	Fuel Section One
90-SK-1977	Fuel Section Two
90-SK-1978	Fuel Section Three
90-SK-1979	Fuel Section Four
90-SK-1980	Top Reflector
90-SK-1992	Fuel Bed Details
90-SK-2477	Fuel Zone One Assembly
90-SK-2478	Fuel Zone Two Assembly
90-SK-2479	Fuel Zone Three Assembly
90-SK-2480	Fuel Zone Four Assembly
90-SK-1988	Handling Tool Assembly
90-SK-2309	Shipping Cask Assembly
90-SK-2353	Aligning and Spacer Pipe
90-SK-2314	Bumper for Bottom Connector - Proof Test Element
90-SK-2354	Proof Test Fuel Element and Shipping Cask Assembly

Drawing No.	Title
90-SK-2320	Shipping Cushion for Proof Test Element
90-SK-2208	Collar Assembly and Details
90-SK-2073	Assembly and Details for Proof Test Element Assembly Fixture
90-SK-2072	Details - I Beam
90-SK-2071	Proof Test Element Assembly Fixture
90-SK-2209	Jig Assembly for Proof Test Element
SKPTE-1	Thermocouple Cold Junction
SKPTE-2	Lift Block
SKPTE-13	Proof Test Element Handling Tool - Reference Dimensions
SKPTE-11	Handling Tool Life Knob and Thrust Bearing Details
SKPTE-7	Handling Tool Lifting Tee - Details
SKPTE-8	Handling Tool Spring Rod and Extension Rod - Details
SKPTE-9	Handling Tool Guide Core - Details
SKPTE-10	Handling Tool Lower Spring Cup - Details
SKPTE-12	Handling Tool Spring
SKPTE-14	Handling Tool Holder-Canister Insert
SKPTE-15	Handling Tool Storage Canister
SKPTE-17	Handling Tool Wrench
SKPTE-18	Lift Block Dowel Pins - Details
SKPTE-16	Handling Tool Operation Sequence Schematic

The following is a complete list of all specifications used for PTE-2.

Specification No.	Title
X-18-U-3, Issue - A	Tungsten Rhenium Fuel Element Thermocouple
X-18-U-4, Issue - A	Chromel Alumel Fuel Element Thermocouple

Specification No.	Title
X-18-U-6, Issue C	Coated Fuel Particles for Second FSV Fuel Test Element
X-18-U-7, Issue B	Fuel Rods for Second FSV Proof Test Element
X-18-U-8, Issue A	Fort St. Vrain Proof Test Element Assembly
X-18-U-9, Issue A	Fort St. Vrain Proof Test Element Fabrication
396-FO-1M, Issue C	Fuel Element Graphite and Replaceable Reflector Graphite for the FSV Reactor
33-R-3, Issue C	Low Permeability Sleeve and Bottom Connectors for Peach Bottom Fuel Element.
QA Plan 90-48	Quality Assurance Plan - Peach Bottom and PSC Proof Test Element

REFERENCES

1. Philadelphia Electric Company, Peach Bottom Atomic Power Station, "Final Hazards Summary Report," Vol. II, Sect. II.A.4.
2. "Target. A Program for a 1000-MW(e) High-Temperature Gas-Cooled Reactor, Quarterly Progress Report for the Period Ending February 28. 1965" USAEC Report GA-6113, General Dynamics, General Atomic Division, March 31, 1965; and for the period ending May 31, 1965, Report GA-6418, June 30, 1965.
3. "HTGR Base Program Quarterly Progress Report for the Period Ending Aug. 31, 1965," USAEC Report GA-6671, General Dynamics, General Atomic Division, Sept. 30, 1965; for the period ending Nov. 30, 1965, Report GA-6869, Jan. 15, 1966; and for the period ending February 28, 1966, Report GA-7010, May 15, 1966.
4. "Target. A Program for a 1000 MW(e) High-Temperature Gas-Cooled Reactor," Quarterly Progress Report for the Period Ending May 31, 1965, USAEC Report GA-6418, General Dynamics, General Atomic Division, June 30, 1965.
5. Turner, R. F., et al., "Irradiation Test of the GAIL-III-B Fuel Element in the General Atomic In-Pile Loop," USAEC Report GA-5314, General Dynamics, General Atomic Division, July 10, 1964.
6. Winkler, E. O., "GAIL-IV Irradiation Assembly Design Summary and Information Data Package," USAEC Informal Report GAMD-5535, General Dynamics, General Atomic Division, August 11, 1964.
7. Winkler, E. O., et al., "Irradiation Test and Postirradiation Examination of the GAIL-IV Fuel Element in the General Atomic In-Pile Loop," USAEC Report GA-7997, General Dynamics, General Atomic Division, June 30, 1967.
8. "HTGR Base Program. Quarterly Progress Report for the Period Ending February 28, 1967," USAEC Report GA-7801, General Dynamics, General Atomic Division, April 20, 1967.

9. Goeddel, W. V., and J. C. Bokros, "HTGR Coated Particle Fuel," Proceedings of the AIME Nuclear Metallurgy Symposium on High Temperature Nuclear Fuels 42, 85 (1968).

10. Turner, R. F., and W. V. Goeddel, "Advances in Fuel Element Design and Materials," USAEC Report GA-7183, General Dynamics, General Atomic Division, June 17, 1966.

11. "HTGR Base Program. Quarterly Progress Report for the Period Ending May 31, 1967," USAEC Report GA-7981, General Dynamics, General Atomic Division, Sept. 29, 1967.

12. Philadelphia Electric Company, Peach Bottom Atomic Power Station, "Final Hazards Summary Report," Vol. V, Annex B, Table B-3.

13. Langer, S., et al., "The Retention of Iodine by Pyrolytic Carbon-Coated Nuclear Fuel Particles," USAEC Report GA-8524, Gulf General Atomic, March 6, 1968.

14. "HTRDA Fuel and Fuel Cycle Development Program. Semiannual Report for the Period July 31, 1967 to December 31, 1967," unpublished data.

15. Langer, S., C. C. Adams, and J. N. Graves, Gulf General Atomic, "Status and Recommendations on Fission Product Release Measurements for HTGRs," Unpublished data.

16. Mills, R. G., Gulf General Atomic,"Specification for Coated Particles for Second Fort St. Vrain Proof Test Element," unpublished data.

17. Goeddel, W. V., and J. N. Siltanen, "Materials for High Temperature Nuclear Reactors," Annual Review of Nuclear Science 17, 189 (1967).

18. Jaye, S., and W. V. Goeddel, "High-Temperature Gas-Cooled Reactor Fuel and Fuel Cycles - Their Progress and Promise," Nuclear Engineering and Design 7, 283 (1968).

19. Hooker, J. R., Gulf General Atomic, "Fuel Rods for the Second Proof Test Element," unpublished data.

20. "Public Service Company of Colorado 330-MW(e) High-Temperature Gas-Cooled Reactor Research and Development Program. Quarterly Progress Report for the Period Ending Sept. 30, 1968," USAEC Report GA-8879, Gulf General Atomic, October 31, 1968.

21. "Public Service Company of Colorado 330-MW(e) High-Temperature Gas-Cooled Reactor Research and Development Program. Quarterly Progress Report for the Period Ending September 30, 1969," USAEC Report GA-9720, Gulf General Atomic, October 29, 1969.

22. "Public Service Company of Colorado 330-MW(e) High-Temperature Gas-Cooled Reactor Research and Development Program. Quarterly Progress Report for the Period Ending June 30, 1969," USAEC Report GA-9440, Gulf General Atomic, July 31, 1969.
23. Luby, C. S., D. P. Harmon, and W. V. Goeddel, "HTGR Fuel Design and Irradiation Performance," USAEC Report GA-10468, Gulf General Atomic, January 5, 1971.
24. "Public Service Company of Colorado 330-MW(e) High-Temperature Gas-Cooled Reactor Research and Development Program. Quarterly Progress Report for the Period Ending December 31, 1971," USAEC Report GA-A10980, Gulf General Atomic, January 31, 1972.
25. "HTGR Fuel Specifications," Gulf General Atomic, unpublished data.